MEASUREMENT OF AWARENESS AT THE END OF LIFE

by

Elizabeth G. Blundon

B.Sc., University of British Columbia

M.A., University of British Columbia

A THESIS SUBMITTED IN PARTIAL FULFILLMENT OF

THE REQUIREMENTS FOR THE DEGREE OF

DOCTORATE OF PHILOSPHY

in

THE FACULTY OF GRADUATEAND POSTDOCTORALSTUDIES

(Psychology)

THE UNIVERSITY OF BRITISH COLUMBIA

(Vancouver)

April 2020

The following individuals certify that they have read, and recommend to the Faculty of Graduate and Postdoctoral Studies for acceptance, the dissertation entitled:

Measurement of awareness at the end of life

submitted by Elizabeth Blundon in partial fulfillment of the requirements for

the degree of Doctor of Philosophy

in Psychology

Examining Committee:

Lawrence Ward, Professor, Cognitive Psychology, UBC

Supervisor

Rebecca Todd, Associate Professor, Cognitive Psychology, UBC

Supervisory Committee Member

Janet Werker, Professor, Developmental Psychology, UBC

University Examiner

Anthony Herdman, Associate Professor, School of Audiology & Speech Sciences

University Examiner

Additional Supervisory Committee Members:

Todd Handy, Professor, Cognitive Psychology

Supervisory Committee Member

Abstract

Here I report evidence of awareness among unresponsive hospice patients at the end of life. Chapter 2 describes the neurotypical neural networks underlying some EEG measures used to assess awareness, particularly activations of different attention networks associated with the P3a and P3b event-related potential (ERP) sub-components of the P300 ERP. I found that the primary neural generators of the P3a were frontal regions associated with exogenous attention processes, such as the Ventral Attention (Corbetta & Shulman, 2002) and Saliency (Menon & Uddin, 2010) networks. The neural generators of the P3b, by contrast, were parietal regions associated with endogenous attention processes, such as the Dorsal Attention Network (Corbetta & Shulman, 2002), and regions often involved in detecting oddball targets (H. Kim, 2014). Chapter 3 reports evidence of auditory cortical processing (Näätänen et al., 2007) among all unresponsive patients, and attention orienting or context updating (Polich, 2007) among some unresponsive patients. Chapter 4 describes the spatio-temporal dynamics of attention networks reported in Chapter 2 among individual neurotypical control participants, and both responsive and unresponsive hospice patients. While these results are highly nuanced, some unresponsive patients showed some fronto-parietal connectivity, and may have engaged in motor imagery. Chapter 5 reports evidence of stimulus-independent cognition occurring in the default mode network (Buckner et al., 2008a; Christoff et al., 2016; Raichle et al., 2001; Smallwood et al., 2012) among unresponsive patients during a period of rest. Chapter 6 reports evidence of a decrease in alpha-band oscillation power in the posterio-parietal cortex in response to music among unresponsive patients. As such a decrease in alpha-band power is associated with orienting of attention, this implies that these patients may be paying attention to the music. The results of this research suggest that some unresponsive hospice patients at the end of life may be

aware. These results lend credence to the belief that “hearing is the last to go”, and that loved ones at the bedside should be encouraged to interact with their dying relatives for as long as possible. Furthermore, attention to music could be a promising new biomarker of awareness that has potential for clinical adaptation.

Lay Summary

Many people believe that, as we die a natural death, our “hearing is the last to go”. This implies that even as our bodies weaken, and we can no longer interact with our loved ones, we can still hear them, or even feel their touch. I measured brain signals from a small group of unresponsive hospice patients and found that some of them may have been listening to simple tones, listening to music, or mind-wandering. There could, therefore, be some truth to the belief that “hearing is the last to go”, and that friends and family should continue to interact with their dying loved ones for as long as possible.

Preface

Neurotypical data were collected in the Psychophysics and Cognitive Neuroscience Lab at the University of British Columbia Vancouver Campus, where Dr. Lawrence Ward is the Principal Investigator. Hospice patient data were collected at Saint John's Hospice, where Dr. Romayne Gallagher was the supervising physician of this project. I conducted and/or supervised all data collection. I analyzed the data and was the primary writer of the dissertation. My supervisor, Dr. Ward, assisted with project conceptualization and suggested edits to the dissertation. Dr. Gallagher also suggested edits to some of the dissertation. The experiments reported were approved by the University of British Columbia's Behavioural Research Ethics Board [Fast dynamics of brain regional networks underlying cognition: H00-80505; Awareness in the last hours of life: H12-03333].

A version of Chapter 2 has been published: Blundon: E. G., & Ward, L. M. (2019). Search asymmetry in a serial auditory task: Neural source analyses of EEG implicate attention strategies. *Neuropsychologia*, *134*, 107204. I was the lead researcher in charge of collecting all data, performing all analyses, and the primary author of the manuscript. Dr. Ward supervised the research, provided funding, and contributed to the manuscript.

A version of Chapter 3 has been submitted for publication: Blundon, E. G., Gallagher, R. E., & Ward, L. M. (2019a). Electrophysiological evidence of preserved hearing at the end of life, manuscript submitted for publication. I was the lead researcher in charge of collecting all data, performing all analyses, and the primary author of the manuscript. Dr. Ward supervised the research, provided funding, and contributed to the manuscript. Dr. Gallagher assisted in data collection and contributed to the manuscript.

A version of Chapter 5 has been submitted for publication: Blundon, E. G., Gallagher, R. E., & Ward, L. M. (2019b). Default-mode network activation and functional connectivity in the dying brain, manuscript submitted for publication. I was the lead researcher in charge of collecting all hospice data, performing all analyses, and the primary author of the manuscript. Dr. Ward supervised the research, provided funding, and contributed to the manuscript. Dr. Gallagher assisted in data collection and contributed to the manuscript. Control data were donated by Dr. Todd Handy and Diana Pricop.

Table of Contents

Abstract iii

Lay Summary v

Preface vi

Table of Contents viii

List of Tables xiii

List of Figures xv

List of Acronyms xvii

List of Abbreviations xix

Acknowledgements xx

Dedication xxi

Chapter 1 : Introduction 1

1.1 Is it possible for a dying brain to sustain awareness? *1*

1.2 How can we assess awareness of unresponsive patients at the end of life? *3*

1.3 What are some possible neural signatures of awareness? *4*

1.4 Overview of electrophysiological measures used to assess awareness *7*

1.4.1 Event-related potentials (ERPs) *8*

1.4.2 Event-related spectral perturbations (ERSPs) *8*

1.4.3 Phase-locking values (PLVs) *8*

1.5 Dissertation summary *9*

Chapter 2 : Spatiotemporal neural dynamics underlying the P3a and P3b among neurotypical control participants. 12

2.1 Materials and Methods 20

2.1.1 Ethics Statement 20

2.1.2 Participants 21

2.2 Stimuli 21

2.3 Procedure 22

2.3.1 EEG recording and preprocessing 24

2.3.2 Independent Component Analysis 25

2.3.3 Artefact rejection and source localization 26

2.3.4 IC Source Clustering 27

2.3.5 Cluster to channel ERP projections 28

2.3.6 Event Related Spectral Perturbations (ERSPs) 29

2.3.7 Phase-locking Values (PLVs) 30

2.4 Results 31

2.4.1 Behavioural data 31

2.4.2 Cluster Results 32

2.4.3 Cluster to channel ERP projection results 36

2.4.4 ERSP results 37

2.4.5 Phase Locking Value Results 41

2.5 Discussion 43

Chapter 3 : Electrophysiological evidence of hearing at the end of life 49

3.1 Materials and Methods 50

3.1.1 Ethics Statement *51*

3.1.2 Participants *51*

3.2 Stimuli and Procedure *55*

3.2.1 EEG recording and preprocessing *56*

3.2.2 Behavioural and ERP Analyses *57*

3.3 Results *62*

3.3.1 Controls *62*

3.3.2 Patients *65*

3.4 Discussion *66*

Chapter 4 : Individual spatio-temporal dynamics underlying P3a and P3b among neurotypical and hospice patients 71

4.1 . Materials and Methods *71*

4.1.1 . Artefact rejection and source localization *72*

4.1.2 . ROI clustering *73*

4.1.3 . Event Related Spectral Perturbations (ERSPs) *74*

4.1.4 . Phase-locking Values (PLVs) *74*

4.2 . Results *75*

4.2.1 . Cluster Results *75*

4.2.2 . ERSP Results *76*

4.2.3 . Connectivity results *80*

4.3 . Discussion *83*

Chapter 5 : Electrophysiological evidence of default mode activation at the end of life..... 90

5.1 Materials and Methods *91*

5.1.1 . Controls and Ethics statement *92*

A total of 30 participants were recruited through the community via posting at the Paid Participants Study List hosted by Psychology Graduate Student Council website, and remunerated $20 (CAD) for their participation (23 females; M = 24.5 years old, SD = 7.98; 28 were right-handed). All had no history of neurological problems and had normal or corrected-to-normal vision. Participants provided written informed consent to the experimental procedure, and the UBC Behavioral Review Ethics Board approved all procedures and protocols of this experiment. *92*

5.1.2 Patients and Ethics Statement *92*

5.1.3 Procedure *92*

5.1.4 Artefact rejection and source localization *92*

5.1.5 ROI clustering *93*

5.1.6 Phase-locking Values (PLVs) *94*

5.2 Results *95*

5.2.1 Controls *95*

5.2.2 Patients *98*

5.3 Discussion *102*

Chapter 6 : Electrophysiological evidence of music listening at the end of life 105

6.1 . Experiment 6.1-Neurotypical Control Participants *107*

6.1.1 . Materials and Methods *107*

6.1.2 . Results *111*

6.1.3 . Discussion *119*

6.2 . Experiment 6.2-Hospice Patients *120*

6.2.1 . Materials and Methods *120*

6.2.2 . Results *121*

6.2.3 . Discussion *125*

Chapter 7 : General Discussion **127**

7.1 . Relation of current results to other work *127*

7.2 . Is hearing the last to go? *131*

7.3 . How do neural network dynamics change at the end of life? *135*

7.4 . Strengths, limitations, future directions, and clinical recommendations *140*

References **144**

Appendix A **193**

Appendix B **195**

Appendix C **196**

Appendix D **198**

List of Tables

Table 2.1 Details of the 9 valid clusters that were retained for further analysis after seeding. 34

Table 2.2 Percentage of electrode power accounted for by cluster activation projected to midline electrodes. 37

Table 3.1: Details of responsive hospice patient diagnosis and medications consumed on the day of each recording..... 53

Table 3.2: Details of unresponsive hospice patient diagnosis and medications consumed on the day of each recording. 54

Table 3.3: List of electrodes from which ERP analyses were performed. 61

Table 4.1. Details of the 9 valid control clusters identified in Chapter 2. 73

Table 4.2. Characteristics of seeded ROIs per participant group. 76

Table 4.3. Number of valid IC pairs per network and per participant group. 81

Table 5.1. DMN regions and their seed coordinates in Talairach space. 94

Table 5.2. Details of seeded ROIs within DMN. 96

Table 5.3. p values of McNemar's test to compare the IC contributions of PCC and RIPL to other ROIs withing DMN..... 97

Table 5.4. The number of ICs localized to regions within the DMN (either hemisphere) per patient..... 99

Table 5.5. List of p values for McNemar's tests comparing vMPFC and PCC (rows) to the remaining regions within DMN (columns), for both responsive (top) and unresponsive (bottom) patients. 100

Table 6.1. Clusters uncovered in between-subjects comparisons of Active and Passive conditions separately. 112

Table 6.2. Clusters containing ICs from both Active and Passive conditions. 114

Table 6.3. Clusters containing ICs from both Responsive and Unresponsive patients. 122

Table 6.4. The number of posterio-parietal and frontal ICs with sustained alpha suppression for each participant. 125

Table 7.1. Strong (++) and weak (+) evidence of 6 different potential biomarkers of cognition among responsive (top) and unresponsive (bottom) palliative care patients. 133

List of Figures

Figure 2.1. Midline ERPs to tone change and pattern change runs. 14

Figure 2.2. Stimuli and study design. 22

Figure 2.3. Sequence Design. 24

Figure 2.4. Nine clusters retained for further analysis. 35

Figure 2.5. Projections from frontal and parietal clusters to CZ and PZ, respectively. 37

Figure 2.6. Time course of ERSP differences between rare and common runs for each condition, grouped by frequency band, and in 100ms bins following the onset of the final stimulus in the run. 39

Figure 2.7. PLV connections within networks (VAN, DAN, ODD) and between networks (VAN-DAN, VAN-ODD, DAN-ODD). 42

Figure 3.1: Individual differences in ERP and reaction time (RT) responses from neurotypical control participants (N001-N17) to local tone deviants (left) and global pattern deviants (right). 64

Figure 3.2: Individual differences in ERP responses from both responsive (top panel) and unresponsive hospice participants (P001-P009) to local tone deviants (left) and global pattern deviants (right). 66

Figure 4.1. Proportion of participants that evinced early theta ERS (top) and later beta ERD (bottom) to tone changes (left) and pattern changes (right) for each ROI. 78

Figure 4.2. The proportion of participants that showed early frontal (ACC/SMA/Cing) theta ERS (top) or later centro-parietal (SMA/Cing/R SPC/L PreCG) to tone changes (top) or pattern changes (bottom). 79

Figure 4.3. The proportion of participants with early (0 – 500ms) theta connectivity within each network. 82

Figure 5.1. Proportion of controls with at least one meaningful connection between each ROI for each frequency band. 98

Figure 5.2. Functional connectivity between regions within the DMN between responsive and unresponsive patients. 101

Figure 6.1. Study 2 consisted of 4 blocks of alternating imagery and music trials, where imagery trials also alternated between auditory (“Birthday”) and visual-spatial (“Room”) trials. 109

Figure 6.2. Clusters with at least 10 Active and 10 Passive ICs. 115

Figure 6.3. The proportion of controls with alpha suppression in each ROI. 118

Figure 6.4. The proportion of patients with alpha suppression in each ROI. 123

Figure 6.5. The proportion of participants with at least one IC with sustained alpha suppression in frontal and posterio-parietal ROIs. 124

Figure 7.1. Comparison of within-network (VAN, DAN, ODD) and between-network (VANDAN, VANODD, DANODD) connectivity for all patient groups reported in Chapter 4.139

List of Acronyms

Acronym	Definition
ACC	Anterior Cingulate Cortex
ANOVA	Analysis of Variance
BA	Brodmann Area
BOLD	Blood Oxygen Level Dependent
DAN	Dorsal Attention Network
DMN	Default Mode Network
dMPFC	Dorso-Medial Prefrontal Cortex
DOC	Disorder of Consciousness
EEG	Electroencephalogram
EMG	Electromyogram
ERD	Event-Related Desynchronization
ERP	Event-Related Potential
ERS	Event-Related Synchronization
ERSP	Event-Related Spectral Perturbation
fMRI	Functional Magnetic Resonance Imaging
IC	Independent Component
ICA	Independent Component Analysis
IFC	Inferior Frontal Cortex
IFG	Inferior Frontal Gyrus
IPL	Inferior Parietal Lobule
MCS	Minimally Conscious State
MFG	Medial Frontal Gyrus
MMN	Mismatch Negativity
MNI	Montreal Neurological Institute
NCC	Neural Correlates of Consciousness
NDE	Near-Death Experience
ODD	Oddball Network
OFC	Orbito-Frontal Cortex
PCC	Posterior Cingulate Cortex
PCU	Precuneus
PLV	Phase-Locking Value
PO	Per Os
PPAF	Percentage of Power Accounted For
PreCG	PreCentral Gyrus
PVAF	Percentage of Variance Accounted For
REM	Rapid Eye Movement
ROI	Region of Interest
RT	Reaction Time
SMA	Supplementary Motor Area
SNR	Signal to Noise Ratio
SOA	Stimulus Onsert Asynchrony

SON	Subject's Own Name
SPC	Superior Parietal Cortex
STG	Superior Temporal Gyrus
TBI	Traumatic Brain Injury
TPJ	Temporo-Parietal Junction
UWS	Unresponsive Wakefulness Syndrome
VAN	Ventral Attention Network
vMPFC	Ventro-Medial Prefrontal Cortex
VS	Vegetative State

List of Abbreviations

Abbreviation	Definition
Aud	Auditory Cortex
Cing	Cingulate Cortex
Ins	Insula
Mtr	Motor Cortex
Occ	Occipital Cortex
Par	Parietal Cortex
SUBCUT	Subcutaneous
Vis	Visual Cortex

Acknowledgements

Thanks to Tricia Sernande, Yana Pertels, Naima Mansuri, Brittney Mallet, Bridget Gallagher, Carolina Daffara, and Will Alvarez for assisting with data collection and analysis. Thanks to St. John Hospice staff for their support of this project, and to Dr. Romayne Gallagher for making the collaboration with the hospice possible. Thanks to Dr. Todd Handy and Diana Pricop for generously providing the control data for Chapter 5.

Thanks to Yvette, Anna, Trish, Natasha, Nick, Sam, Julia, and Rebecca for their emotional support. Thanks to my mom for (literally) going through this process alongside me. Thanks to my dad for paving the way.

Thanks to Dr. Lawrence Ward for his guidance over the past 10 years. I couldn't have asked for a better mentor and friend. Thanks for making me the best scientist I can be. And thanks for believing in me.

Thanks to Jesse for being my biggest fan, and for never letting me doubt myself for too long. I could not have done this without you.

And finally, thanks to the hospice patients and their loved ones for donating some of the most precious hours of their lives to the collection of these data. They gave me an invaluable gift, for which I am deeply grateful.

This work was supported by the Natural Sciences and Engineering Research Council of Canada and the University of British Columbia.

Dedication

This is for the patients and their loved ones.

Chapter 1: Introduction

In the last hours before an expected, natural death, many people enter a period of unresponsiveness, during which they no longer respond to their environment. This can be a profound and spiritual time for families, as it is currently unknown whether unresponsive patients are aware of the touch or words of their loved ones. There is a persistent belief, however, that some unresponsive patients may still be aware of touch and sound (Tapson et al., 2015), despite being unable to reliably indicate their awareness. Much of this belief comes from reports of near-death experiences (NDEs), where a common recurring element of this experience is hearing unusual noises or hearing oneself pronounced dead (French, 2005; Greyson, 2000; Parnia & Fenwick, 2002). Reports from NDEs, however, are difficult to interpret, because incidence of NDEs is low, between 6% (Parnia et al., 2001) and 12% (van Lommel et al., 2001) of cardiac arrest survivors, and the cognitive neuroscience underlying NDEs remains both poorly understood and hotly debated (Charland-Verville et al., 2014; Facco & Agrillo, 2012; Greyson et al., 2012; Lake, 2017; Mobbs & Watt, 2011; Thonnard et al., 2013). Further perpetuating the belief that "hearing is the last to go" are some family members and health care providers who have reported that unresponsive patients will occasionally groan or make a small facial movement in response to hearing a familiar voice, but there is no systematic empirical evidence to corroborate these anecdotes (Villanueva, 1999).

1.1 Is it possible for a dying brain to sustain awareness?

Neuroprotective mechanisms, mainly the blood-brain barrier, reduce neuronal firing in response to ischemia (a common physiological cause of unresponsiveness at the end of life), which could protect the brain from irreversible brain damage under these conditions (Raichle, 1983). The brain's tolerance to ischemia has been demonstrated in autopsy, as only about 60% of

patients who had been declared brain dead before death showed signs of moderate to severe cortical ischemia, and only about 30% in deep brain structures such as the thalamus and basal ganglia, and a similar percentage in the cerebellum (Wijdicks & Pfeifer, 2008) (see also the following responses: Evans, 2009; Machado & Korein, 2009). The brain, therefore, may be somewhat resistant to the effects of ischemic damage while the rest of the body shuts down just before death. In addition, opioids can reduce behavioural responses to external stimulation, without necessarily reducing awareness (Rady & Verheijde, 2016). Pain and shortness of breath are common symptoms among the physiological changes that occur at the end of life (Kehl & Kowalkowski, 2013; Singer et al., 1999; Solano et al., 2006), and are frequently controlled with opioids (Chou et al., 2009; Fainsinger et al., 1991; Qaseem et al., 2008). Patients who are being treated for pain with opioid medications could, therefore, become less responsive to their external environment as they enter the final stage of dying, but may retain some covert awareness. Finally, a surge of cortical gamma power and connectivity is present in the rat brain for 30 seconds immediately following cardiac arrest (Borjigin et al., 2013) (see also the following response: Greyson et al., 2013). Because synchronous gamma oscillations have been linked to conscious cognitive processing in humans (Doesburg et al., 2009, 2012; Fries, 2009; Rodriguez et al., 1999; Sanders et al., 2012), increased gamma synchrony could generate an NDE immediately after cardiac arrest (this interpretation is, however, debated) (Greyson et al., 2013). Although these studies point to the potential for awareness in the dying brain, they speak to neurophysiological states after sudden cardiac arrest, and may not be generalizable to the period of unresponsiveness that can occur before death from other “natural” causes. In a scoping review of 39 human and animal studies investigating brain activity in the period before cardiac arrest, Pana et al. (2016) found that “[t]here are no studies describing clinical brain function in

the context of progressive hypoxia or ischemia leading to circulatory arrest (pg 79)". While there is some, but limited, physiological and anecdotal evidence to support the assertion that "hearing is the last to go", the capacity for awareness during the unresponsive period leading to a "natural" death remains unknown.

1.2 How can we assess awareness of unresponsive patients at the end of life?

The standard clinical neurologist's method of measuring consciousness is to evaluate brain function indirectly by observing behavioural responses to physical stimulation and verbal command (Giacino et al., 2009; Seel et al., 2010). Example assessment behaviours include eye opening (arousal/vigilance), visual pursuit (visual functioning), and response to verbal request (auditory and language functioning) (Giacino et al., 2004, 2009). Among TBI patients, however, behavioural signs of consciousness can be difficult to detect because such behaviours are often "impaired, inconsistent, or easily fatigued" (Giacino et al., 2009, p. 34) (see also Wannez et al., 2017). There has been growing concern, therefore, that assessment of consciousness (and subsequent prognosis) among TBI patients using *only* behavioural measures is disturbingly inaccurate (Casali et al., 2013; Di Perri et al., 2016; Fingelkurts et al., 2013; Giacino et al., 2014; Lutkenhoff et al., 2015; Naccache, 2018; Noirhomme et al., 2014; Owen, 2013), with misdiagnosis rates estimated at up to 43% (Andrews et al., 1996; Childs et al., 1993; Schnakers et al., 2009; Tresch et al., 1991). Recently, some patients with disorders of consciousness (DOC) (who were diagnosed using conventional behavioural measures) have shown signs of residual cognitive function by means of neuroimaging (Bekinschtein et al., 2009; Cruse et al., 2011, 2012; Fernández-Espejo & Owen, 2013; Goldfine et al., 2013; Laureys, 2005; Owen et al., 2006). Neuroimaging methods of consciousness assessment more directly evaluate brain function by observing *neural* responses to verbal command (Blume et al., 2015; Di Perri et al.,

2014; Giacino et al., 2014; Gibson et al., 2014; Hannawi et al., 2015; Lemaire et al., 2014; Owen, 2013, 2014; Stender et al., 2014). For example, in a seminal fMRI study, one DOC patient, who had not previously demonstrated any behavioural signs of awareness of her environment, showed patterns of BOLD activation consistent with neurotypical controls when she was asked to engage in motor and visual-spatial mental imagery (Owen et al., 2006). This was the first demonstration of possible covert awareness among behaviourally unresponsive TBI patients (Owen et al., 2007). Subsequent studies have uncovered neural signs of covert awareness among DOC patients using fMRI (Coleman et al., 2007; Fernández-Espejo et al., 2014; Fernández-Espejo & Owen, 2013; Martin M. Monti et al., 2010), EEG (Bekinschtein et al., 2009; Curley et al., 2018; Gibson et al., 2016; Peterson et al., 2013), and PET (Boly, Faymonville, et al., 2008; Laureys et al., 1999; Owen et al., 2005). Neuroimaging is a useful tool to assess awareness among behaviourally unresponsive TBI patients (H. Di et al., 2008; Gibson et al., 2014; Laureys, 2005; M. M. Monti et al., 2009; Owen & Coleman, 2008), the application of which could be extended to unresponsive patients at the end of life.

1.3 What are some possible neural signatures of awareness?

Because the neural correlates of consciousness (NCC) are still unknown (see Koch et al., 2016 for a recent review), there is no way to directly measure awareness from an unresponsive patient. Much like behavioural methods of awareness assessment, neuroimaging can, instead, detect neural responses to stimulation and verbal command that indirectly demonstrate awareness. For example, when a conscious neurotypical person detects a deviation in an auditory regularity, their brain generates electrophysiological signals, such as event-related potentials (ERPs), that are associated with different aspects of conscious auditory processing. Some of these aspects include detection of the deviation by auditory cortex (as measured with the

mismatch negativity, MMN) (Näätänen et al., 2007), exogenous attention orienting toward the deviation (the P3a) (Polich, 2007), and memory processes associated with detection of the deviation (P3b) (Polich, 2007). Each of these responses has been used to assess the capacity for information processing among DOC patients (Bekinschtein et al., 2009; Boly et al., 2011; Fischer et al., 2010, 2010; King et al., 2011; Kotchoubey et al., 2005; Laureys et al., 2005; Morlet & Fischer, 2014; Perrin et al., 2006; Rappaport et al., 1991; Real et al., 2016; Schiff & Plum, 1999; Sharova et al., 1998; Vanhaudenhuyse et al., 2008), and successful measurement of these ERPs predicts better recovery from TBI (Cavinato et al., 2009; Gott et al., 1991; Wijnen et al., 2007). The P3b is the only such ERP that appears to be generated exclusively in the context of *conscious* detection of a target stimulus, as it is only elicited in active search conditions (i.e. the participant is asked to search for the target deviation) and not when the stimulus is ignored, nor to non-target distractors (Katayama & Polich, 1998; Polich, 2007; Polich & McIsaac, 1994; Wronka et al., 2008), and rarely in states of low arousal such as during sleep (Atienza et al., 2001; Chennu & Bekinschtein, 2012; Cote, 2002) or sedation (Heinke & Koelsch, 2005; J.-W. Kim et al., 2019; Koelsch et al., 2006; Nourski et al., 2018; Plourde & Boylan, 1991). Notable exceptions include during REM sleep (Cote, 2002), and during “passive” conditions (i.e. participants are asked to ignore the target) when the target stimulus is the subject’s own name (Eichenlaub et al., 2012; Holeckova et al., 2006, 2008). There is a general consensus, therefore, that if an unresponsive participant generates a P3b to an auditory deviant, they are presumed to have been aware of that deviant (Chennu & Bekinschtein, 2012).

On the other hand, should an unresponsive participant not generate a P3b, or any similar electrophysiological signal measured at the scalp, this does not necessarily indicate that the patient was unaware of the auditory irregularity. To generate an ERP, multiple neural regions

must be functionally connected, over multiple trials, to produce measurable neural responses that can indicate awareness (Bressler, 1995; Goldman-Rakic, 1988; Hipp et al., 2011; Palva & Palva, 2011; Siegel et al., 2012; Sporns, 2002). Depending on the location and severity of a patient's brain injury, reduced cortical activity in key regions underlying the ERP could prevent a patient from generating a measurable response, while isolated functional networks may be preserved elsewhere in the brain (Schiff et al., 2002). In the case of unresponsive patients at the end of life, decreased overall metabolic activity and the psychoactive effects of pain medications, such as benzodiazepines or opioids, may suppress electrophysiological signals such that they become difficult to detect (Engelhardt et al., 1992; Jääskeläinen et al., 1999; Kivisaari et al., 2007; Milligan et al., 1989; Polich & Criado, 2006; Rockstroh et al., 1991). While evidence of certain electrophysiological signals among unresponsive patients may be sufficient to assume awareness, a lack of evidence of such signals is not sufficient to assume unawareness (Peterson et al., 2013). A more thorough characterization of the spatiotemporal neural dynamics underlying electrophysiological signals detected at the scalp would benefit the development of a more specific measurement of consciousness.

Implicit in the previous discussion is that behavioural and ERP measures of consciousness only evaluate whether an unresponsive patient is capable of conscious *externally*-oriented cognition, i.e. whether an unresponsive patient is aware of physical touch or sound. There is growing evidence, however, that altered activity within the default mode network (DMN) (Raichle, 1983), which is associated with *internally*-oriented thought (Buckner et al., 2008a), is correlated with reduced levels of consciousness (Boly, Phillips, et al., 2008; J. S. Crone et al., 2011, 2015; Danielson et al., 2011; Deshpande et al., 2010; Fernández-Espejo et al., 2012; Greicius et al., 2008; Horovitz et al., 2009; Vanhaudenhuyse et al., 2010). The DMN

consists of medial frontal and parietal regions that are preferentially active during states of rest compared to when participants are asked to perform attention-demanding tasks (Andrews-Hanna et al., 2010; Buckner et al., 2008a; Raichle et al., 2001). The contents of conscious thought that are associated with DMN activation include (but are not limited to) mind-wandering (Christoff et al., 2016), autobiographical planning (Spreng et al., 2008) and scene construction (Hassabis & Maguire, 2007). Reduced DMN activity has been detected in states of low arousal, such as deep sleep (Horovitz et al., 2009), light sedation (Greicius et al., 2008) and anesthesia (Deshpande et al., 2010), unconsciousness due to epileptic seizure (Danielson et al., 2011), and among DOC patients (Cauda et al., 2009; J. S. Crone et al., 2011, 2015), and in states of reduced self-awareness such as hypnosis (Demertzi et al., 2011), and meditation (Garrison et al., 2015). Although the precise relationship between DMN activation and/or connectivity and internally-oriented mental activity is currently unknown (c.f. Gerlach et al., 2014; Hassabis & Maguire, 2007; Schacter et al., 2012), functionally-connected cortical activity within DMN may be a necessary, if not sufficient, property of consciousness (Boly, Phillips, et al., 2008). Regardless, an analysis of activation within the DMN among unresponsive patients may be a beneficial complement to any neuroimaging method of awareness assessment, as diagnosis of DOC patients is improved by incorporating multiple EEG measures (Rossi Sebastiano et al., 2015).

1.4 Overview of electrophysiological measures used to assess awareness

The experiments described in this dissertation involve several different electrophysiological measures that are used to characterize cognitive function. Each of these measures can tell us different information pertaining to cognitive processing and will be briefly described here as they pertain to assessment of awareness.

1.4.1 Event-related potentials (ERPs)

Event-related potentials (and evoked potentials) are neural signals measured at scalp electrodes (Paul Sauseng et al., 2007; Tallon-Baudry & Bertrand, 1999). They represent the average cortical response that is time-locked to an event or stimulus. Because cortical responses have very low amplitude and are embedded in noise, ERPs are generated by averaging channel EEG over many trials to enhance the signal to noise ratio of the response. Averaging over many trials reduces noise while preserving the signal, as oscillations that are out of phase with one another will cancel each other out when averaged, but phase-locked signals will remain.

1.4.2 Event-related spectral perturbations (ERSPs)

ERSPs are the time-frequency decomposition of neural signals measured either at the electrode or at the source level (David et al., 2006; Pfurtscheller & Lopes da Silva, 1999; Tallon-Baudry & Bertrand, 1999). They represent the average cortical response that is *not* phase-locked to the stimulus (also called induced responses). ERSPs are generated by first computing time-frequency power for each trial, then averaging across trials. They may represent so-called 'higher order cognitive processes' that are not entrained by the presentation of a stimulus, such as object representation (Tallon-Baudry & Bertrand, 1999), maintenance of a current sensorimotor state (Engel & Fries, 2010), selective attention (Klimesch, 2012), or memory processes (Buzsáki, 2002).

1.4.3 Phase-locking values (PLVs)

PLVs, conceptually, represent the degree to which the phase difference between two neural signals are constant over time (Lachaux et al., 1999). This is often referred to as "phase locking". They are a measure of functional connectivity between two neural signals and are used as a measure of long-range neural communication.

1.5 Dissertation summary

This dissertation consists of attempts to measure awareness among unresponsive patients at the end of their lives. I measured EEG activity from both conscious neurotypical participants and from hospice patients (both when they were responsive and again when they became unresponsive) both at rest and in response to auditory stimulation. The primary objective of this research was to uncover any evidence of cortical activity among unresponsive patients that could indicate conscious auditory processing (Chapters 3, 4, and 6), or stimulus-independent thought (Chapter 5). A secondary objective was to describe the differences in spatio-temporal network activity underlying potential biomarkers of awareness (P3a, P3b, DMN) between responsive participants (both neurotypical and responsive hospice patients) and unresponsive patients.

Chapter 2 characterizes the neural networks underlying some ERPs (P3a & P3b) that have previously been used to assess awareness among unresponsive patients with traumatic brain injury. This chapter includes group-level analyses of neurotypical P3a and P3b responses. Based on previous research, both on the neural source(s) of the P3a and fMRI work on attention networks, my initial hypothesis was that the spatio-temporal dynamics underlying the P3a would reflect fast cortical activation within neural networks associated with attention orienting to highly salient stimulus features, such as the ventral attention (Corbetta & Shulman, 2002) and salience networks (Seeley et al., 2007). By contrast, and similarly based on previous research, I expected that the P3b would be associated with slower cortical activation within networks associated with maintaining target features in memory and context updating, such as the dorsal attention network (Corbetta & Shulman, 2002).

Chapter 3 reports evidence of auditory cortical processing (Näätänen et al., 2007) among all unresponsive patients, and attention orienting or context updating (Polich, 2007) among some

unresponsive patients. My initial hypotheses were that hospice patients would exhibit neurotypical auditory cortical processing and attention mechanisms when they were responsive, albeit with longer P300 ERP latencies compared to controls. I also expected that unresponsive hospice patients would generate neurotypical MMN responses to auditory irregularities, as the MMN is widely considered “preconscious” (Näätänen et al., 2007).

Chapter 4 describes individualized network dynamics underlying the P3a and P3b subcomponents among neurotypical control and hospice patients. I expected that most participants who exhibited evidence of a P3a would have cortical activity localized to regions within the ventral attention network and show patterns of local power and connectivity within those regions indicative of exogenous attention orienting to highly salient features. By contrast, I expected that most participants who exhibited a P3b would have neural sources, local power, and connectivity within the dorsal attention network. The analyses from Chapter 2 inform those of Chapter 4.

Chapter 5 characterizes functional connectivity within the default-mode network (DMN) among neurotypical control participants, and both responsive and unresponsive hospice patients, during a period of rest (Buckner et al., 2008a; Christoff et al., 2016; Raichle et al., 2001; Smallwood et al., 2012). I expected that responsive patients would show neurotypical levels of connectivity, and that unresponsive patients, similarly to DOC patients, would show reduced connectivity, within DMN (Laureys et al., 2005; Vanhaudenhuyse et al., 2010).

Chapter 6 reports exploratory analyses of neural power underlying active and passive music listening among neurotypical and hospice patients. These data were from an active listening task initially intended to be a distractor in an EEG adaptation of a mental imagery paradigm (not reported in this dissertation) previously used to assess awareness among DOC

patients (Owen et al., 2006, 2007). I, therefore, had no specific a priori hypotheses associated with this experiment, although I did expect to detect evidence of music processing among some unresponsive patients. While the study of music as a diagnostic or therapeutic tool for use among DOC patients is still in its infancy (Magee et al., 2016; O'Kelly et al., 2013; Okumura et al., 2014; Rollnik & Altenmüller, 2014; Varotto et al., 2012), some DOC patients have shown evidence of music processing (Castro et al., 2015; Heine et al., 2015; O'Kelly et al., 2013), although the results are mixed and have only been studied in the context of passive music listening. To my knowledge, this experiment represents a novel approach to evaluating attention and awareness among behaviourally unresponsive patients.

Chapter 7 summarizes the main results and discusses their implications for our current understanding of cognition and consciousness in people with DOC and for future research in this area. This work is a first attempt to describe changes in cortical activity in the dying brain, and whether such activity supports consciousness. Because this work represents one of very few attempts to record EEG data in a hospice setting (c.f. Droney & Hall, 2008), I also provide some recommendations for how awareness can be measured in a manner that is consistent with the goals and values of palliative care providers.

Chapter 2: Spatiotemporal neural dynamics underlying the P3a and P3b among neurotypical control participants.

In this chapter I characterize the neurotypical spatio-temporal dynamics underlying two subcomponents of the P300, the P3a and the P3b, which are potential biomarkers of conscious awareness among behaviourally unresponsive patients (Bekinschtein et al., 2009; Kotchoubey et al., 2005; Laureys et al., 2005; Pan et al., 2014; Real et al., 2016). The paradigm involves a conceptual replication of a study that has demonstrated evidence of command following in individual neurotypical control participants and minimally conscious patients, but not unresponsive wakeful patients (Bekinschtein et al., 2009) (see Chapter 3 for a more thorough discussion of the results of the original study). In this study all participants listened to oddball sequences, where stimuli consisted of two different types of five-tone auditory patterns: “change runs”, which contained a frequency deviant, and “flat runs”, which did not (see Materials and Methods; see also Figure 2.1). In half the oddball sequences, flat runs were common and change runs were rare targets, and in the other half change runs were common and flat runs were rare targets. Whereas in the original study all target runs were treated as equivalent, in a previous study I show that neurotypical behavioural and ERP responses to target change runs were different from those to target flat runs (Blundon et al., 2017). Reaction times and P300 latencies to target change runs were significantly shorter than those to target flat runs. Moreover, scalp topography of P300 responses to target change runs indicated significant contribution of both P3a and P3b subcomponents, whereas scalp topography of P300s to target flat runs only indicated the P3b. I interpreted this discrepancy as an indication that participants were employing different search strategies to identify each of the targets. As the P3a is typically associated with exogenous attention orienting to highly salient, infrequent stimuli (Polich, 2007), the P3a

response to target change runs indicated that the frequency deviant contained within the change runs was essentially “popping out” to participants, implying a passive or diffuse search strategy. In contrast, the flat runs, which did not contain a frequency deviant, did not generate a P3a, implying that participants were not using a passive search strategy to identify flat targets. This asymmetry bore a striking resemblance to visual search asymmetry (Treisman & Souther, 1985), wherein search for a target that differs from distractors in some simple feature, as for example Q differs from a field of Os, participants are quicker to identify the target, and P300 latencies are faster (Luck & Hillyard, 1994), than if participants search for the converse, an O in a field of Qs. Borrowing from the search-asymmetry nomenclature, search for a feature-present target (which are the change runs in the present experiment) may initially recruit exogenous attention processes to detect the salient feature, whereas search for feature-absent targets (flat runs) would not. I reasoned that a more thorough analysis of the EEG results, in which I infer neural sources from scalp data, and perform time-frequency and functional connectivity analyses on these source activations, would reveal more clearly which brain networks were activated, and how they communicated, during the different types of search task.

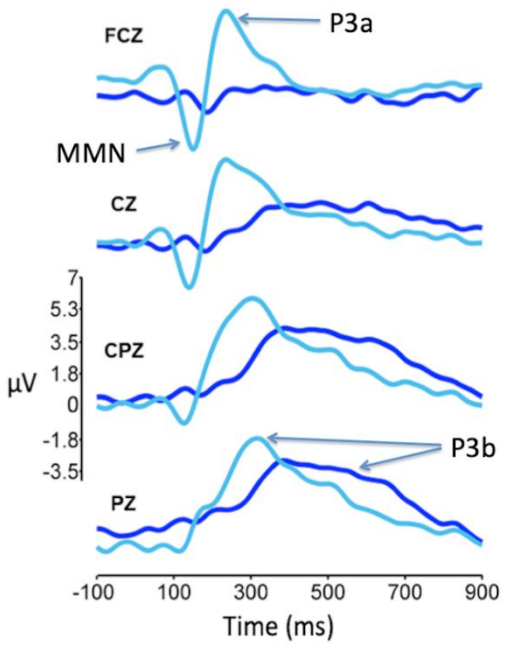

Figure 2.1. Midline ERPs to tone change and pattern change runs.

Tone changes in light blue, pattern changes in dark blue. P3a is typically maximal over central electrodes (FCZ and CZ), and peaks approximately 200-300 ms post stimulus. The P3b is typically maximal over parietal electrodes (CPZ and PZ), and peaks approximately 300 ms post stimulus (Polich, 2007); ERP data from (Blundon, Rumak, & Ward, 2017).

My reasoning is based on the extensive literature that shows a strong association between neural oscillations in specific frequency bands, stimulus processing, and attention orienting. It has been shown repeatedly that the onset of a stimulus not only evokes ERPs, but also induces bursts of oscillatory power (event-related synchronization, ERS), in the relevant sensory cortex, that often persist for hundreds of milliseconds (see the following for reviews: Doesburg et al., 2015; Palva & Palva, 2011; Varela et al., 2001). These bursts of power occur in specific frequency bands, especially theta (4-8 Hz) and so-called low gamma (30-50 Hz). Importantly, a decrease of power in the alpha band (8-14 Hz), or event-related desynchronization (ERD) usually accompanies the ERS in the other bands. Moreover, alpha-band ERD also occurs, before a visual

stimulus is presented, over visual sensory areas (occipital cortex) responsive to the part of visual space where the stimulus is expected to occur, implicating this oscillatory activity in attention orienting (Doesburg et al., 2008, 2009; Rihs et al., 2007; Worden et al., 2000). Functional connectivity in these frequency bands, measured by phase-locking analysis or in other ways, has been associated both with stimulus processing and with attention orienting (Doesburg et al., 2008, e.g. 2009) (see the following for reviews: Palva, 2016; Palva & Palva, 2011; Varela et al., 2001). Briefly, it has been proposed that information exchange between spatially-separated regions of the brain networks underlying perceptual and cognitive processes is enabled by synchronization of neural oscillations generated within each separate region (e.g. Fries, 2005; Varela et al., 2001). Phase synchronization is a measure of functional connectivity, where functional connectivity is construed to mean information exchange that informs perceptual and cognitive processing (e.g. Lachaux et al., 1999). Specifically relevant to the present work, functional connectivity between brain regions, measured by phase synchronization in theta, alpha, and gamma frequency bands, has been closely associated with attention orienting (Doesburg et al., 2008, 2009; Ribary et al., 2017). Until now, however, oscillatory power and functional connectivity associated with scalp EEG measurements have not been specifically characterized within the attention networks identified through fMRI brain imaging. In this chapter I describe such an analysis aimed at delineating the neural activity underlying the subcomponents of the P300 ERP, the P3a and the P3b, in relation to processing of auditory oddball stimuli in the serial search asymmetry context.

The neural generators of the P3a ERP are most likely frontal regions (Bledowski et al., 2004; Polich, 2007; Wronka et al., 2012) within the Ventral Attention Network (VAN), which is associated with stimulus-driven task-relevant search (Corbetta et al., 2002, 2008; Corbetta &

Shulman, 2002). P3b neural generators, by contrast, are likely parietal regions (Bledowski et al., 2004; Polich, 2007; Wronka et al., 2012) within the Dorsal Attention Network (DAN), which is associated with voluntary (endogenous) orienting of attention and maintaining attentional sets (Corbetta et al., 2002, 2008; Corbetta & Shulman, 2002). In addition, many parietal regions outside the DAN, such as the posterior cingulate cortex and visual cortex, have been associated with the P3b response to oddball target detection (see H. Kim, 2014 for a meta-analysis).

The time course of power fluctuations measured at scalp electrodes associated with the P300 has been well-documented. Even though the P300 response is maximal over parietal electrodes, it is preceded by theta and low alpha (8-10Hz) ERS that is maximal over frontal electrodes (Klimesch et al., 1998; Kolev et al., 1997; Missonnier et al., 2006; Yordanova et al., 2001; Yordanova & Kolev, 1998a, 1998b). These low frequency ERS bursts typically occur immediately after stimulus onset, and last until approximately the onset of the P300 (and can persist throughout the P300 timeframe) (see Bernat et al., 2007). Early frontal electrode low frequency ERS is sensitive to task demands and stimulus context (Klimesch, 2012). For example, pre-P300 theta ERS is also generated by single tones during a passive listening task. These tones do not generate a P300 response, but nonetheless pre-P300 theta ERS persists longer in response to oddball tones than to standards (Yordanova & Kolev, 1998a). Furthermore, whereas the time course and scalp topography of slow oscillations associated with the P300 are similar for both P3a and P3b subcomponents, the amplitude of theta ERS preceding the P3a is larger for more novel distractor stimuli (Demiralp et al., 2001). The amplitude and duration of low frequency ERS are, therefore, modulated by the attentional “state” of participants, as well as the novelty of the stimulus itself. To my knowledge, however, the neural generators of pre-P300 low frequency

ERS are currently unknown, though considering its scalp topography it is most likely generated in frontal regions for both P3a and P3b.

The P300 is also followed by alpha-band ERD that is maximal over posterior electrodes (Klimesch et al., 1998; Missonnier et al., 2006; Yordanova et al., 2001; Yordanova & Kolev, 1998b). As I am primarily interested in exploring the network dynamics underlying the generation of the P300, post-P300 alpha ERD is beyond the scope of this chapter (though it will be discussed in Chapter 6) (see Klimesch, 2012 for a review; see also Klimesch et al., 1998; Peng et al., 2012; Yordanova et al., 2001).

Like the low frequency oscillations, fronto-central gamma-band ERS is typically observed shortly after target onset (Başar et al., 2015; Fell et al., 1997; Gurtubay et al., 2001, 2004; Marshall et al., 1996), followed by gamma-band ERD during the P300 timeframe (though Gurtubay et al (2001) and (2004) observed gamma-band ERS during the P300 timeframe). Gamma-band oscillations associated with the P300 have been localized to frontal regions, such as the ACC, inferior and superior frontal gyri, and SMA, for both P3a and P3b subcomponents (B. Lee et al., 2007). To my knowledge, any differences in the time course of gamma oscillations between P3a and P3b subcomponents, either at the scalp or at the source level, have not been reported. Because gamma-band oscillations are associated with maintenance of short-term and working memory (Jensen et al., 2007) as well as selective attention (Fell et al., 2003), gamma ERD may represent a disruption in the maintenance of an attentional set, triggered by the oddball stimulus (Jensen et al., 2007; Marshall et al., 1996). Finally, the timecourse of beta-band oscillations associated with the P300 have not been well-documented, nor is the beta-band's role in attention well-understood (Engel & Fries, 2010; Wróbel, 2000). There is some evidence, however, that beta-band oscillations may be involved in maintenance of a current attentional

state, and that beta power is modulated by whether or not a participant is anticipating a change in their environment (Engel & Fries, 2010). Beta band desynchronization is also involved in generating small motor movements (Alegre et al., 2002) and motor imagery (McFarland et al., 2000), which is relevant to oddball paradigms such as this one, where participants are required to generate a behavioural response to targets.

The P300 response to oddball targets is also accompanied by an increase in functional connectivity between electrodes underlying the P300 (Giani et al., 2015; Güntekin & Başar, 2010; Kabbara et al., 2016; Karamzadeh et al., 2013; Peng et al., 2012) . Greater overall connectivity (between all electrodes) is associated with oddball targets compared to standards, and that connectivity peaks around the P300 timeframe (Kabbara et al., 2016). Phase coherence is strongest between frontal, parietal, and temporal electrodes for the P3b response (Giani et al., 2015; Güntekin & Başar, 2010), and between frontal and central electrodes for the P3a (Karamzadeh et al., 2013; Li et al., 2016). Li and colleagues (2016) found not only overall greater inter-electrode connectivity to targets than to standards associated with the P3a response, they also showed how the central nodes of that connectivity shift from temporal electrodes before the P3a, to central and frontal electrodes around the P3a latency. To my knowledge, however, a similar analysis has not been performed on the P3b subcomponent, nor has such a detailed time course of connectivity been described at the neural source level for either subcomponent.

Thus, in what follows, I report further analyses of high-density EEG from Experiment 1 of Blundon et al. (2017) to characterize the functional dynamics underlying the P3a and P3b subcomponents to feature-present and feature-absent targets within a serial auditory search paradigm. I emphasize that these are the first analyses, to my knowledge, of the neural dynamics

underpinning a *target-elicited* P3a ERP subcomponent, and of its role in facilitating responses in a search asymmetry context. While the P3a is typically measured in response to *task-irrelevant* salient stimuli, all P300 ERPs are likely comprised of a combination of P3a and P3b subcomponents, and the contribution of either depends on stimulus features and task demands (Polich & Criado, 2006). In addition, this is the first time, to my knowledge, that EEG-based time-frequency and functional connectivity analyses have been conducted for neural sources inferred to be within fMRI-identified attention networks in the brain.

First, I used independent component analysis (ICA) to locate single equivalent-current dipole sources corresponding to regions of interest (ROIs) that were active during the auditory oddball task. I expected that ROIs would correspond to neural regions commonly associated with the P3a and P3b subcomponents, namely frontal and parietal regions associated with the ventral and dorsal attention networks, as well as regions that have been associated with detecting auditory oddball stimuli (see H. Kim, 2014 for a meta-analysis; see also Polich, 2007). Second, each ROI was "projected" to midline scalp electrodes (where the P3a and P3b are maximal) using channel weights determined by the ICA decomposition. The contribution of each of these ROIs to the P3a and P3b subcomponents was determined by comparing the scalp power of the ROI ERP "projections" to the scalp power of the P300 subcomponents measured directly from those same electrodes. Consistent with EEG scalp recordings, I expected that projections from frontal ROIs would account for more of the scalp power of the P3a subcomponent than would projections from parietal regions, and the reverse would be true for the P3b subcomponent. Third, a time-frequency analysis of the IC activations corresponding to each ROI was performed for the 500 ms after the final tone of both feature-present and feature-absent rare and common runs. These event-related spectral perturbations (ERSPs) characterise the fluctuations in power at

each frequency band in response to the auditory stimuli. Consistent with the literature reviewed earlier, I expected to see greater power in sources associated with the VAN in the P3a timeframe (approximately 100-300 ms after the feature-present targets), and greater power in sources associated with the DAN and other regions sensitive to oddball detection in the P3b timeframe (approximately 200-500 ms after either feature-present or feature-absent targets). Finally, the degree of functional connectivity at different frequency bands between ROIs in the several networks was determined using a phase synchrony analysis. Again, consistent with the literature reviewed earlier, I expected that regions in both VAN and DAN would be functionally connected when participants identified feature-present targets, whereas only regions in the DAN and other oddball-sensitive regions would be functionally connected when participants identified feature-absent targets.

2.1 Materials and Methods

Some of the following descriptions of the materials and methods, including ethics statement, description of participants, stimuli, procedure, EEG recording, and EEG preprocessing, are identical to those detailed in the published article that describes the ERP analysis component of this study (Blundon et al., 2017). The remainder are unique to the present neural network source analyses of those data.

2.1.1 Ethics Statement

All aspects of the experimental protocol, including the recruitment and consent procedures, were approved by the University of British Columbia Behavioural Research Ethics Board in accordance with the provisions of the World Medical Association Declaration of Helsinki. All participants gave written informed consent by reading and signing the approved

consent document. Controls were offered monetary compensation ($10/hr) for their participation. This ethics statement applies to all studies that include control participants.

2.1.2 Participants

Data were collected initially from 20 participants who were recruited via the UBC Psychology Department's online experimental participant recruitment site and via a poster on the Department's participant recruitment bulletin board. From 15–25 participants has been shown in previous studies in our lab and others to yield reliable EEG data for either ERP or connectivity analyses given the numbers of stimulus trials in the study design. Data collection was stopped after the indicated number of participants had been included. Data from three participants were excluded because of excessive noise in their EEG. Thus, the analysis to be described is based on 17 participants (10 female, age 18 to 30 years, mean age 23.1 years). Participants were all right-handed and reported no hearing or neurological difficulties.

2.2 Stimuli

Stimuli consisted of 50-ms duration pure tones with 7.5 ms onset and offset ramps, using the ascending first half of a Hann window for the onset and the descending second half of the Hann for the offset, using a custom MATLAB (MathWorks, Natick USA) script. The tones were administered binaurally at 70 dB through insert earphones (EAR 3A) in a sound-attenuating chamber. Stimuli were presented and responses registered using Presentation software (Neurobehavioral Systems Berkeley CA USA). Tone runs were generated using Audacity (Sourceforge). Auditory stimuli consisted of two types of five-tone runs called flat runs and change runs (see Figure 2.2). Flat runs consisted of five pure tones of the same frequency while change runs consisted of four pure tones of the same frequency followed by a fifth tone of a different frequency. All runs contained a combination of 500-Hz and 1000-Hz tones which

generated two versions of each type of run: one in which 1000-Hz tones comprised the first four tones in a change run and all the tones in the flat run (change-down and flat-high), and the same for the 500-Hz tones (change-up and flat-low see). Successive 50-ms duration tones in a run were separated by 100 ms of silence. Each run lasted 650 ms from the onset of the first tone to the offset of the last tone. Intervals between the offset of the final tone of a given run and the onset of the first tone of the next run varied randomly from 700 ms to 1000 ms.

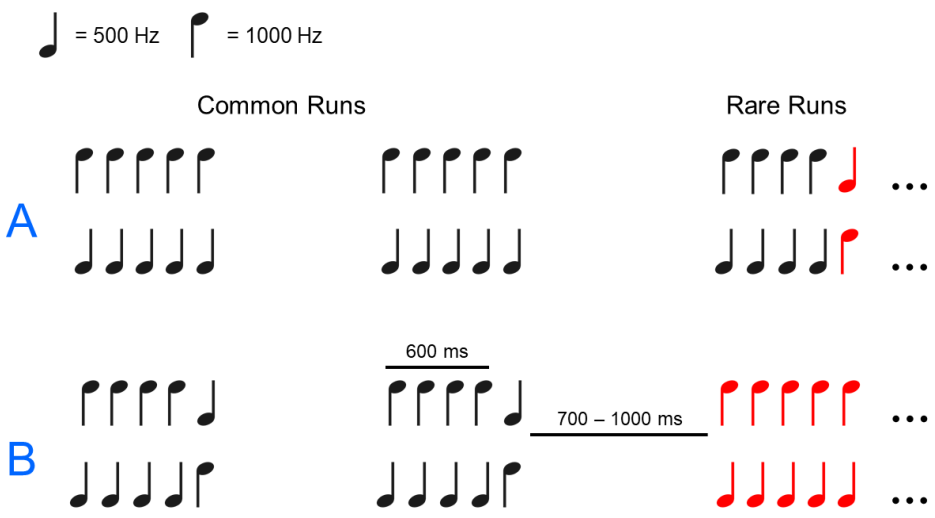

Figure 2.2. Stimuli and study design.

Stem-down notes are 1000 Hz and stem-up notes are 500 Hz. Flat runs consisted of five pure tones of the same frequency; change runs consisted of four pure tones of the same frequency followed by a fifth tone of a different frequency. Participants each heard four sequences. In two of the sequences participants were instructed to search for rare change runs among common flat runs (A), whereas in the other two sequences participants were instructed to search for rare flat runs among common change runs (B). Rare runs are targets to be detected in the longer sequence of common runs. A describes the feature-present condition, and B describes the feature-absent condition.

2.3 Procedure

Data were collected in a sound attenuating chamber located in the UBC Psychophysics and Cognitive Neuroscience Laboratory. All task instructions were presented in written format on a laptop, with simultaneous audio recordings of the instructions presented through insert-ear headphones. Each participant heard four extended oddball sequences of tone runs (about 35 mins total) in randomized order per subject (see Figure 2.3). Each sequence began with 30 instances of the common run. From then on, the rare run was presented on a random 20% of occasions among 80% common runs. In each sequence rare runs were heard between 18 and 30 times. There were always at least 2 common runs before and after each rare run. The four sequences of runs consisted of the following: (1) common flat-low, rare change-up; (2) common change-up, rare flat-low; (3) common flat-high, rare change-down; (4) common change-down, rare flat-high. Participants were instructed to click the mouse as quickly as possible to each pattern oddball (rare run) they heard during each block. It was made clear to participants that they were only to count or to respond to runs that represented a change in the global pattern, i.e. a rare run, not every time they heard a tone that differed from the previous tone.

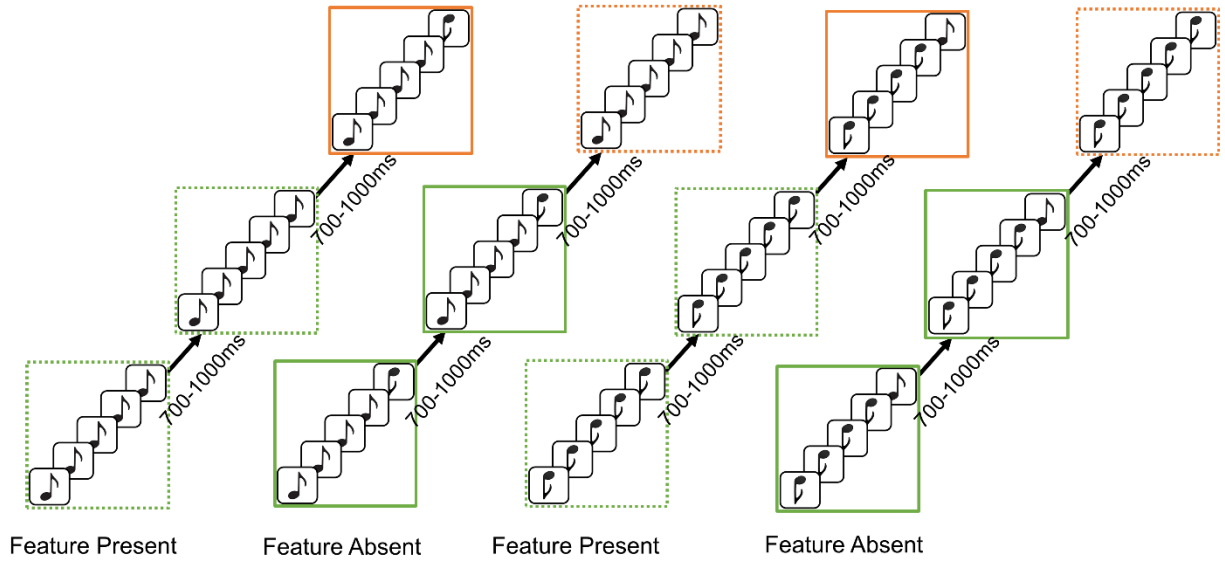

Figure 2.3. Sequence Design.

Participants each heard four sequences. In two of the sequences participants were instructed to search for rare change runs, whereas in the other two sequences participants were instructed to search for rare flat runs. Stem-down high notes are 1000 Hz and stem-up low notes are 500 Hz. Rare runs are targets to be detected in the longer sequence of common runs. Green borders are around common runs; orange borders are around rare runs. Dashed lines are around flat runs; solid lines are around change runs (reprinted with permission; Blundon, Rumak & Ward, 2017).

2.3.1 EEG recording and preprocessing

EEG signals were digitized at 500 Hz (National Instruments Inc., Vaudreuil-Dorion QC Canada) from a 60-channel electrode cap (Electrocap Inc., Eaton OH USA, International 10±10 placement) referenced to the right mastoid. Before digitization EEG signals were amplified and analog bandpass filtered from 0.1 Hz to 100 Hz (SA Instrumentation, San Diego CA USA). Eye movements were recorded with four periocular electrodes. All electrode impedances were kept below 10 kΩ (input impedance of the amplifier was > 2 gΩ)

All participant EEG data were analyzed using EEGLAB software (Delorme & Makeig, 2004). Raw data were down-sampled to 250 Hz and re-referenced to average reference. Line noise was removed online by applying a notch filter between 55 and 65Hz. Data were visually inspected for large muscle artefacts. Eye-blink and EMG artefacts were removed using ICA (see Independent Component Analysis section for a more detailed description).

2.3.2 Independent Component Analysis

What follows are descriptions of network analyses that were not part of the published ERP study (Blundon et al., 2017) and were conducted specifically to inform the present chapter. Artefact rejection, source localization, ROI to channel projections, time-frequency analysis, and functional connectivity analyses were all conducted on independent components from an infomax ICA (runica algorithm EEGLAB) (Viola et al., 2009). ICA is a machine learning method of blind source separation that, given *n* channels of EEG data, which are believed to be linear combinations of independent neural sources projected to the scalp (Delorme et al., 2012), generates *n* independent components (ICs), each of which are temporally independent, sharing minimal mutual information (see Onton et al., 2006 for a review of ICA applications to EEG data analysis). The ICs are characterized by weights for each scalp electrode (channel) that describe that IC's contribution to the recorded scalp potential. ICA has been shown to successfully isolate cortical (Bedo et al., 2014; MacLean et al., 2015; MacLean & Ward, 2014, 2016; Onton et al., 2006) and artefactual signals (Delorme et al., 2007; Jung et al., 2000) (see also Fitzgibbon et al., 2016 for a validation of the use of ICA to isolate and remove EMG contamination from EEG signals) from EEG (see again Onton et al., 2006) and fMRI (see Calhoun et al., 2009 for a review) data. In the case of EEG, ICs are also free from distortions due to volume conduction (Delorme et al., 2012).

I performed ICA on the combined EEG data from both feature-present and feature-absent conditions, rather than performing ICA on each condition separately. This strategy allows for detection of differences in the activations of, and connectivity between, neural sources that are active in both conditions, as well as allowing contrasts between sources that are predominantly active on one condition or the other. This is in contrast to the usual techniques of locating ERP sources, which attempt to find a sharp discontinuity between sources active in each experimental condition. Such techniques not only omit relevant sources that might be active in all conditions, for example those located in attention networks, but also preclude analyses of network connectivity between those sources.

2.3.3 Artefact rejection and source localization

All ICs that were classified as either eye-blinks or EMG artefacts were removed from each participants' EEG recording. The neural source of each remaining IC was localized using the EEGLAB dipfit algorithm. This algorithm estimates the location of each IC by fitting the scalp projection of a single equivalent current dipole to the pattern of scalp activity of each IC (this pattern of scalp activity is estimated from the weight matrix generated by the ICA decomposition). This means that only ICs with scalp topographies that are highly similar to those projected from a single dipole were retained for further analysis. I included only ICs with single dipole characteristics because source-estimation of a single dipole has a unique solution (as opposed to source-estimation of multiple-dipole ICs, which is an ill-posed problem; see Onton et al., 2006), and because spatially localized populations of synchronously firing neurons typically generate single-dipole-like activity (Delorme et al., 2012; Nunez, 1974; Onton et al., 2006; see also Stok, 1987). Electrode locations were co-registered to the Montreal Neurological Institute (MNI) average brain, allowing for IC sources to be visualized in brain space. ICs were only

included for further analysis if their power spectra followed a *1/f* shape (which is characteristic of a single dipole neural source), if their source was fitted to a single dipole that accounted for at least 80% of the variance of the IC's electrode weights, and if their source was localized inside of MNI brain space.

2.3.4 IC Source Clustering

The retained ICs (hereafter referred to as "valid ICs") were grouped into spatially similar clusters based on the MNI coordinate estimate of each IC's single equivalent current dipole (hereafter referred to as a valid IC's "dipole location"). Grouping of spatially similar dipoles (hereafter referred to as "clustering") was performed using a combination of the *k*-means clustering method used in EEGLAB (Delorme & Makeig, 2004), and a seed clustering algorithm developed in our lab. This seed clustering algorithm seeds centroid MNI coordinates of ROIs determined a priori, and groups ICs into ROI clusters if their dipole locations fall within a predetermined Euclidean distance (here d = 35 mm) of the cluster centroid. A distance of 35 mm is appropriate for our clustering analysis because after attempting many iterations of this seeding algorithm using different distances, it was found that smaller distances reject too many nearby ICs, and larger distances include too many ICs that fall outside the ROI Brodmann area. Seeding ROIs was applied in this case because it has been found in our lab that the clusters generated by the *k*-means algorithm can be unstable, wherein the IC composition of each cluster, or centroid location of each cluster, can change somewhat every time the *k*-means algorithm is applied to the same set of valid ICs. This is because the algorithm begins with a different random distribution of ICs into groups on each run. The seeding algorithm was, therefore, only used if the location of a *k*-means cluster centroid was ambiguous, or if the *k*-means algorithm did not reveal a cluster that would be expected based on previous literature (examples to follow).

A cluster (revealed with either *k*-means or seeding) was retained for further analysis (hereafter referred to as a "valid cluster") if it contained ICs from at least 50% of the participants in the study (minimum 9 participants). Only a single IC per participant was permitted into any single cluster to avoid biasing the contribution of a subset of participants to the cluster. If more than one valid IC per participant was within the predetermined distance of a cluster centroid, the IC closest to the centroid was kept in the cluster.

2.3.5 Cluster to channel ERP projections

Cluster IC activations were projected to scalp electrodes using an EEGLAB extension. ICs were projected to electrodes where the P3a and P3b were found to be maximal in the previous study, namely midline electrodes from FCZ to PZ. An ERP was recalculated for each IC within a cluster by multiplying each IC's activation (epoched by condition) with the channel weights generated by the ICA decomposition. In other words, an ERP for an IC was recalculated according to the following formula:

$$C = WA,$$

where A is the activation of a given IC, C is the channel data, and W is the pseudoinverse of the standardized (whitened) weight matrix. The mean percentage of scalp ERP power that each projected IC accounted for (PPAF) was determined for each cluster. Recall that scalp ERPs were free from eye-blink and EMG artefact contamination. PPAFs were compared across clusters and electrodes within the P3a timeframe (100-300 ms after the rare change run) and P3b timeframe (200-400 ms after the rare change run, and 300-500 ms after the rare flat run). P3a and P3b timeframes represent approximately 100 ms before and after the peak amplitude of the P3 waveform at FCZ (for P3a, feature-present condition only) and at PZ (for P3b, both feature-present and feature-absent conditions). It was expected that ERPs projected from frontal clusters

would account for more of the scalp power of the P3a (frontal electrodes FCZ and CZ, 100 to 300 ms post stimulus) than would the parietal clusters. Conversely, it was expected that the ERPs projected from the parietal clusters would account for more of the scalp power of the P3b (parietal electrodes CPZ and PZ, 200 to 500 ms post stimulus) than would the frontal clusters.

2.3.6 Event Related Spectral Perturbations (ERSPs)

ERSPs are a measure of induced oscillatory power dynamics of the broad-band EEG signal time-locked to a stimulus or an event (see the following for overviews: Delorme & Makeig, 2004; Makeig et al., 2004). Oscillatory power in each epoch at every timepoint, and at each frequency between 4 Hz and 45 Hz, to include all frequencies analysed, was computed from a time-frequency (wavelet) decomposition of all ROI cluster IC activations in the time window immediately following the last tone of every run. ERSPs were normalized to a common (average) baseline between 150 and 50 ms before the onset of the run (i.e. before the first tone of each run). Thus, ERSP in decibels at each timepoint equals 10 log (timepoint power/baseline power). Differences in ERSPs averaged over epochs were computed between rare and common runs within each condition (rare change – common flat in feature-present, rare flat – common change in feature-absent). Significant differences between runs were masked at $p < 0.01$ by EEGLAB's permutation test.

Meaningful ERSP differences between rare and common runs were quantified in two ways. First, the time course of the ERSP differences immediately following the last tone in each run were mapped for each frequency band. Significant time-frequency points were coded as 1, whereas masked (not significant at $p < 0.01$) time-frequency points were coded as 0. Difference time-frequency points were summed (separately) across Gamma (35 - 45 Hz), Beta (20 - 25 Hz), Alpha (8 - 12 Hz), and Theta (4 - < 8 Hz) bands for each time point from 100 ms before to 800

ms after the onset of the final tone in each run. I chose these frequency ranges based on previous literature, particularly those frequencies most commonly associated with attention and stimulus processing (see introduction). Note that for phase synchronization analysis the signals to be analysed must be narrow-band enough to have a definable phase. I thus chose to analyse slightly narrower frequency ranges than the broadest ones mentioned in previous literature. The frequency vectors were grouped into 100 ms bins, each containing 24 time points. If a bin contained more than 12 (50%) non-zero time points, then the bin was deemed meaningfully different.

2.3.7 Phase-locking Values (PLVs)

Phase synchrony analyses were conducted to determine the degree to which neural regions associated with the auditory change detection task, seeded a priori and confirmed by the clustering analysis, share information (see introduction). First, a wavelet analysis generated a time-frequency decomposition of the activations of each IC contained in all valid clusters for each condition (Makeig, 1993). This wavelet analysis produced a wavelet coefficient, which comprises a measure of instantaneous amplitude and phase, for each time point of IC activation at each frequency in each condition. Second, phase locking values (PLV) (see Lachaux et al., 1999) were computed across clusters. PLVs were computed in EEGLAB using the following equation (Delorme & Makeig, 2004, p. 9):

$$PLV_{1,2}(f,t) = \frac{1}{N} \sum_{k=1}^{N} \frac{W_{1,k}(f,t)\, W^{*}_{2,k}(f,t)}{\left| W_{1,k}(f,t)\, W_{2,k}(f,t) \right|},$$

where *Wi,k(f,t)* are the wavelet coefficients for each time point, *t*, and frequency, *f*, for each IC, *i*, and *k* =1 to *N* is the index of epochs. Possible PLVs range from 0, which represents no phase locking, to 1, which represents perfect phase locking between ICs across all trials. PLVs between

IC pairs were statistically compared against a surrogate distribution (N = 200 permutations) generated for each time-frequency point. Only PLVs outside this distribution were considered significant for further analysis ($p < 0.01$). PLVs between clusters represent only the mean PLVs computed between pairs of ICs common to the same participant. The PLVs between cluster pairs represent the mean of the significant PLVs obtained between each pair of ICs at each timepoint. Cluster PLVs were compared across conditions (rare vs common) at each timepoint from 0 to 500 ms after the final tone of the rare run ($p < 0.05$, one-tailed). Significant PLVs between conditions were grouped into 100 ms bins from 0 ms to 500 ms post stimulus onset (5 time-bins in total). Because each 100 ms bin contains 24 time points, only bins with at least 7 between-condition-significant PLV timepoints within each frequency band were considered meaningful. If the PLVs for each time point were independent, the binomial probability of obtaining 7 successes out of 24 where binomial $p = 0.05$ and binomial $q = 1 - p = 0.95$ is 0.000127. Thus, our estimated family-wise error for this analysis, with 10 connections x 5 time bins x 4 frequency bands x 2 conditions = 400 comparisons, is less than 0.000127 x 400 = 0.05. As the time points are contiguous, is it unlikely they all give rise to independent PLVs. Thus, this is a liberal estimate of the experiment-wise Type I error probability for this test.

2.4 Results

2.4.1 Behavioural data

To set the context for the analyses to follow I briefly review the behavioural data from Experiment 1 of Blundon et al. (2017). Responses in the feature-present condition were reliably faster and more accurate than those in the feature-absent condition. The average response time difference was 163 ms ($p < 0.0004$) and the average accuracy difference was 1.195 in units of *d'* ($p < 0.0001$). In addition, the peak latency of the P300 (but not its amplitude) in the EEG data

was also different between the conditions, shorter for the feature-present condition, with an average significant difference of 135 ms ($p < 0.02$). The shorter-latency P300 in the feature-present condition also had a scalp distribution consistent with the P3a subcomponent, whereas the longer-latency P300 in the feature-absent condition had a scalp distribution more consistent with the P3b subcomponent. In Blundon et al. (2017) we reasoned that the rare, highly salient, unpredictable change runs were attracting attention to the presence of a change run (and generating a P3a subcomponent added to the P3b). When these runs were rare this was sufficient to identify the target, thus allowing the participant to utilize a passive, or diffuse, attention strategy in the feature-present condition. On the other hand, when the flat runs were the targets in the feature-absent condition, it was necessary to scrutinize each run to detect the flat run target, thus forcing participants to utilize an active, "serial" search strategy (and only generating a P3b to the target). As described in the introduction, I expected to find the VAN associated with the detection of change targets and the DAN and perhaps other relevant brain regions associated with the detection of the flat targets.

2.4.2 Cluster Results

K-means clustering generated valid clusters in Supplementary Motor Area (SMA), Middle Cingulate Cortex (Cing), Posterior Cingulate Cortex (PCC), Medial Occipital Cortex (Occ), bilateral Temporoparietal Junction (L/R TPJ), Right Superior Parietal Cortex (R SPC), Left PreCentral Gyrus (L PreCG), and Ventral Frontal Cortex (the location in brain space was ambiguous, but the closest region was Anterior Cingulate Cortex; ACC). Because Cing and SMA were localized very close together (within 20mm of each other), and have been found to be functionally related, particularly in their role in the VAN (Corbetta et al., 2008; Downar et al., 2000; H. Kim, 2014), a single cluster equidistant between SMA and Cing was later seeded. *K*-

means also uncovered an additional cluster localized either to Left anterior ACC or Left Middle Frontal Gyrus (BA 9). Since an ACC cluster had already been found using *k*-means, I favoured the Middle Frontal Gyrus interpretation. In addition, I expected to find a cluster in anterior Frontal Gyrus as part of the VAN (see Corbetta et al., 2002 for a review), which has been previously implicated in efficient search paradigms (Ossandón et al., 2012). I, therefore, chose to seed a region in the left Middle Frontal Gyrus that had been previously found by Corbetta, Kincade, & Shulmann (2002). This cluster will hereafter be referred to as the Left Middle Frontal Gyrus (LMFG) cluster, however, much like all clusters localized using this method, this interpretation should be viewed cautiously. Additionally I chose to seed bilateral Superior Temporal Gyrus (STG) and bilateral Inferior Frontal Cortex (IFC) as these regions have also been associated with the ERP components of interest. Bekinschtein et al. (2009) found strong bilateral STG activity associated with the MMN response (response to final tone in all change runs minus that in all flat runs), so these regions were also seeded. Recall that the present paradigm is a conceptual replication of the original paradigm by Bekinschtein and colleagues (2009), so I expected to uncover similar neural sources. As Bekinschtein et al. (2009) did not provide MNI coordinates for bilateral STG, coordinates for these regions were taken from Doeller et al. (2003), who combined EEG and fMRI to uncover the neural regions associated with the MMN. In addition, using sLORETA (a method of EEG source localization) (Pascual-Marqui, 2002), Wronka et al. (2012) found that bilateral IFC (as well as the ACC and MFG), were most strongly associated with the P3a. Bilateral IFC was, therefore, seeded using MNI coordinates provided by Wronka et al. (2012).

Five ROIs in total were seeded, but only 2 contained ICs from at least 50% of the participants in the study. Table 2.1 summarizes these valid clusters from both *k*-means and

seeding, and Figure 2.4 displays images of the dipole clusters and their associated VAN, DAN, or so-called "oddball detection network" (ODD). The ODD network classification was used simply to refer to a collection of ROIs that were found using *k*-means clustering, and are frequently active during oddball tasks (H. Kim, 2014). Inferior frontal and superior temporal clusters did not contain ICs from at least 50% of participants, so they were not retained for further analysis. ICs free from EMG contamination in the superior temporal regions, and occasionally inferior frontal regions, have been difficult to uncover for a large enough group of participants in our lab, as these neural sources are close to muscle groups that can engage in involuntary muscle activity, namely jaw muscles, ossicles in the ears, and muscles in the forehead (Goncharova et al., 2003).

Region of Interest (ROI)	Brodmann Area (BA)	Number of participants	Cluster Centroid Talairach Coordinates	Average % variance accounted for
LMFG*	9	13 (76%)	-30, 22, 25	89.10
SMA/Cing*	6/24	12 (71%)	6, -4, 52	88.68
ACC**		12 (71%)	-1, 7, 11	85.46
PCC**	31	16 (94%)	9, -59, 23	90.84
RTPJ**	40	11 (65%)	40, -56, 36	89.34
LTPJ**	39	13 (76%)	-30, -67, 26	90.43
RSPC**	5	15 (88%)	18, -34, 50	88.35
LPreCG**	4	15 (88%)	-21, -23, 49	88.84
Occ**	18	13 (76%)	1, -89, 9	90.34

Table 2.1 Details of the 9 valid clusters that were retained for further analysis after seeding.

*Because EEGLAB typically visualizes dipole locations in Talairach space, all valid cluster centroids have been transformed from MNI to Talairach coordinates. ROIs and BAs represent the closest anatomical regions to resulting cluster centroid Talairach coordinates. Because the ACC only represents the closest region to the Talairach centroid (localized to the lateral Ventricle), no Brodmann Area is provided. *seeded clusters, **k-means clusters*

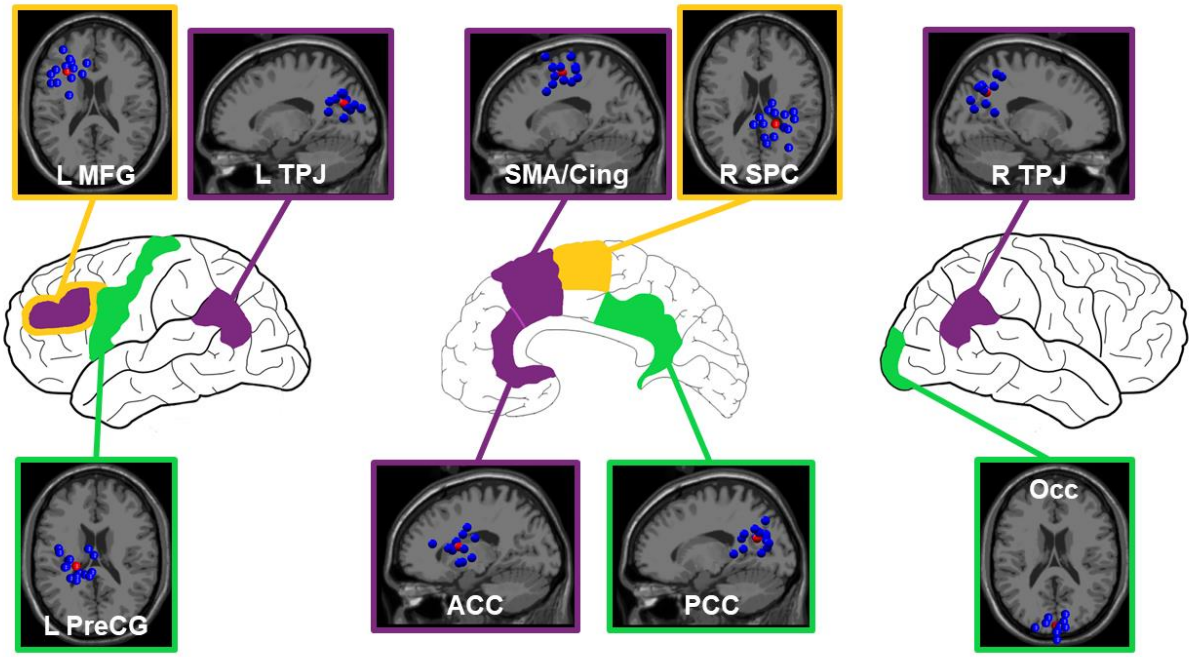

Figure 2.4. Nine clusters retained for further analysis.

Clusters include Left Middle Frontal Gyrus (L MFG), Left Temporo-parietal Junction (L TPJ), Supplemental Motor Area/Middle Cingulate Gyrus (SMA/Cing), Right Superior Parietal Cortex (R SPC), Left Precentral Gyrus (L PreCG), Anterior Cingulate Cortex (ACC), Posterior Cingulate Cortex (PCC), and Occipital Cortex (Occ). Clusters in purple are most strongly associated with Ventral Attention Network (VAN), clusters in gold with Dorsal Attention Network (DAN). Clusters in green are associated with detecting auditory oddball stimuli (Kim, 2014). Note that the MFG is labeled as part of both the DAN and the VAN as it has been known to coordinate between these two networks (Corbetta, Patel, and Shulman, 2008).

Of the nine clusters retained for further analysis, four clusters have been associated with the VAN (ACC, SMA/Cing, R/L TPJ) (Corbetta et al., 2008; Downar et al., 2000), one cluster has been associated with the DAN (R SPC) (Corbetta et al., 2008; Downar et al., 2000), and three clusters were found to be involved in detecting auditory oddball targets (PCC, L PreCG, and Occ) (H. Kim, 2014). One cluster, the MFG, has previously been associated with both the VAN and DAN, as it is believed to coordinate top-down and stimulus-driven control between these two networks (Corbetta et al., 2008).

2.4.3 Cluster to channel ERP projection results

Table 2.2 summarizes the percentage of electrode power accounted for by cluster projections to midline electrodes CZ and PZ, and Figure 2.5 displays examples of these projections for several of the most revealing results. This analysis revealed that frontal clusters ACC and SMA/Cing contributed the most to CZ during the P3a subcomponent timeframe (100-300 ms after the last tone of rare change runs). ACC and SMA/Cing contributed less to PZ during the P3a and P3b timeframes. PCC and R SPC contributed the most to parietal electrodes (CPZ and PZ) during the P3b timeframe in both the feature-present (200-400 ms) and the feature-absent condition (300-500 ms).

Feature-Present	Early (100-300 ms)			Late (200-400 ms)	
	CZ	PZ		CZ	PZ
L MFG	2.2	0		2	0
ACC	44.4	4.9		38.2	5.7
SMA/Cing	26.5	19.6		19.2	15.5
R TPJ	3.4	2.2		0	6.1
L TPJ	2.3	2.6		1	1.7
R SPC	7.2	18.3		6.8	20.7
PCC	5.9	25.8		6.2	27.5
L PreCG	4.9	12.4		1.7	9.3
Occ	2.8	1.8		4	0.7
Feature-Absent	Early (100-300 ms)			Late (300-500 ms)	
	CZ	PZ		CZ	PZ
L MFG	0	0		0	6.9
ACC	45	2		29.3	0
SMA/Cing	16.1	15.2		6.4	11.4
R TPJ	0	0		4	4.6
L TPJ	0	8.7		2.9	0
R SPC	5.7	12.7		12.1	20.5
PCC	6	7.4		0	31
L PreCG	9.8	2.9		3.5	10.4
Occ	4.1	0		0	2.7

Table 2.2 Percentage of electrode power accounted for by cluster activation projected to midline electrodes.

Only positive values or zeros are presented, because only positive values are meaningful.

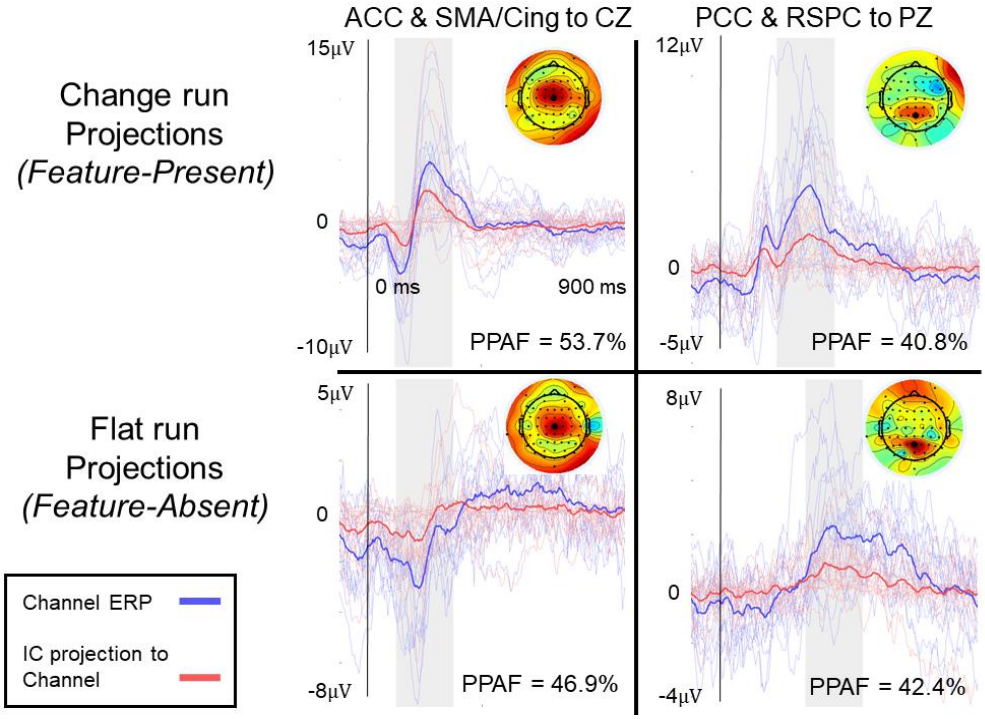

Figure 2.5. Projections from frontal and parietal clusters to CZ and PZ, respectively.

Only rare runs were projected. Projections are plotted from -100 to 900ms after the onset of the final tone in the run. PPAF values were computed during the early timeframe (100-300ms) at CZ, and during late timeframes (200-500ms) at PZ.

2.4.4 ERSP results

The time course of the ERSP differences between rare and common runs immediately following the last tone in each run was mapped for each frequency band in 100 ms bins (see Figure 2.6). Since ERSP generalizes both event-related synchronization (ERS) and event-related desynchronization (ERD), the significant differences between rare and common runs did not account for the direction of power difference between rare and common runs. The direction was,

however, estimated based on the ERSP plots for rare and common runs (see Appendix A for representative examples). Hereafter (for both feature-present and feature-absent ERSP results), ERS will refer to ERSPs significantly larger in the rare relative to common runs, whereas ERD will refer to ERSPs significantly smaller in the rare relative to common runs.

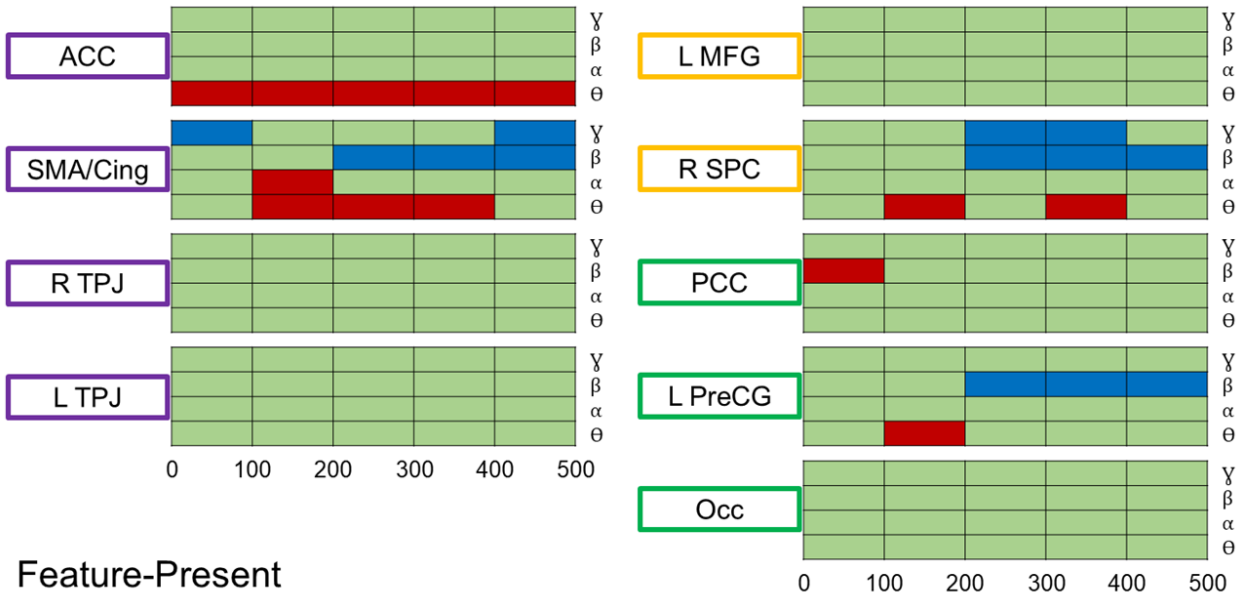

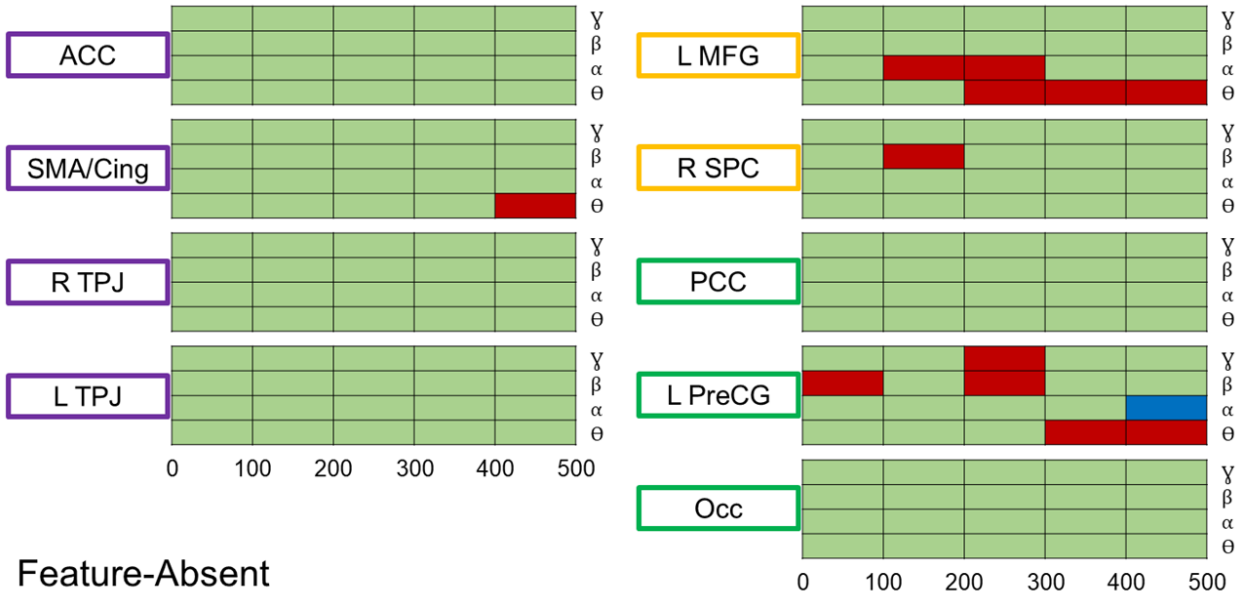

Figure 2.6. Time course of ERSP differences between rare and common runs for each condition, grouped by frequency band, and in 100ms bins following the onset of the final stimulus in the run.

Red represents a significant difference in power with rare > common (ERS), blue represents a significant difference in power with common > rare (ERD), and green represents no significant difference between conditions. Each cluster time course is grouped by gamma (highest position), beta, alpha, and theta (lowest position) frequency bands. If a bin contained more than 50% non-zero difference time points, then the bin was deemed meaningful. Coloured boxes around the cluster names are the same as those used in Figure 2.4: purple indicates clusters associated with the VAN, gold with DAN, and green with oddball detection.

2.4.4.1 Feature-present ERSPs

From 0 to 500ms after the last tone in the run, significant ERS was observed in lower frequencies (theta and alpha bands), whereas ERD was observed in higher frequencies (beta and gamma bands). ERSP results will be broken down by early (P3a) and late (P3b) timeframes.

Early (P3a, 100-300 ms): Lower frequency ERS was observed in clusters associated with VAN (ACC and SMA/Cing), DAN (R SPC only), and detecting oddball stimuli (L PreCG) during the P3a timeframe. Higher frequency ERD was also observed in clusters associated with VAN (SMA/Cing), DAN (R SPC), and detecting oddball stimuli (L PreCG) during this same time frame.

Late (P3b, 200-400 ms): Because of the temporal overlap between P3a and P3b in the feature-present condition, ERSP results were similar across both subcomponents timeframes. Lower frequency ERS was observed in clusters associated with VAN (ACC, SMA/Cing) and DAN (RSPC) during the P3b timeframe. Higher frequency ERD was observed in clusters associated with VAN (SMA/Cing), DAN (R SPC), and detecting oddball stimuli (L PreCG).

Finally, there appears to be a latency difference between the onset of ERS and ERD across clusters, where ERS appears earlier (between 0 and 200 ms post stimulus) than ERD (200 ms, save for SMA/Cing, which begins immediately after stimulus onset).

2.4.4.2 Feature-absent ERSPs

From 0 to 500 ms after the last tone in the run, significant ERS was observed in both lower and higher frequencies. ERD was only observed during a single time bin. As in the feature-present results, ERSP results will be broken down by early and late timeframes. Recall that only a P3b during the late timeframe was observed in the feature-absent condition.

Early (100-300 ms): Both high and low frequency ERS was observed in clusters associated with DAN (L MFG and R PSC) and ODD (L PreCG) networks. Low frequency ERS was observed in MFG, whereas high frequency ERS was observed in R SPC and L PreCG. There were no significant ERS or ERD observed in clusters associated with VAN.

Late (P3b, 300-500 ms): Low frequency ERS was observed in a single cluster associated with VAN (SMA/Cing), and a single cluster associated with DAN (L MFG). No high frequency ERS was observed during this timeframe. A single instance of low frequency ERD was observed in a single cluster associated with the ODD network (L PreCG). The feature-absent ERSPs suggest that only DAN and ODD networks are associated with detecting oddball patterns lacking any salient rare features.

2.4.5 Phase Locking Value Results

PLVs were computed on clusters that are associated with VAN (ACC and SMA/Cing), DAN (L MFG and R SPC), and ODD (PCC and L PreCG) networks. Only these six clusters were retained for the final PLV analysis because these were either the largest contributors to the P3a and P3b subcomponents at the scalp, or they showed significant ERS and ERD during the P3a and P3b timeframes. Figure 2.7 shows the proportion of significant connections relative to the total possible connections within each subnetwork (VAN, DAN, ODD), and between each subnetwork pair (VAN-DAN, VAN-ODD, DAN-ODD) across all frequency bands at each time bin. Only PLVs that were meaningfully larger in response to the rare stimulus (the change stimulus in the feature-present condition, the flat stimulus in the feature-absent condition) than to the common stimulus are reported (see Methods). Appendix B displays representative brain maps from which Figure 2.7 was derived, with significant functional connections indicated between cluster centroids in the various networks.

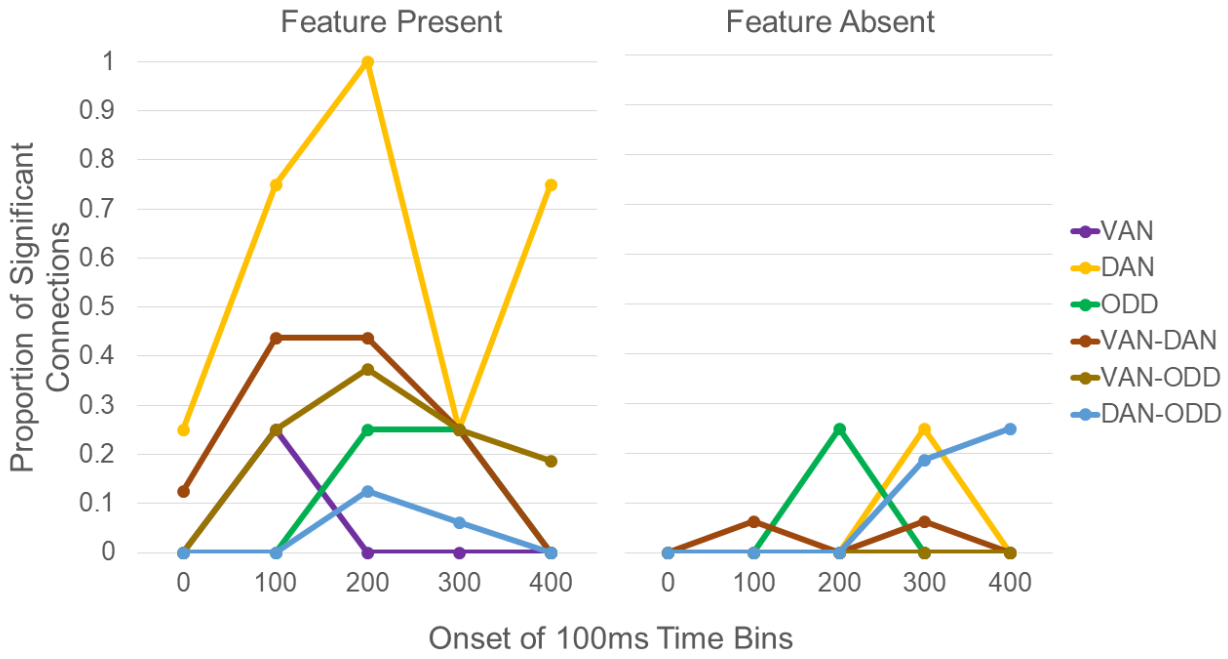

Figure 2.7. PLV connections within networks (VAN, DAN, ODD) and between networks (VAN-DAN, VAN-ODD, DAN-ODD).

The total number of significant connections was calculated for each network or network pair, across all four frequency bands, and at each 100 ms time bin. The total number of connections was weighted by the total number of possible connections that could be made within or between networks. As there are two regions in each network, the total number of possible connections within VAN, DAN, or ODD is 4 (1 connection per frequency band), and between each network pair is 16 (4 connections per frequency band).

Figure 2.7 shows not only that there are many more connections, but also that the regions begin to communicate earlier (0 ms post stimulus onset), in the feature-present than in the feature-absent condition (100-200 ms post stimulus onset). Consistent with the ERSP results, there is strong VAN connectivity (within the VAN network, and between VAN and the other two networks) in the feature-present condition, whereas there is little to no VAN connectivity in the feature-absent condition. Connectivity involving the VAN appears to peak earlier (100 ms) than

connectivity involving DAN and ODD (200-300ms) in both feature-present and feature-absent conditions, though, as previously mentioned, the VAN connectivity is meager in the feature-absent condition. Importantly, notice that the DAN in the feature-present condition has the largest relative proportion of connections during the P3a timeframe. This is in contrast to the channel projection and ERSP results, where neural power and scalp projections underlying the P3a were dominated by regions associated with the VAN.

2.5 Discussion

Channel projection, ERSP, and PLV results are consistent with the involvement of attention orienting processes using dorsal and ventral attention networks in the behavioural search asymmetry that were found in a previous auditory serial search study (Blundon et al., 2017). Broadly speaking, the ventral attention network (VAN) is associated with orienting attention to salient and unexpected stimuli (exogenous attention). The neural regions typically associated with the VAN consist of right hemisphere ventral frontal cortex (MFG, IFG, or ACC), bilateral TPJ (Christoff et al., 2016; Corbetta et al., 2008; Downar et al., 2000; H. Kim, 2014), and though not considered a core member, have also included the SMA/Cing (Downar et al., 2000; H. Kim, 2014; Thomas Yeo et al., 2011). Our source localization revealed most of those same regions, though the MFG was localized to the left hemisphere. Of those regions, the ACC and SMA/Cing had the strongest contributions to the P3a scalp ERP, accounting for 44% and 27% (respectively) of the power at CZ during the P3a timeframe.

ERSP analysis also revealed a large increase in power at the low frequencies (theta and alpha) during the P3a timeframe in response to rare change runs relative to common flat runs

localized to both the ACC and the SMA. Finally, the PLV analysis revealed that these two regions were far more functionally connected with each other, and with other regions, in the feature-present condition than in the feature-absent condition. This is compelling evidence that the ACC and SMA/Cing, and by extension the VAN, are primary neural generators of the P3a in this paradigm, and possibly for all target-related P3a activity.

The dorsal attention network (DAN) is associated with top-down (endogenous) focus of attention and consists of bilaterial superior parietal regions (superior parietal lobule, for example), and frontal eye fields (Brodmann area 8). Of those regions, source localization revealed only right superior parietal cortex (R SPC). Since this was an auditory study, it's not surprising that no clusters were found in the frontal eye fields. While the R SPC was one of the strongest contributors to the P3b (approx. 20% of the power at PZ during the P3b timeframes), the largest contributor was the PCC (28-31%). This is consistent with previous research that has also found PCC (and PreCG) activation associated with detecting auditory oddball stimuli (H. Kim, 2014). Despite the PCC's strong contribution to the P3b at the scalp, there was no significant difference in local spectral power in response to rare runs relative to common runs. In contrast, the L PreCG contributed very little to the scalp P3b but showed significant high frequency ERD in response to rare change runs, and significant low frequency ERS in response to rare flat runs, during the P3b timeframes. This is evidence that this region is showing preferential activation for rare target runs over common runs, and is most likely a movement signal associated with the button press that controls were asked to make when they heard a rare run (see Pfurtscheller & Lopes da Silva, 1999 for a review). Contralateral beta ERD is commonly found over centro-parietal electrodes starting about 2 seconds before movement initiation, then becoming bilateral immediately before a voluntary movement (Alegre et al.,

2002; N. E. Crone et al., 1998; Engel & Fries, 2010; Pfurtscheller & Lopes da Silva, 1999). While the PCC appears to play a critical role in the generation of the P3b at the scalp, and the PreCG may be involved in the detection of rare targets, the specific function of this oddball network remains unclear.

Of special interest is the L MFG. While the MFG is considered part of the VAN (Corbetta & Shulman, 2002), the channel projection and ERSP results for this region are very different from that of the two VAN regions in this study (ACC and SMA/Cing). The L MFG contributes very little to either the P3a or the P3b at the scalp, and there is no ERSP evidence that the L MFG is involved in detecting rare change runs. There is evidence, however, of significant low frequency ERS in response to rare flat runs over common change runs. This could suggest that the L MFG plays a role in the detection of targets that require focused, endogenous attention, making it a stronger candidate for the DAN than the VAN in the context of this study. Furthermore, the L MFG may be acting as a coordinating hub between the VAN (ACC) and the DAN (R SPC), as it is very strongly connected to one or both of those regions in response to feature-present targets during the P3a timeframe (see Figure S2). This is consistent with the hypothesis that MFG plays a key role in coordinating both ventral and dorsal attention networks (Corbetta et al., 2008). During tasks requiring focused attention, the DAN sends top-down signals via the MFG to suppress the activation of the VAN, and to limit its response to only task-relevant stimuli. When a participant perceives a highly salient and unexpected input, the VAN sends bottom-up information to the DAN through the MFG to orient attention toward the salient stimulus. Further analysis of the functional connectivity involving the MFG, as well as the direction of information transfer between the VAN and DAN through the MFG, is required to confirm this hypothesis.

This study also revealed that the neural generators of low frequency oscillations observed at the scalp may be different for different task demands. In the feature-present condition, low-frequency (theta and alpha) ERS was observed in ACC and SMA, and the time course of the low frequency ERS in SMA matches the time course commonly observed at the scalp (Klimesch et al., 1998; Kolev et al., 1997; Missonnier et al., 2006; Yordanova et al., 2001; Yordanova & Kolev, 1998a, 1998b). In contrast, low-frequency ERS was observed in L MFG in the feature-absent condition, and its time course too matches that typically observed at the scalp. While not exactly the same, this is reminiscent of research previously conducted in our lab, where we found that the neural generators of the MMN varied with task demand (MacLean et al., 2015). Future studies should explore the relationship between frontal theta oscillations and how their neural sources vary with task demand or stimulus context.

High frequency (beta and gamma) ERD during the P300 timeframe was only observed during the feature-present condition, and was distributed among the three different networks, observed in SMA, R SPC, and L PreCG. This is perhaps consistent with the interpretation that gamma ERD may reflect a disruption in the maintenance of an attentional set, triggered by a change in auditory stimulus (Jensen et al., 2007; Marshall et al., 1996). This further suggests that gamma (and maybe even beta in this case) may be more sensitive to changes in sensory environment than to changes in attentional sets, per se. In fact, high-frequency ERD in the feature-present condition, and high-frequency ERS in the feature-absent condition shown in Figure 2.6, are the result of local decreases in high frequency power to the change runs, and local increases in high frequency power to the flat runs, regardless of stimulus context (see Appendix A). Future research should explore more thoroughly how the neural generators of gamma ERD during the P300 time frame may be different for different task demands.

Corbetta et al. (2008, p. 314) state that "Enhanced responses to oddballs are observed in a set of regions that includes most consistently the temporo-parietal junction and the lateral prefrontal cortex but also dorsal regions in parietal and frontal cortex involved in shifting attention. Because the oddball is usually defined by a different feature(s) than the standard, rather than by a different location […], the enhancement to the oddball is not related to a spatial shift of attention." This points to a significant difference between search asymmetry in the visual domain (and possibly the touch domain as well) and what we have documented in the serial auditory domain. The feature oddball of the change run is *not* spatial, and therefore should not particularly engage spatial attention maps in the parietal cortex or elsewhere. It should, however, engage tonotopic maps in auditory cortex and attention shifting networks generally, the latter of which is seen in these analyses. It might also be expected to engage the closely-related salience network, which consists of the ACC and the anterior insula (Cole et al., 2013; Kucyi et al., 2012; Menon & Uddin, 2010; Power et al., 2011). Some (e.g. Kucyi et al., 2012) even consider the salience regions to be part of the VAN. From this point of view, I hypothesize that the early and persisting ERSP activity observed in the theta band in the ACC in the feature-present condition could represent the alerting function of the salience network. Indeed, when the oddball is not spatial, it could be the primary way by which a rare, salient, unpredictable oddball engages the VAN. A more direct test of this hypothesis would involve comparison of spatial and non–spatial oddballs in the auditory domain.

The purpose of this chapter was to describe neurotypical spatio-temporal dynamics underlying the generation of the P3a and P3b subcomponents, which are commonly used to establish awareness among DOC patients (c.f. Bekinschtein et al., 2009; Chennu & Bekinschtein, 2012; Fischer et al., 2008, 2010; Morlet & Fischer, 2014). It appears that the P3a is associated

with exogenous attention processes (ventral attention and salience networks), while the P3b may be associated with endogenous attention processes (dorsal attention network) and a network of regions typically involved in detection of oddball targets. In the following chapters I will characterize the ERP (Chapter 3) and spatio-temporal network dynamics (Chapter 4) among the same individual control participants and compare them to a small group of responsive and unresponsive hospice patients. The network dynamics described in this chapter will inform Chapter 4.

Chapter 3: Electrophysiological evidence of hearing at the end of life

This chapter reports individual event-related potential (ERP) results of the study reported in Chapter 2 among neurotypical control participants and both responsive and unresponsive hospice patients. Recall that this is a conceptual replication of a study that has demonstrated ERP evidence of command following in individual neuro-typical control participants and minimally conscious participants, but not unresponsive wakeful patients (Bekinschtein et al., 2009). The results of the original study revealed that both minimally conscious and (most) unresponsive wakeful patients generated an MMN or P3a (which they called a "local effect") to simple tone changes, but only minimally conscious participants generated a P3b (which they called a "global effect") to changes in auditory patterns. The MMN and P3a have been widely implicated with pre-attentive and pre-conscious processing of acoustic irregularities (Näätänen et al., 2007; Rinne et al., 2001; Sussman et al., 2003), although the MMN does seem to operate on a consciously accessible memory trace (Dykstra & Gutschalk, 2015). The P3b, on the other hand, seems to always be associated with conscious awareness of task-relevant oddball targets (Bekinschtein et al., 2009; Polich, 2007). Recall that I have previously shown that this paradigm generates a reliable P3a to tone changes, and P3b to both tone and pattern changes, among neurotypical participants (Blundon et al., 2017) (see Figure 2.1 for neurotypical MMN, P3a and P3b ERPs). The P3a and P3b are subcomponents of the P300 response (Linden, 2005; Polich, 2007) and, as demonstrated in Chapter 2, are associated with different attentional processes. The P3a is associated with exogenous attention orienting toward highly salient, rare, and unpredictable oddballs, whereas the P3b is associated with context updating and working memory processes relevant to target detection (Blundon & Ward, 2019). Whereas the P3a and MMN often co-occur, whether the P3a operates on unconscious or conscious memory traces is

also currently a matter of debate (Friedman et al., 2001; Muller-Gass et al., 2007; Sculthorpe et al., 2009). The P3b, however, is considered a reasonably reliable marker of conscious detection of target stimuli (Bekinschtein et al., 2009; Polich, 2007; Sergent et al., 2005; Vogel et al., 1998), though this interpretation has recently been debated (Koch et al., 2016; Naccache et al., 2016; Silverstein et al., 2015).

By applying a similar paradigm to actively-dying unresponsive patients, the capacity for unresponsive patients to engage in auditory perceptual processes (MMN), attentional (P3a and P3b), and memory (P3b) processes can (tentatively) be inferred. In the present chapter I report the MMN, P3a, and P3b responses to auditory tone and pattern changes both from neurotypical control participants, from responsive hospice patients, and from unresponsive, actively-dying, hospice patients. In order to properly appreciate the results of this study, however, it is important to understand that even the responsive hospice patients differed from the neurotypical controls in several respects. First, they were all terminally ill (usually cancer; see Tables 3.1, 3.2) and were being medicated (Tables 3.1, 3.2), often with opioids, to ameliorate the symptoms of the illness. Second, they were as a group considerably older than the controls, on average by nearly five decades. All of these factors can be expected to affect patients' EEG responses in the auditory task.

3.1 Materials and Methods

All aspects of the experimental procedure and EEG analysis apply to both responsive and unresponsive sessions of hospice patients and to the single sessions of neurotypical control participants, unless otherwise specified. Hereafter, neurotypical control participants will be referred to as "controls", and hospice patients will be referred to as "patients". Information about

control participants, stimuli, procedure, and EEG recording/preprocessing are the same as what was reported in Chapter 2.

3.1.1 Ethics Statement

All aspects of the experimental protocol that pertain to hospice patients, including the recruitment and consent procedures, were approved by the University of British Columbia Behavioural Research Ethics Board in accordance with the provisions of the World Medical Association Declaration of Helsinki. All participants gave written informed consent by reading and signing the approved consent document. Hospice patients explicitly extended their consent to the time when they became unresponsive. In addition, patients' families (when available) gave verbal assent to the procedures. This ethics statement applies to all studies that include hospice patients.

3.1.2 Participants

3.1.2.1 Controls

The following analyses were conducted on the same data as was presented in Chapter 2. Recall that these data were collected from 17 university-aged neurotypical participants.

3.1.2.2 Hospice Patients

Data were collected initially from 13 participants, residing in a hospice facility in Vancouver, over a time period of more than two years. A hospice in British Columbia is a facility that accepts patients with advanced disease with an estimated prognosis of 3 months or less at the time of admission to hospice, although prognosis is notoriously variable.

Hospice Patient Eligibility Criteria: Patients were eligible to participate if they showed no signs of psychiatric or neurological deficits, or cognitive impairment, including delirium,

which can be common in the last days to hours. These clinical assessments for eligibility were performed by hospice physicians. In addition, eligible patients must have been proficient in the English language to understand the task instructions, and their hearing must have been sufficient to distinguish between the tone patterns. If there was concern about a patient's hearing, or if the patient wore a hearing aid, a hearing screening was performed.

I intended to record each patient twice, once as soon as possible after admission to the care facility and given consent, and once when unresponsive and actively-dying. Actively-dying is defined as "the hours to days preceding imminent death during which time the patient's physiologic functions wane" (Hui et al., 2014). Time between sessions varied from 8 to 12 weeks, depending on the time elapsed between enrolment in the study (first session) and when the patient became unresponsive prior to death (second session). Typically, an "unresponsive" actively-dying patient was defined using the Palliative Performance Scale (PPS) rating of 10%. The PPS is a valid and reliable eleven-point scale designed to measure in 10% decrements the decline from 100% (healthy) to 0% (death) based on five observable parameters: ambulation, ability to do activities, ability to do self-care, food/fluid intake and consciousness level. (Palliative Performance Scale (PPSv2). copyright Victoria Hospice Society, 2006. Accessed at: https://victoriahospice.org/how-we-can-help/clinical-tools/ on August 27, 2019) This assessment was performed by the nursing staff at the facility. Between responsive and unresponsive sessions, I frequently visited the patients (approximately every 1-2 weeks) to collect verbal assent to continue to participate in the study. Various forms of attrition, including rapid progression to death or remission, reduced the number of patient participants. One family revoked assent at the time of the unresponsive recording. Data from four patients were excluded because of excessive noise in their EEG. The patient analysis to be described is based on nine

patients (four female, age 28 to 88 years, mean age 68.2 years). Eight patients were recorded when they were responsive, five when they were unresponsive. Four patients were recorded once when they were responsive, and again when they were unresponsive, as originally intended. Details of patients' diagnoses and medications can be found in Tables 3.1a and 3.1b. Note that most patients were receiving various forms of opioids at both recording sessions. See Appendix C for information about these medications and their typical usage.

Responsive							
Subject ID	*Diagnosis*	*Approx. age at recording*	*Approx. time of recording*	*Medication*	*Dose*	*Time of Med. Admin.*	*Method of Med. Admin.*
P002	Lung Cancer	66	14:00	Clonazepam Dexamethasone Hydromorphone Lorazepam	0.25 mg 4 mg 0.25 mg 0.25 mg 0.5 mg 1 mg	10:00 10:00 8:00 12:00 13:25 13:25	PO PO SUBCUT SUBCUT SUBCUT PO
P003	Head & Neck Cancer	81	14:00	No relevant medications to report	--	--	--
P004	Lung Cancer	67	13:00	Gabapentin	200 mg 200 mg	10:00 12:00	PO PO
P005	Astrocytoma	28	14:00	Dexamethasone Levetiracetam	1 mg 250 mg	10:00 10:00	PO PO
P006	Colorectal Cancer	55	11:00	Dexamethasone Escitalopram Oxycodone	4 mg 30 mg 90 mg	10:00 10:00 7:30	PO PO PO
P007	Ovarian Cancer	87	12:00	Escitalopram Fentanyl (patch)	10 mg 18 mcg	10:00 22:00	PO Transdermal
P008	Lung Cancer	61	12:00	Dexamethasone Hydromorphone	4 mg 9 mg	9:00 10:00	PO PO
P009	Congestive Heart Failure	77	15:00	Fentanyl (patch) Levothyroxine Methylphenidate	6 mcg 25 mcg 5 mg	18:00 10:00 10:00	Transdermal PO PO

Table 3.1: Details of responsive hospice patient diagnosis and medications consumed on the day of each recording.

Locations of cancer metastases are not included. Only medications that may affect cognitive function, and were administered before each recording, are included. Medications not included are those designed to treat the following: moderate pain relief (like acetaminophen and lidocaine), fungal infections, gout, blood clotting, hemorrhoids, constipation, skin diseases, nausea, and heartburn. Two patients (N007 and N009) were prescribed sleep aids (Zopiclone

15mg PO, and Trazodone 50mg PO, respectively). These medications are not shown as it is unlikely the patients were still affected by the time of the recording based on medication half-lives. Times are listed using 24-hour clock.

List of abbreviations and acronyms: Approx. = Approximate, Med. = Medication, Admin. = Administration, PO = Per Os (medication taken orally), SUBCUT = Subcutaneously (medication administered by injection into the subcutaneous tissue).

Unresponsive								
Subject ID	*Diagnosis*	*Approx. age at recording*	*Approx. time of recording*	*Medication*	*Dose*	*Time of Med. Admin.*	*Method of Med. Admin.*	*Approx. time between recording and death*
P001	Prostate Cancer	88	16:00	Hydromorphone	0.25 - 0.5 mg	6:00 12:00	SUBCUT SUBCUT	76 hrs
P002	Lung Cancer	66	15:00	Dexamethasone Lorazepam Hydromorphone	4 mg 0.5 mg 0.5 mg 1 mg 0.5 mg 1 mg	8:00 14:00 10:00 12:00 12:45 14:30	SUBCUT SUBCUT SUBCUT SUBCUT SUBCUT SUBCUT	6 hrs
P004	Lung Cancer	67	23:00	Dexamethasone Gabapentin Methadone Hydromorphone Glycopyrrolate	4 mg 200 mg 7 mg 2 mg 2 mg 2 mg 0.2 mg 0.2 mg	10:00 10:00 14:00 11:20 13:30 17:00 14:00 16:00	SUBCUT PO PO SUBCUT SUBCUT SUBCUT SUBCUT SUBCUT	116 hrs
P007	Ovarian Cancer	87	14:00	Glycopyrrolate	0.2 mg	11:15	SUBCUT	5 hrs
P008	Lung Cancer	61	20:00	Dexamethasone Hydromorphone Glycopyrrolate	6 mg 2 mg 2 mg 1 mg 2 mg 2 mg 2 mg 0.2 mg 0.2 mg	10:00 10:00 14:00 14:30 17:05 18:00 20:00 14:30 20:00	SUBCUT SUBCUT SUBCUT SUBCUT SUBCUT SUBCUT SUBCUT SUBCUT SUBCUT	79 hrs

Table 3.2: Details of unresponsive hospice patient diagnosis and medications consumed on the day of each recording.

Locations of cancer metastases are not included. Only medications that may affect cognitive function, and were administered before each recording, are included. Medications not included

are those designed to treat the following: moderate pain relief (like acetaminophen and lidocaine), fungal infections, gout, blood clotting, hemorrhoids, constipation, skin diseases, nausea, and heartburn. For P001 a range of hydromorphone doses is reported because the specific dosage administered was not specified. P004 was able to take medications PO earlier in the day because they did not become unresponsive until the evening on the day of the recording. It was also verbally reported that P004 regained responsiveness sometime after the recording, but no written record of this is available to us. Times are listed using 24-hour clock.

List of abbreviations and acronyms: Approx. = Approximate, Med. = Medication, Admin. = Administration, PO = Per Os (medication taken orally), SUBCUT = Subcutaneously (medication administered by injection into the subcutaneous tissue).

3.2 Stimuli and Procedure

Stimuli and basic procedure were identical to those described in Chapter 2 for both controls and patients (see Figures 2.2 and 2.3). All aspects of the procedure specific to controls are described in Chapter 2. Only procedural details specific to patients will be described here.

Hospice patient data were collected using a portable EEG system in each patient's room. Each patient lay in their bed for data collection. The bed was adjusted so that the patient could lie upright comfortably, with their head supported by a rolled towel wrapped around their neck to keep the back of their head clear of the bed. Once the EEG was set up and the patient was fitted with the cap, pictures were taken of the patient from many angles using a digital camera without internet access. These pictures served as a record from which to recreate the conditions of the responsive session as faithfully as possible during the unresponsive session. All photos were deleted once the patient had completed, or was no longer enrolled, in the study. Before the experiment began, each patient performed a short loudness screening to make sure they were comfortable with the loudness of the stimuli and instructions.

All task instructions were presented in written format on a laptop, with simultaneous audio recordings of the instructions presented through over-ear headphones. Recall that controls

were instructed to click the mouse as quickly as possible to each pattern oddball (rare run) they heard during each block. Patients were instead instructed to *count* the rare runs they heard during each block. This modification was made to accommodate expected patient paralysis when they became unresponsive. It was made clear to participants that they were only to count or to respond to runs that represented a change in the global pattern, i.e. a rare run, not every time they heard a tone that differed from the previous tone. If at any point during the responsive session the patient needed to ask a question about the procedure, or the patient appeared not to understand the procedure, the recording was paused, and the procedure was clarified. During the unresponsive session, the conditions of the responsive session were recreated as faithfully as possible, including head and bed position, laptop placement, and stimulus loudness. Family members were permitted to stay in the patients' room during the unresponsive session and were encouraged to talk to their loved one between blocks.

3.2.1 EEG recording and preprocessing

Control EEG signals were digitized at 500 Hz (National Instruments Inc., Vaudreuil-Dorion QC Canada) from a 60-channel electrode cap (Electrocap Inc., Eaton OH USA, International 10±10 placement) referenced to the right mastoid. Before digitization EEG signals were amplified and analog bandpass filtered from 0.1 Hz to 100 Hz (SA Instrumentation, San Diego CA USA). Eye movements were recorded with four periocular electrodes. All electrode impedances were kept below 10 kΩ (input impedance of the amplifier was > 2 gΩ)

EEG signals from patients were digitized at 2048 Hz (BioSemi, ActiveTwo) from a 128-channel electrode cap (only 64 channels were used, BioSemi equiradial placement) referenced to the CMS electrode. Before digitization, EEG signals were amplified and analog bandpass filtered

from 0.1 Hz to 100 Hz. Eye movements were recorded with two periocular electrodes, one to the right and one above the right eye.

All participant EEG data were analyzed using EEGLAB software (Delorme & Makeig, 2004). Raw data were down-sampled to 256 Hz and re-referenced to average reference. Line noise was removed online by applying a notch filter between 55 and 65Hz. Data were visually inspected for large muscle artefacts. Eye-blink and EMG artefacts were removed using ICA (see Independent Component Analysis section of Chapter 2 for a more detailed description).

3.2.2 Behavioural and ERP Analyses

Reaction times and accuracy to target runs were recorded for controls only. The response times to correctly detect the rare target run (hits) were calculated from the onset of the fifth tone in the run separately for the two stimulus types (change and flat). Correct responses were defined as a response to a rare target run that occurred before the onset of the final tone of the following non-target run. This time window varied between 1300 ms and 1900 ms after the onset of the final tone in a target run. Reaction times for individual neurotypical participants will be reported with the ERP results for this study. Group behavioural results are reported in (Blundon et al., 2017).

ERP analyses were conducted using ERPLAB (Lopez-Calderon & Luck, 2014) software running in EEGLAB. Artefacts were removed using independent component analysis (Viola et al., 2009). The continuous EEG record for each individual participant was epoched from -1000 to +2000 ms relative to the onset of the first tone of each run, low-pass filtered at 30 Hz using a FIR filter, and baseline corrected (-200 to 0 msec re onset of fifth tone in each run). Shortened segments of these epochs were selected for display purposes. EEG trials containing data with

amplitudes greater than 100µV, and step-like artefacts consistent with saccadic eye movements, were removed from further analysis.

Consistent with the analyses performed by Bekinschtein et al. (2009), MMNs were characterized as the difference between change runs and flat runs (change – flat), regardless of whether they were rare or common, across all four blocks of stimuli. After trials containing artefacts were removed, MMN data (control or patient) was based on 188 to 284 trials of each run type (382 to 576 trials total). P300s, however, were characterized as the difference between rare and common (rare – common) runs, sorted by run type. In other words, I compared rare vs common change runs (now defined as "tone change" comparison) and rare vs common flat runs (now defined as "pattern change" comparisons). This allowed a determination of the effect of the longer-sequence role alone on the P300 subcomponents, independent of the physical makeup of the run. Because each block contained many more common runs than rare runs, only common runs immediately preceding rare runs were retained for further analysis. After trials containing artefacts were removed, P300 data (neurotypical or hospice patient) were based on 29 to 55 rare runs of each type (between 60 and 107 rare trials total).

As our study requires reporting ERP responses for individual participants, I adopted definitions of the latency and scalp topography of the MMN, P3a, and P3b that were amenable to capturing individual differences in ERP spatio-temporal characteristics among neurotypical and hospice patients. Whereas the MMN typically peaks between 150 ms and 250 ms post stimulus onset (Näätänen et al., 2007), and the P300 can peak anywhere between 250 ms and 500 ms post stimulus onset (Polich, 2007), latencies of both ERPs are sensitive to stimulus properties and task demands. For example, MMN latencies are often shorter for larger frequency deviations (Näätänen et al., 2007), and P300 responses to targets that deviate in semantic compatibility are

often longer than those to targets that deviate in spatial compatibility (Polich, 2007). I expected, therefore, that MMN peak latency among neurotypical participants could be near the beginning of the typical interval. On the other hand, I expected that the peak latency of P300 responses would be different for each condition. In Blundon et al. (2017) I found that P3b peak latency was earlier (by about 135 ms) to tone-change targets than to pattern-change targets among neurotypical participants (Blundon et al., 2017), and that P3b peak latency to pattern-change targets was quite late (about 500 ms post stimulus onset). Recall that, in this latter condition, participants were asked to identify targets that were missing a tone change among standards that contained that tone change, making this a difficult search task to perform (Blundon et al., 2017). Finally, I expected that all ERP latencies for hospice patients could also be later, as P300 latencies can be longer among older adults (Anderer et al., 1996; Polich, 1996, 1997), and opioid medications may slow ERP latencies for some patients. While there is currently insufficient data to predict the effects of active opioid ingestion on MMN or P300 responses, some research has shown longer MMN and P300 latencies in opioid-dependent patients (Bauer, 2001; Kivisaari et al., 2007; Singh et al., 2009). On the other hand, some suggest that this relationship is an endophenotypic marker of substance-abuse, rather than an effect of the drugs themselves (Singh & Basu, 2009). To the best of my knowledge, there is currently no published research exploring the relationship between P300 amplitude and latency in patients being treated for pain with opioids. I, therefore, defined the MMN as an early negativity (0 and 300 ms), and the P300 as a late positivity (between 200 and 700 ms) after the onset of the last tone of each run type.

The MMN and P3a are typically maximal over fronto-central midline electrodes (eg FCZ or CZ, whereas the P3b is typically maximal over centro-parietal midline electrodes (eg PZ) (Näätänen et al., 2007; Polich, 2007). Because I expected some individual variability at which

electrode each ERP would be maximal (Näätänen et al., 2007; Polich, 1986), I extracted ERP data from the fronto-central (MMN and P3a) and centro-parietal (P3b) electrode where that ERP was maximal within its timerange (0 – 300 ms for MMN, 200 – 700 ms for P3a and P3b) and showed characteristic ERP-like morphology by visual inspection (i.e. had both a positive and negative deflection within its time range, where possible; see Table 3.3 for the list of electrodes used in this analysis). For the MMN, a difference wave was calculated for each participant by subtracting all flat runs from all change runs. Data from the fronto-central electrode with the maximal negative deflection of that difference wave during the MMN timeframe were retained for further analysis. A similar procedure was performed for P300s, where difference waves for each run type (change or flat) were calculated by subtracting common runs from rare runs. For each participant, data from the fronto-central and centro-parietal electrodes with the maximal positive deflections for each difference wave during the P300 timeframe were retained for further analysis. Because the frontal component of the MMN is often localized to anterior electrodes (Näätänen et al., 2012; Ruzzoli et al., 2012), electrodes for the MMN were restricted to fronto-central medial electrodes (midline plus one lateral electrode position, i.e. AF1 to AF2) between AFZ and CZ. The P3a, by contrast, is typically localized more centrally (Comerchero & Polich, 1999; Conroy & Polich, 2007; Polich, 1986, 2007), so fronto-central electrodes for the P3a were restricted to medial electrodes between FZ and CZ. Centro-parietal electrodes for P3b analysis were restricted to medial electrodes between CPZ and POZ.

	Frontal Electrodes			Posterior Electrodes	
	Change – Flat	Change (Rare – Common)	Flat (Rare – Common)	Change (Rare – Common)	Flat (Rare – Common)
Neurotypical					
N001	CZ	CZ	CZ	P1	PZ
N002	FCZ	FCZ	FCZ	POZ	CPZ
N003	CZ	CZ	CZ	PZ	PZ
N004	CZ	CZ	CZ	PZ	PZ
N005	FCZ	FCZ	FCZ	PZ	PZ

N006	C1	C1	C1	PZ	PZ
N007	CZ	CZ	CZ	POZ	PZ
N008	FCZ	FCZ	FCZ	P1	P1
N009	CZ	CZ	CZ	CPZ	CPZ
N010	CZ	CZ	CZ	CPZ	CPZ
N011	CZ	CZ	CZ	PZ	PZ
N012	FCZ	FCZ	FCZ	CPZ	CPZ
N013	CZ	CZ	CZ	PZ	P1
N014	FCZ	FCZ	FCZ	CPZ	CPZ
N015	CZ	CZ	CZ	PZ	PZ
N016	CZ	CZ	CZ	POZ	PZ
N017	CZ	CZ	CZ	PZ	PZ
Responsive					
P002	F2	FC2	FC2	P1	P1
P003	FC1	FCZ	FCZ	PO4	CPZ
P004	F1	FCZ	FCZ	PZ	PZ
P005	C2	C1	C1	PZ	PZ
P006	FZ	FCZ	FCZ	CPZ	PZ
P007	FC1	CZ	CZ	CPZ	CPZ
P008	FCZ	CZ	CZ	P2	P2
P009		FCZ	FCZ	CP1	CP1
Unresponsive					
P001	FC1	FCZ	FCZ	PZ	PZ
P002	F2	FC1	FC1	PZ	PZ
P004	CZ	CZ	CZ	PZ	PZ
P007	FC1	FC1	FC1	PZ	PZ
P008	FCZ	C1	C1	PZ	PZ

Table 3.3: List of electrodes from which ERP analyses were performed.

Meaningful individual ERP difference waves were determined using a modified cluster-based permutations test (Maris & Oostenveld, 2007). First, significant timepoints within individual ERP difference waves were determined by comparing conditions (change with flat for MMN, rare with common for P300s) using a paired *t* test for each timepoint. Similar to the analysis adopted by Bekinschtein et al. (2009), only ERP clusters of at least 5 consecutive significant time points (a sustained effect of approximately 20 ms) were retained for further analysis ($p < .05$ 1-tailed). Clusters calculated from ERP difference waves will hereafter be referred to as “real clusters”. Next, “sham clusters” were computed using the same procedure from surrogate permutations of each comparison ($n = 200$). Sham clusters were retained for

further analysis if they contained at least as many timepoints as the real cluster. To perform the cluster-based permutations analysis, each cluster (real or sham) was represented by the sum of all the *t* values within that cluster. Significance of the real clusters was determined by comparing the representative *t* statistic of each real cluster with a distribution of representative *t* statistics from sham clusters. The proportion of sham *t* statistics that exceeded the real *t* statistic served as each real cluster's *p* value . A cluster was deemed meaningful if its *p* value was smaller than the Bonferroni corrected alpha value (0.05/173 real clusters = 0.0003). While only meaningful clusters are reported in Figures 3.1 and 3.2, each timepoint within those clusters is represented by its own *p* value so that the reader can appreciate the morphology of each individual difference wave. A significant positive deflection (i.e. a significant real cluster where the rare run was larger than the common run) at a fronto-central electrode was classified as a P3a, whereas a positive deflection at a centro-parietal electrode was classified as a P3b. A negative deflection at a fronto-central electrode (i.e., a significant real cluster where the change run was more negative than the flat run) was classified as an MMN. I adopted a somewhat less conservative version of the analysis employed in the original study because, unlike Bekinschtein et al. (2009), my goals were not to develop a diagnostically helpful tool for assessing awareness in behaviourally unresponsive patients, but to explore whether some cognitive mechanisms required to support auditory attention may remain functional close to death. In other words, the goal of this Chapter was to see if hearing is even possible for unresponsive, actively dying hospice patients.

3.3 Results

3.3.1 Controls

Grand average ERPs for controls are shown in Figure 2.1. Recall that controls generated a P3b to both tone and pattern changes, and a P3a to tone changes only. P3b to tone changes was

approximately 150ms earlier than that to pattern changes. Additionally, controls generated an early negativity to tone changes but not to pattern changes. Consistent with Bekinschtein et. al. (2009) I'm interpreting this negativity as an MMN, as its scalp topography (maximal at fronto-central electrodes, inversion at temporal sites) and latency (within 100-250ms post-stimulus onset) is consistent with that of an MMN (c.f. Näätänen et al., 2007).

All (17/17; 100%) controls showed some evidence of early (0 – 300ms) frontal negativity (MMN) or late (200 – 700 ms) fronto-central positivity (P3a) to tone changes (see Figure 3.1 for an overview of individual ERP and RT results for the neurotypical participant group). Similarly, most generated a late centro-parietal positivity (P3b) to tone changes (16/17; 94%) or to pattern changes (15/17; 88%). Several (13/17; 76%) control participants generated a late fronto-central positivity to pattern changes, but many of these responses were weak ($0.5 < p <= 0.1$), and, like the centro-parietal responses to pattern changes, the latencies of the responses varied considerably more than those to tone changes. Hit rates were at or near ceiling for most participants (93 – 100 %), save for participant N011, who only detected 29% of the tone changes, and participants N003 and N015, who detected 78% and 59% of pattern changes, respectively. Reaction times (RT) and P3b peak latencies appear to co-vary (statistics not reported due to insufficient variability in the RT and peak latency data).

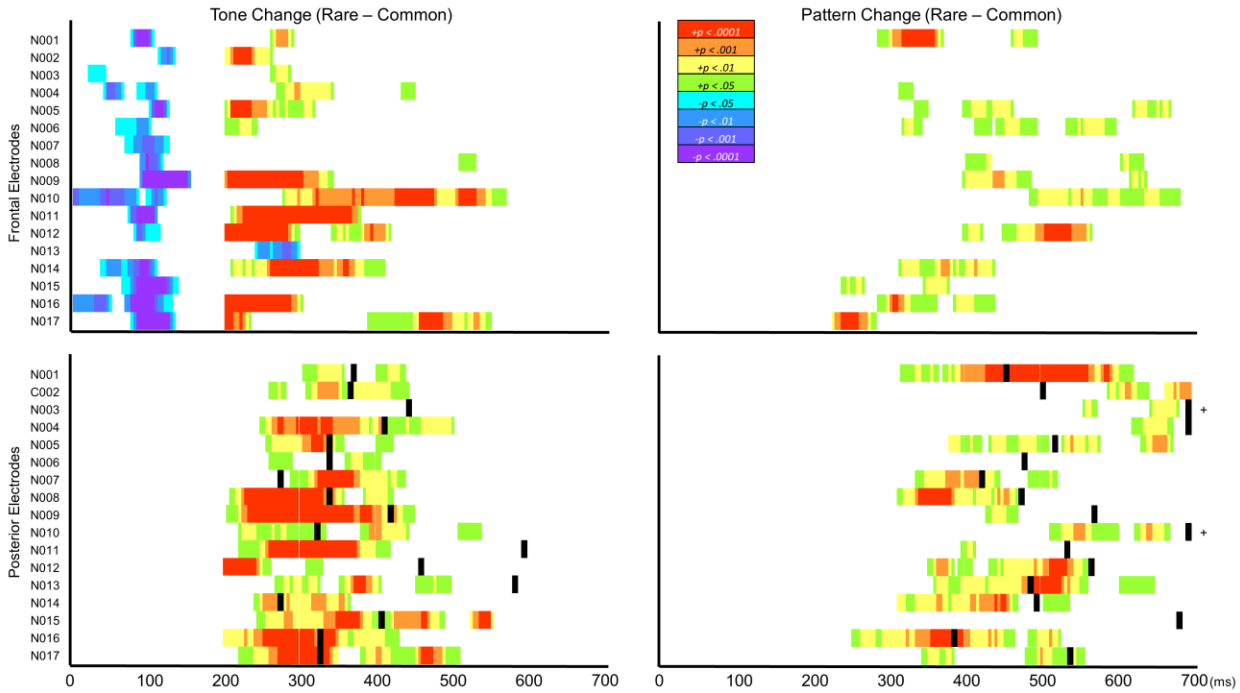

Figure 3.1: Individual differences in ERP and reaction time (RT) responses from neurotypical control participants (N001-N17) to local tone deviants (left) and global pattern deviants (right).

Warm colours (green through red) represent positive deflections in the difference wave for tone and pattern deviants when they were rare targets (rare – common). Cool colours (blue through purple) represent negative deflections in the difference wave for all tone deviants regardless of whether they were common or rare (change – flat). Black represents each participants' approximate reaction time. Black time points with a plus sign (+) outside the grid represent RTs that were longer than the last time point in the grid. Each row represents a participant (participant ID is listed to the left of each row). MMN (cool colours) and P3a (warm colours) responses were measured from the fronto-central electrode, and P3b (warm colours) responses were measured from the centro-parietal electrode, where the response to the rare run (or change run for MMN) was largest for each participant (see Table 3.3 for the list of electrodes used in this analysis). Only significant time points at $p < .05$ (1-tailed) are in colour. Only significant timepoints ($p < 0.05$) within meaningful time point clusters ($p < 0.0003$ determined from permutations cluster test) within the MMN (0 – 300ms) and P300 (200 – 700ms) timerange are shown. Colours correspond to the probability (p value) that the difference between rare and common runs (or change and flat runs) at that time point is 0.

3.3.2 Patients

3.3.2.1 Responsive Hospice Patients

Similar to control participants, all responsive hospice patients showed some evidence of either an early frontal negativity (MMN), or a late fronto-central positivity (P3a), or both, to tone changes. By contrast, only half (4/8; 50%) showed some evidence of late centro-parietal positivity (P3b) to tone changes. Latencies of both fronto-central and centro-parietal positivities to local tone changes were, in general, longer among responsive hospice patients compared to controls. Very few (2/8, 25%) responsive patients showed evidence of centro-parietal positivity (P3b), and none showed evidence of fronto-central positivity, to pattern changes.

3.3.2.2 Unresponsive Hospice Patients

Consistent with control and responsive participants, all (5/5) showed some evidence of either an early fronto-central negativity (MMN), or a later fronto-central positivity (P3a), or both, to tone changes. None of the unresponsive patients showed a centro-parietal positivity (P3b) to the tone changes. One unresponsive patient (20%) showed evidence of a weak late fronto-central positivity (P3a) to pattern changes, and two patients showed stronger centro-parietal positivity (P3b) to pattern changes. See Figure 3.2 for an overview of the results for both responsive and unresponsive hospice patients.

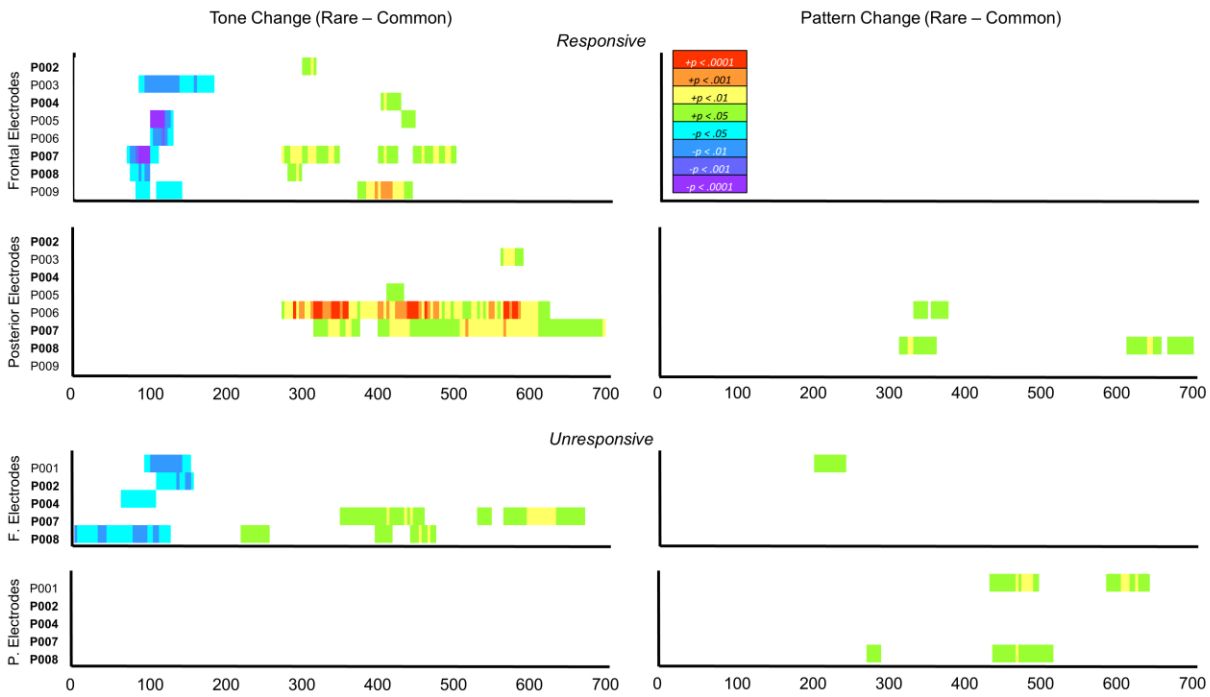

Figure 3.2: Individual differences in ERP responses from both responsive (top panel) and unresponsive hospice participants (P001-P009) to local tone deviants (left) and global pattern deviants (right).

Warm colours (green through red) represent positive deflections in the difference wave for tone and pattern deviants when they were rare targets (rare – common). Cool colours (blue through purple) represent negative deflections in the difference wave for all tone deviants regardless of whether they were common or rare (change – flat). Each row represents a participant (participant ID is listed to the left of each row). MMN (cool colours) and P3a (warm colours) responses were measured from the fronto-central electrode, and P3b (warm colours) responses were measured from the centro-parietal electrode, where the response to the rare run was largest for each participant (see Table 2.3 for the list of electrodes used in this analysis). Only significant timepoints ($p < 0.05$) within meaningful time point clusters ($p < 0.0003$ determined from permutations cluster test) within the MMN (0 – 300ms) and P300 (200 – 700ms) timerange are shown. Colours correspond to the probability (p value) that the difference between rare and common runs (or change and flat runs) at that time point is 0.

3.4 Discussion

This chapter presents evidence that at least a few actively-dying hospice patients, when they are unable to respond to family or healthcare provider verbal stimuli, nonetheless seem to be

hearing and giving neural responses to sequences of simple auditory stimuli. This is consistent with the trope that hearing is the last to go when a person is dying and lends some credence to the advice that loved ones should keep talking to a dying relative as long as possible. Importantly, this analysis revealed a "local effect," either an MMN or a P3a or both, to tone changes in 100% (17/17) neurotypical participants, and a "global effect," namely a P3b, to both tone and pattern changes in most (88 – 94%) of the neurotypical participants. For comparison, using their highly similar paradigm, Bekinschtein et al. (2009) were able to detect both local and global effects in all 11 of their neurotypical participants who counted oddballs. It should be noted, however, that although Bekinschtein et al. (2009) defined local and global effects similarly, they did not clearly differentiate between P3a and P3b effects by separating analyses of stimuli expected to produce the two effects (here tone change and pattern change). They simply combined all rare global targets, whether tone change or pattern change, together in their analyses of the global effect, similarly to how they (and I) combined all local tone change stimuli together in analyses of the MMN. Moreover, they assessed responses recorded at several (10 or 20) electrodes to measure both local and global effects. In contrast, I analysed responses to tone change and pattern change stimuli separately and observed the effects at specific electrodes where P3a and P3b effects are typically largest. This latter approach allows a more precise inference about which underlying brain processes are likely still functioning effectively. Nonetheless, in combination with the results of Bekinschtein et al. (2009), it seems that this paradigm is a valid one for indexing functioning of auditory change detection networks in neurotypical participants, which implies that similar results with unresponsive patients can be taken to indicate functioning of these networks.

The results for responsive and unresponsive patients are also consistent with reports that minimally conscious state (MCS) and unresponsive wakefulness state (UWS, formerly vegetative state, or VS) (Laureys et al., 2010) patients in a similar auditory search paradigm evidence local effects, and a few even show global effects (Bekinschtein et al., 2009). Because neurotypical participants who were engaged in mind wandering or a distracting task seldom showed global effects, this implies especially that when global effects are seen in an individual participant, in particular the P3b, there is some reason to believe conscious awareness of the stimuli is mediating responses. At the least, the presence of local and/or global effects in a DOC or unresponsive patient in this paradigm implies that auditory change networks in these patients are functioning similarly to those of healthy neurotypical participants. Moreover, a few patients in UWS also give fMRI evidence that they can control their brain responses on request (Bekinschtein et al., 2009; Cruse et al., 2011, 2012; Fernández-Espejo & Owen, 2013; Goldfine et al., 2013; Laureys et al., 2005; Owen et al., 2006, 2007). Thus, either when severely damaged or even when near death, some brains can evidence functioning in some systems.

It is worth pointing out that even some young, healthy, neurotypical participants failed to generate clear P3b responses to auditory change targets, and that the absence of these P3b responses does not imply that the participant was not attending to the targets. Recall that four neurotypical participants failed to generate detectable P3b responses to either tone or pattern changes, but neither reduced accuracy nor longer reaction time consistently co-occurred with the missing P3b responses (see Figure 3.1 and results section). In fact, for 3 of these participants, hit rates in the condition with the missing P3b were near ceiling (94 – 100 %). This suggests that should a participant fail to generate a P3b response to auditory change targets during a single EEG recording session, this does not imply that they were not able to detect the targets during

that session. Furthermore, one participant (N011) generated a clear P3b response to tone changes despite having only behaviourally responded to 30% of the targets. This may be due to a lapse in focused attention (somnolence?) in the middle of each tone change block, as their accuracy was high at the beginning and the end of those blocks, but they stopped responding in the middle.

These inconsistencies in neurotypical performance can inform the interpretation of the hospice patient performance. For example, both P001 and P008 generated a P3b to pattern changes, but not to tone changes, when they were unresponsive. This implies a rather shocking result; that these participants were able to perform the more difficult task of counting rare patterns that contained no salient feature but could not perform the much easier task of counting rare patterns that contained a highly salient feature. While this pattern of responses was atypical among responding neurotypical participants, N003 showed a similar pattern, where they failed to generate a P3b to tone changes but generated a P3b to pattern changes. Furthermore, N003's behavioural accuracy in the tone change condition was much higher (100%) than in the pattern change condition (78%). Finally, P008 also only generated a P3b to pattern changes and not to tone changes when they were responsive. This means that the pattern of responding demonstrated by both P001 and P008 when they were unresponsive is consistent with a pattern of responding demonstrated by a conscious, healthy, neurotypical brain, and a responsive hospice patient. It is, therefore, plausible, that P001 and P008 were aware of their auditory environment at the end of their lives.

It is still unclear how the partial functioning of the auditory change detection system I have reported here relates to normal conscious awareness, in spite of arguments from the existing literature (Fernández-Espejo & Owen, 2013; Ribary et al., 2019) It is simply unknown how much cortical and sub-cortical functioning is required to support even simple phenomenal

conscious awareness. It has been shown that conscious awareness is not lost even when up to half of cortex is removed during resections done to ameliorate epilepsy, although of course there are clear cognitive deficits in these cases (Penfield & Jasper, 1954). It is possible that even partial functioning of a cortical-sub-cortical system results in some awareness even if that awareness cannot be communicated to observers.

Chapter 4: Individual spatio-temporal dynamics underlying P3a and P3b among neurotypical and hospice patients

In this Chapter I characterize the spatio-temporal network dynamics underlying exogenous (P3a) and endogenous (P3b) attention processes among individual neurotypical controls, as well as among responsive and unresponsive hospice patients. In Chapter 3 I showed that most neurotypical controls, but only some hospice patients, generated a P3a to highly salient deviant tones, and a P3b to both tone and pattern deviant auditory patterns. Failure to generate either or both of these ERP responses to auditory deviants does not necessarily imply that a patient was not attending, in some manner, to the tones (c.f. Schiff et al., 2002). Complex functional networks of neural regions underly each of the attentional processes associated with the P3a and P3b (c.f. Corbetta & Shulman, 2002; Fox et al., 2005; Polich, 2007). In Chapter 2 I established that the primary (neurotypical) neural generators of the P3a are midline frontal regions associated with the ventral attention network (VAN), and that the primary neural generators of the P3b are parietal regions associated with dorsal attention network (DAN) and with detecting auditory oddballs (ODD). It is possible that some aspects of these networks remained engaged, even when a patient did not generate an ERP response to tone deviants. The goal of this chapter was, therefore, to identify any evidence of attention network activity among hospice patients, whether or not they produced clear ERP signals to tone and pattern deviants. The control data analysed here are the same as those reported in Chapters 2 and 3.

4.1. Materials and Methods

All aspects of the study participants (control and patients), ethics statement, stimuli, procedure, EEG recording, and EEG preprocessing are identical to those described in Chapters 2 (controls) and 3 (patients), unless otherwise specified.

4.1.1. Artefact rejection and source localization

As in Chapter 2, all artefact rejection and source localization were performed using independent component analysis. For both controls and patients, a notch filter between 55-65Hz, was applied to channel data before running ICA. An additional 3Hz high-pass FIR filter was applied to channel data before ICA. This additional filter was applied to patient data because many had considerable contamination from low frequency noise. While ICA was able to isolate this low-frequency noise (allowing for its removal from the channel data in Chapter 3), remaining data quality was so low that most remaining ICs did not have good single dipole fits. After applying the filter, IC source fits improved considerably.

For patients, rejection of EMG and eyeblink artefacts, source localization, local spectral power, and functional connectivity analyses were all conducted on independent components (ICs) from an infomax ICA (runica algorithm, EEGLAB) (Viola et al., 2009). Using a machine learning algorithm that was trained on 500,000 ICs, some labeled by EEGLAB experts (ICLabel in EEGLAB) (Pion-Tonachini et al., 2019) each IC was classified as the most likely generator of the IC (i.e. brain, eyeblink, channel noise, etc.) based on IC parameters, e.g., activation, shape of the power spectrum, and localization inside Montreal Neurological Institute (MNI) brain space. The neural source of each IC was estimated using the EEGLAB dipfit algorithm, based on electrode locations co-registered to the MNI average brain. ICs included for further analysis ("valid ICs") met the following criteria: 1) single dipole source fit accounted for at least 80% of the variance of the IC's electrode weights, 2) highest probability classification was "brain", 3)

probability the IC was classified as "brain" was at least twice that of the next highest classification. ICs that didn't meet the 3rd criterion were still retained for further analysis if they displayed 1/*f* –like power spectra and scalp maps resembling that of a single dipole. This method of artefact rejection was not used in previous chapters because the machine-learning algorithm was not yet available when those analyses were conducted. For control data, all subsequent analyses were performed on valid ICs localized to one of the network clusters reported in Chapter 2.

4.1.2. ROI clustering

ROI locations identified in Chapter 2 were seeded for each patient's valid ICs. These seed locations are reported again in Table 4.1. Like the seeding algorithm described in Chapter 2, the Euclidean distance between each seeded ROI and each patient's valid ICs was computed for each patient separately. Only ICs within a maximum distance of 35mm from any seeded ROI were retained for further analysis. If an IC was within 35mm of more than one seeded ROI, then it was classified as the nearest ROI.

Region of Interest (ROI)	Brodmann Area (BA)	Number of participants	Cluster Centroid Talairach Coordinates	Average % variance accounted for
LMFG	9	13 (76%)	-30, 22, 25	89.10
SMA/Cing	6/24	12 (71%)	6, -4, 52	88.68
ACC		12 (71%)	-1, 7, 11	85.46
PCC	31	16 (94%)	9, -59, 23	90.84
RTPJ	40	11 (65%)	40, -56, 36	89.34
LTPJ	39	13 (76%)	-30, -67, 26	90.43
RSPC	5	15 (88%)	18, -34, 50	88.35
LPreCG	4	15 (88%)	-21, -23, 49	88.84
Occ	18	13 (76%)	1, -89, 9	90.34

Table 4.1. Details of the 9 valid control clusters identified in Chapter 2.

The cluster Talairach centroids were used as seed locations to identify ROIs among patients. This table is identical to Table 2.1.

4.1.3. Event Related Spectral Perturbations (ERSPs)

The analyses described here were common to both controls and patients. As in Chapter 2, local power (ERSPs) of each valid IC was compared between rare and common runs. In this analysis, however, differences in ERSPs averaged over epochs were computed between rare and common runs *of the same type* (rare change – common change, and rare flat – common flat). Significant differences between runs were masked at $p < 0.01$ by EEGLAB's permutation test. ERSPs were grouped into 100 ms bins from 0 to 1000 ms post stimulus onset, and 4 frequency vectors similar to those described in Chapter 2. A longer time interval was used in this analysis (compared to the shorter time interval – up to 500 ms after the final tone in a run – used in the group analysis reported in Chapter 2) because I expected that ERSP latencies to rare runs might be longer among patients compared to controls, as was demonstrated in the ERP analysis reported in Chapter 3 (see Figures 3.1 and 3.2). To accommodate individual variability of participant peak frequencies, a broader definition of alpha (8 - < 15 Hz), beta (15 - < 30 Hz) and gamma (30 - < 50 Hz) was applied. The theta band (4 - < 8 Hz) remained the same as in Chapter 2. If a 100ms bin contained more than 12 (50%) non-zero time points, then the bin was deemed meaningfully different. Family-wise error estimates are reported in the results.

4.1.4. Phase-locking Values (PLVs)

Intracortical coherence (PLVs) analyses were similar to those described in Chapter 2, with some modifications to preserve individual variability within participant groups. The analyses described here were common to both controls and patients. Like Chapter 2, phase locking values were computed from the wavelet decomposition of each IC's activation. All ICs localized to a seeded region were included in this analysis, including those localized to bilateral TPJ and occipital cortex, which were removed from the synchrony analysis in Chapter 2. For

each IC pair, PLVs were first baseline corrected from -150 to -50 before the onset of the first tone in the run. Then they were compared across conditions (rare - common) against a surrogate distribution of sham differences between PLVs compiled from rare and common epochs of the same run type (N = 200 permutations). Only PLVs above the maximum value of this distribution were retained for further analysis ($p < 0.005$, 1-tailed). Significant PLVs between conditions were grouped into 100 ms bins from 0 ms to 1000 ms post stimulus onset (10 time-bins in total). Because each 100 ms bin contained 24 time points, only bins with at least 7 between-condition-significant PLV timepoints within each frequency band were considered meaningful. Family-wise error estimates are reported in the results. PLVs were grouped into their network of interest based on the brain region their ICs were localized to (see Chapter 2).

4.2. Results

4.2.1. Cluster Results

Control cluster results were the same as those reported in Chapter 2 (see Table 4.2). Among responsive patients, 8 of the 9 seeded ROIs had at least 50% of the patients contribute ICs. Talairach coordinates of responsive clusters remained within their seeded regions. Unresponsive patient clusters, however, were not as consistent with the seeded ROIs. The cluster seeded with Talairach coordinates localized to R SPC resulted in a cluster centroid localized to the PCC, and the cluster seeded with coordinates localized to PCC (which only contained one IC) resulted in a cluster centroid localized to Occ. These regions were relabeled accordingly. Only 6 clusters had at least 50% of the unresponsive patients contribute ICs.

ROI	*Control (n = 17)*	*Tal Coords (x, y, z)*	*Resp. (n = 8)*	*Tal Coords (x, y, z)*	*Unresp. (n = 5)*	*Tal Coords (x, y, z)*

L MFG	13 (76%)	-30, 22, 25	5 (63%)	-33, 15, 19	3 (60%)	-35, 33, 41
SMA/Cing	12 (71%)	6, -4, 52	5 (63%)	7, 2, 54	4 (80%)	7, -4, 57
ACC	12 (71%)	-1, 7, 11	7 (88%)	1, 14, 16	5 (100%)	6, 22, 20
PCC	16 (94%)	9, -59, 23	5 (63%)	8, -49, 19	4 (80%)	21, -24, 37
R TPJ	11 (65%)	40, -56, 36	3 (38%)	41, -58, 36	3 (60%)	33, -50, 31
L TPJ	13 (76%)	-30, -67, 26	5 (63%)	-32, -70, 11	3 (60%)	-31, -55, 14
R SPC	15 (88%)	18, -34, 50	5 (63%)	18, -26, 47	0	--
L PreCG	15 (88%)	-21, -23, 49	8 (100%)	-19, -20, 48	3 (60%)	-19, -29, 54
Occ	13 (76%)	1, -89, 9	4 (50%)	7, -82, 17	2 (40%)	-20, -99, 3
Total ICs	***120***		***47***		***27***	
Mean ICs per participant	***8***		***6***		***6***	

Table 4.2. Characteristics of seeded ROIs per participant group.

Cochran's Q tests (IC contributions to each region were treated as binary: participant score =1 if at least 1 IC localized to that region, = 0 if none), performed on all regions revealed that ICs were not evenly distributed among all ROIs (control: $Q(8) = 1069.43$, $p < .001$; responsive: $Q(8) = 101.29$, $p < .001$; unresponsive: $Q(8) = 66.38$, $p < .001$). McNemar's tests to determine if the brain regions with the largest proportion of patient IC contribution (SMA/Cing, ACC, and PCC) were significantly larger in area than other regions were not significant (Bonferroni corrected $p = 6.94\text{x}10^{-4}$).

4.2.2. ERSP Results

ERSP analyses were conducted on a total of 194 ICs across all three participant groups. The cumulative probability of obtaining at least 12 successes out of 24 at $p = 0.01$, $q = 1 – p = 0.99$, is = $2.42\text{x}10^{-18}$. Family-wise error for conducting such analyses on 10 time bins x 4 frequency bands x 2 conditions x 194 ICs = $3.72\text{x}10^{-14}$.

4.2.2.1. Controls

Because of the large volume of individual ERSP data computed for this analysis, I used the group results reported in Chapter 2 to guide the characterization of the time course and spatial distribution of local power changes among individual control participants (see Fig 4.1). Recall from Chapter 2 that SMA/Cing and ACC showed sustained post-stimulus (100-400ms) theta ERS (and alpha ERS in SMA/Cing) to tone changes, but not to pattern changes. This pattern of local power activity was also found among individual responses to tone changes, as 75-83% of ICs localized to those ROIs evinced early (0 to 500ms) theta ERS. This resulted in 14/17 (82.4%) of all controls with early (0 to 500ms) theta ERS in either one or both of those ROIs. Interestingly, 67-75% of ICs also evinced early theta ERS to *pattern* changes, resulting in 13/17 (76.5%) of all controls with early theta ERS to pattern changes, and 11/17 (64.7%) with early theta ERS to both tone and pattern changes, in these same ROIs. Early theta ERS to pattern changes was not observed in the group average results of ACC and SMA/Cing activity reported in Chapter 2. Early frontal theta ERS was not significantly correlated with the presence of a P3a in the individual data, regardless of deviant type (tone or pattern) ($r(16) = 0.15$, $p = .40$).

Group-level analyses reported in Chapter 2 revealed post-stimulus (100-200ms) theta ERS in L PreCG to tone changes, and later ERS (300-500ms) to pattern changes. This pattern was not evident in individual responses, as 80% of ICs localized to L PreCG evinced early (0-500ms) theta ERS to tone changes, but only 47% to pattern changes. Furthermore, group-level analyses reported early (0-500ms) theta ERS to tone changes, but not to pattern changes, in R SPC, and the opposite pattern in L MFG. The proportion of ICs localized to either R SPC or L MFG that showed early theta ERS, was, however, similar between tone changes (67% and 54%, respectively) and pattern changes (60% and 62%, respectively).

Chapter 2 reported later (200-500ms) beta ERD to tone changes, but not to pattern changes, in SMA/Cing, R SPC, and L PreCG. This pattern was only evident in R SPC, where 87% of ICs localized to this region showed later (200-700ms) beta ERD to tone changes, but only 67% to pattern changes. The opposite was true for L PreCG, where 60% of ICs showed beta ERD to tone changes, but 80% to pattern changes. A similar proportion of ICs localized to SMA/Cing showed later beta ERD to tone changes (75%) and to pattern changes (83%).

c

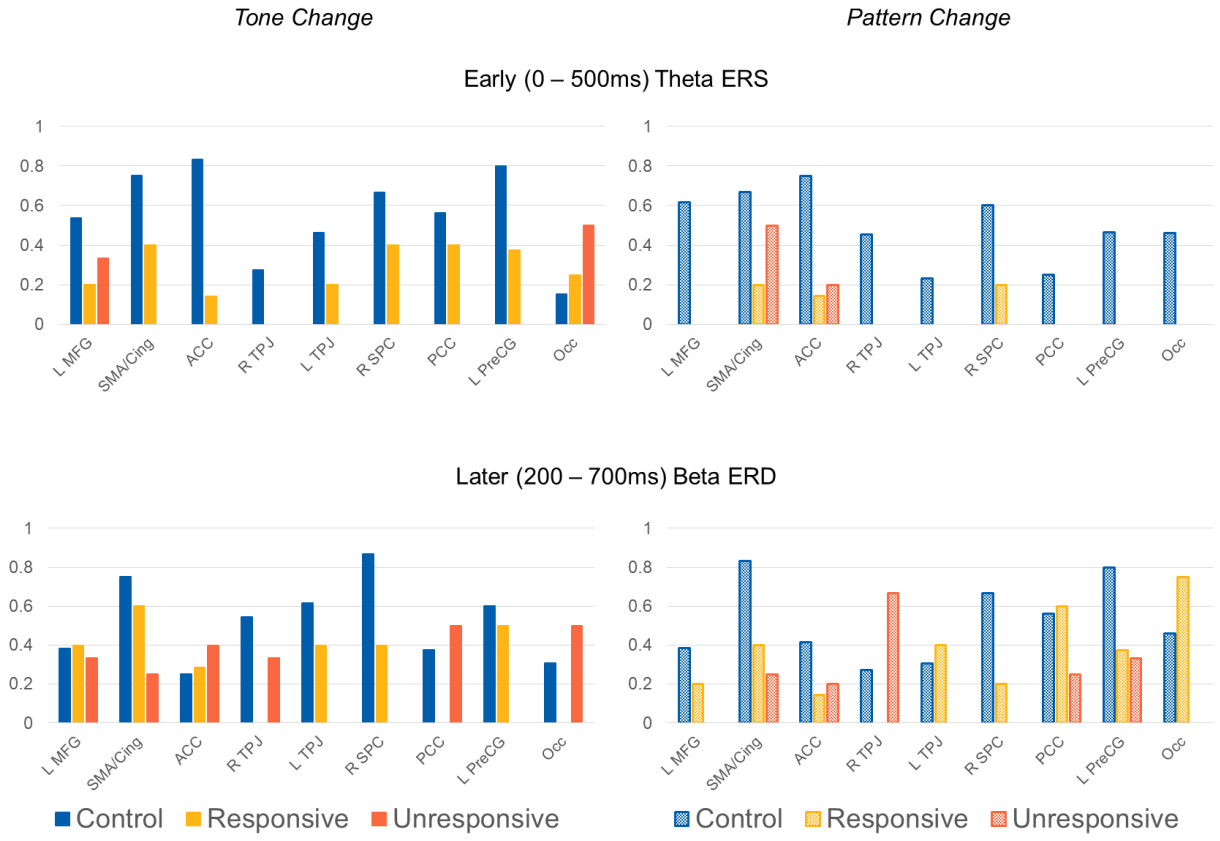

Figure 4.1. Proportion of participants that evinced early theta ERS (top) and later beta ERD (bottom) to tone changes (left) and pattern changes (right) for each ROI.

Taken together, most controls evinced early frontal (ACC or SMA/Cing) theta ERS or later centro-parietal (SMA/Cing, R SPC or L PreCG) beta ERD to both tone (17/17, 100%) and to pattern (15/17, 88%) changes (see Figure 4.2). Because these results are stable and uniformly observed for individual neurotypical controls, they will be used to guide the subsequent analysis of hospice patients.

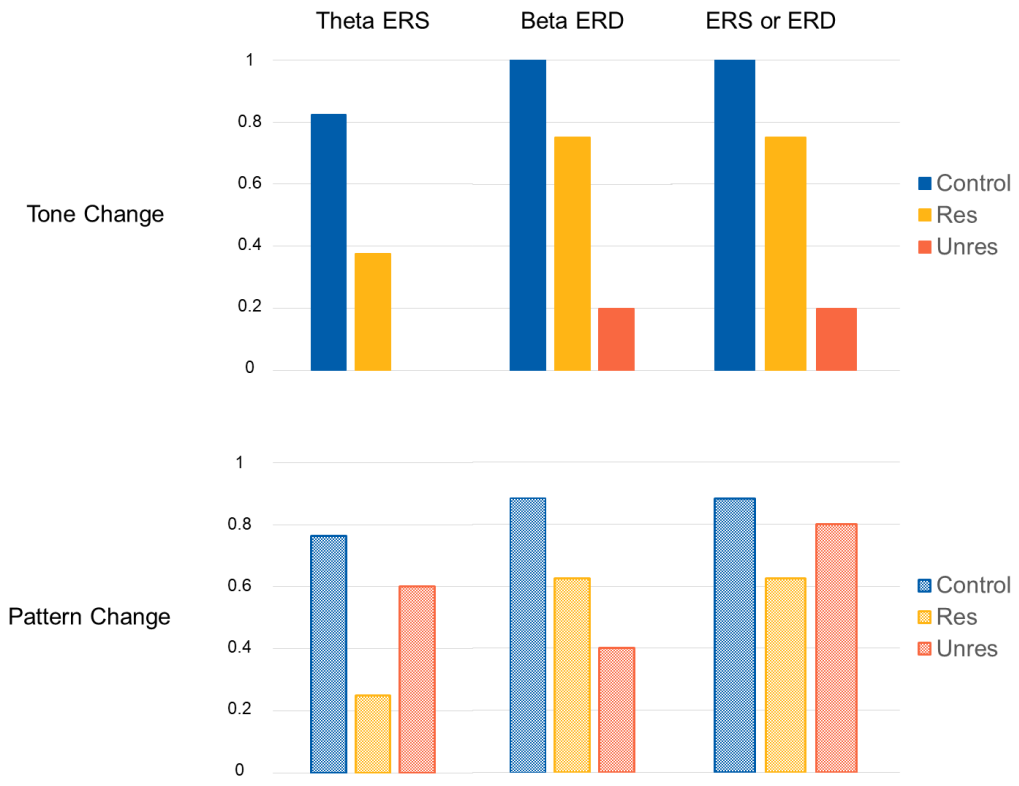

Figure 4.2. The proportion of participants that showed early frontal (ACC/SMA/Cing) theta ERS (top) or later centro-parietal (SMA/Cing/R SPC/L PreCG) to tone changes (top) or pattern changes (bottom).

4.2.2.2. Responsive patients

Only 3/8 (38%) of responsive patients evinced early frontal theta ERS to tone changes, and only 2/8 (25%) to pattern changes. This is inconsistent with the reduction in P3a activity among the responsive hospice patients, and, like controls, there was no correlation between patients who generated a P3a and those who showed early frontal theta ERS, regardless of condition ($r(14) = 0.03$, $p = 0.90$). By contrast, 6/8 (75%) showed evidence of later centro-parietal beta ERD to tone changes, and 5/8 (63%) to pattern changes. Although the proportions are smaller, the similarity between conditions is consistent with controls. There was no correlation between later beta ERD and detection of P3b, regardless of condition ($r(14) = -0.22$, $p = 0.41$). Overall, 6/8 (75%) evinced either early theta ERS, or later beta ERD, to tone changes, and 5/8 (63%) to pattern changes.

4.2.2.3. Unresponsive patients

None of the unresponsive patients showed early frontal theta ERS to tone changes, and 3/5 (60%) showed evidence of early frontal theta ERS to pattern changes. By contrast, a single unresponsive patient (P008) showed evidence of late centro-parietal beta ERD to tone changes, and two patients (P004 & P008) to pattern changes. This resulted in only 1 patient showing evidence either of early theta ERS or of later beta ERD to tone changes, but 4/5 (80%) showing one or both to pattern changes.

4.2.3. Connectivity results

PLVs were computed for pairs of individual ICs associated with VAN (ACC, SMA/Cing, and R/L TPJ), DAN (L MFG and R SPC), and ODD (PCC, L PreCG, and Occ) networks. All ROIs were retained for this analysis because there was no obvious reason to exclude any clusters based on the patient ERSP results. Connectivity analyses were performed on a total of 555 valid

IC pairs across all 3 participant groups (see Table 4.3 for the total number of IC pairs per network per participant group). The cumulative probability of obtaining at least 7 successes out of 24 at $p = 0.005$, $q = 1 – p = 0.995$, is 2.51×10^{-11}. Our family-wise error for conducting such analyses on 10 time bins x 4 frequency bands x 2 conditions x 555 IC pairs = 1.11×10^{-6}.

# IC pairs per network	Control	Responsive	Unresponsive	Total
VAN	49	18	18	85
DAN	12	3	0	15
ODD	38	11	8	57
VANDAN	77	25	11	113
VANODD	121	42	25	188
DANODD	72	20	5	97
Total	369	119	67	**555**

Table 4.3. Number of valid IC pairs per network and per participant group.

4.2.3.1. Controls

As in Chapter 2, meaningful connectivity to tone changes was most prominent within and between VAN and DAN networks, and within the first 500 ms post stimulus onset. PLVs to tone changes were greater than to pattern changes, although when accounting for individual variability and the greater number of ROIs within the VAN network, the differences in connectivity between conditions reported here are less pronounced than in figure 2.7. The largest proportion of meaningful PLVs was in the theta band for both tone and pattern change conditions for all three groups (not shown). Thus I will focus here on those PLVs. The proportion of participants with meaningful early (0 – 500ms post stimulus onset) theta connectivity was similar for all networks between conditions, save for the VANDAN network where 15/17 (88%)

controls showed some evidence of early theta connectivity to tone changes, but only 10/17 (59%) to pattern changes (see Figure 4.3).

4.2.3.2. Hospice patients

Figure 4.3 also shows the proportions of hospice patients who had meaningful PLVs in the theta band between 0 ms and 500 ms after stimulus presentation. Note that the number of patients with ICs localized to the various regions was significantly lower than for neurotypicals, and thus several PLVs could not be computed. Three results stand out, however. First, and expectedly, overall a smaller proportion of patients evinced meaningful connectivity in these networks than did neurotypicals. This is true even of the responsive patients, likely, again, because of the medication regime they were experiencing. Second, individual responsive patients do show considerable evidence of connectivity, particularly between the networks, and responsive patients are more likely to show this connectivity than are unresponsive patients, again what could be expected. Third, the proportion of unresponsive patients who show meaningful VAN and VAN-ODD PLVs is surprisingly high, given the overall lower level of connectivity displayed by this group.

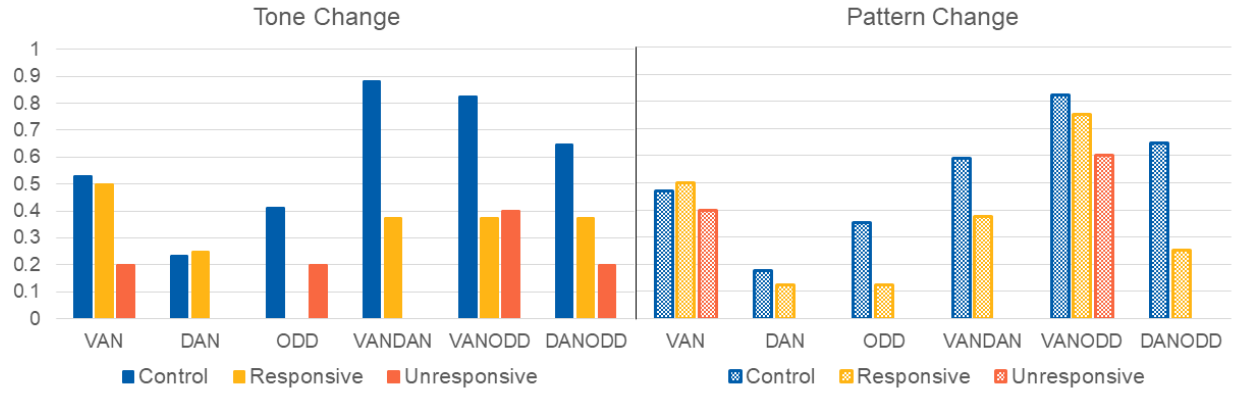

Figure 4.3. The proportion of participants with early (0 – 500ms) theta connectivity within each network.

4.3. Discussion

In this chapter I show that the majority of neurotypical control participants (88-94%) evince either early frontal theta ERS, or late beta ERD, to tone or pattern changes. If these patterns of local spectral activity are assumed to reflect active exogenous and endogenous attention processes in response to the different auditory oddball tasks, then it appears that similar attention mechanisms are being used to detect both tone and pattern changes. It seems that the group-level differences between these conditions reported in Chapter 2 are not reflected in which regions respond to tone or pattern changes, but rather in the timing of those responses. Many controls showed similar temporal dynamics associated with theta ERS and beta ERD to tone changes, but the dynamics associated with pattern changes varied more across participants. For example, theta activity in ACC peaked around 200-300ms post stimulus onset, with about 83% of ICs within ACC showing significant ERS to tone changes at that time bin. Theta activity to pattern changes, by contrast, peaked around 300-400ms post stimulus onset, with 58% of the ICs showing ERS in that time bin. There is a 25% difference in peak theta activity between tone and pattern change conditions, yet nearly the same number of ICs show some evidence of early theta ERS to both conditions. Furthermore, ICs had more time bins with significant ERS or ERD to tone changes than to pattern changes. For example, of the ACC ICs with significant early (0-500ms) theta ERS, the mean number of significant time bins was 4.2 to tone changes, and 2.7 to pattern changes. This is likely a common explanation, but not the only explanation, for the following discrepancies between the group-level ERSP results reported in Chapter 2, and individual results reported in this chapter.

First, group-level analyses revealed early (0-500ms post stimulus onset) theta ERS in ACC and SMA/Cing to tone changes, but not to pattern changes. Individual analyses, however, revealed a similar proportion of participants evinced early frontal theta ERS to both tone and pattern changes. Recall in the Chapter 2 discussion I hypothesized that these regions, which are associated with the ventral attention network (VAN), and saliency network in the case of the ACC, may be preferentially responsive to the salient feature of the change runs, as those regions displayed strong low frequency ERS only to rare change runs, and not to rare flat runs. The results of the present analysis, however, are inconsistent with that hypothesis, as approximately the same proportion of participants evinced theta ERS to pattern changes as to tone changes, and over half to both. This discrepancy may be in part because condition comparisons were different for the different analyses. In Chapter 2, rare change runs were compared to flat common runs, and rare flat runs were compared to common change runs, as this was consistent with typical search asymmetry paradigms. In Chapter 4, however, rare and common runs of the same run type were compared, i.e. rare change to common change, rare flat to common flat. This allowed for an evaluation of the local power changes that were associated with only the attentional demands of the task, without the influence of perceptual processes responding to the different features between change and flat runs. If ACC and SMA/Cing were, therefore, preferentially responsive to the salient feature of the change runs, there should be no difference in local power at those ROIs when comparing rare to common *flat* runs. Since a large proportion of controls showed evidence of early theta ERS to rare flat runs compared to common flat runs, these regions must, therefore, be involved in exogenous attentional processes in general, and not preferentially to detecting highly salient features. As discussed above, the only indication of preferential

engagement with the salient features of the change runs is the greater temporal consistency, and the larger mean number of significant time bins, to tone changes than to pattern changes.

Group-level theta ERS was also observed in R SPC to tone and not pattern changes, and in L MFG to pattern but not tone changes. Individual responses, however, revealed a similar proportion of participants with early theta ERS in R SPC and L MFG to both tone and pattern change. By contrast, group-level early theta was observed to both tone and pattern changes in L PreCG, yet 30% fewer ICs showed early theta ERS to pattern than to tone changes. Individual theta ERS responses are consistent with the network classification of each of these ROIs. Since R SPC and L MFG are associated with the DAN, it follows that DAN activity would be consistent across both conditions, as endogenous attention is required to detect both targets. The L PreCG, by contrast, is associated with detecting oddball targets, and, perhaps, early theta ERS in L PreCG is more strongly associated with detecting feature oddballs (i.e. change runs), rather than semantic oddballs (i.e. flat runs) (although early theta ERS in L PreCG was not correlated with P3a detection, regardless of deviant type) ($r(32) = 0.21$, $p = 0.24$).

Group-level beta ERD was observed to tone changes but not to pattern changes, whereas individual results revealed equivalent proportions of participants with evidence of parietal beta ERD to both tone and pattern changes. The similarity in parietal beta ERD to both tone and pattern changes among individual controls further supports the interpretation that beta ERD is associated with the movement (button press) controls made when they detected a rare target (Pfurtscheller & Lopes da Silva, 1999). The discrepancy between individual and group-level analyses is likely because in Chapter 2 only results until 500ms post stimulus onset are reported, and this time frame didn’t capture most of the beta ERD activity to pattern changes.

Connectivity group results were also different from individual results. Whereas in Chapter 2 connectivity within DAN to change runs was obviously the most prominent, in this analysis connectivity between VAN and DAN and between VAN and ODD were the most prominent. This was an unexpected result and may be partly because there were more possible VANDAN and VANODD connections available in Chapter 4 than there were in Chapter 2. Further work may be required to reconcile the differences between group and individual connectivity analyses.

Later centro-parietal beta activity among responsive patients was similar to that of controls. Interestingly, responsive patients were not asked to press a button when they heard each rare run, instead they were asked to count them because they would not be able to respond when unresponsive. I, however, did not tell patients they couldn't count on their fingers, and I seem to recall (though I have no record of this) that some may have done just that. In a future replication of this study, the relationship between beta ERD and behavioural response to rare runs should be further explored.

There was, by contrast, a considerable reduction in early theta ERS to both tone and pattern changes among responsive patients compared to controls (despite the prevalence of P3a responses to tone changes). The reduction in frontal ERS may imply that fewer responsive patients engaged in exogenous attention processes to detect either run type compared to controls. Essentially, the reduction in frontal theta activity implies that responsive patients had to focus more to detect the rare runs than did controls. This is consistent with my personal impressions of the task difficulty for responsive patients. While patients were all capable of detecting the change runs among flat runs, some indicated that it was difficult to sustain attention throughout each

block. Moreover, some patients could not reliably identify the rare flat runs among common change runs.

The proportion of unresponsive hospice patients that showed later centro-parietal beta ERD was similar to both tone and pattern changes. In fact, P008 showed beta ERD to both tone and pattern changes, and they also happened to be one of the two unresponsive patients who showed evidence of a P3a to tone changes. This is an encouraging sign that some attentional processes may have remained active for this patient when they became unresponsive. Recall that the beta ERD observed among controls and responsive patients may be associated with making small movements in response to rare runs. There is also evidence that beta ERD is generated when movements are imagined (McFarland et al., 2000); beta responses to motor movements have been used in the development of brain-computer interfaces (Coyle et al., 2015; Pfurtscheller & Neuper, 2006), and beta ERD to imagined hand and foot movements have been used as an EEG measure of awareness among DOC patients (Cruse et al., 2011, 2012) (although the results of that study are debated) (Goldfine et al., 2013). The detection of centro-parietal beta ERD among unresponsive patients, particularly P008 because they showed evidence of this response in both conditions, could be taken as a positive sign of motor imagery, and thus awareness of the rare runs, when they were unresponsive.

The fact that one patient, P004, showed evidence of later beta ERD to pattern and not to tone changes, is inconsistent with control and responsive patients, as no conscious participant showed a positive sign of beta ERD to only pattern changes. The pattern of unresponsive patient early theta ERS was atypical and unexpected. While no unresponsive patients generated early frontal theta ERS to tone changes, over half did to pattern changes. This is very inconsistent with control and responsive patients as a group, though 2 individual controls showed a similar pattern

of ERS activity. Given the inconsistency in early frontal theta ERS activity across participant groups, this signal may be less reliable indicators of active attentional processes than later beta ERD and the P3b.

The proportion of participants with early theta connectivity within any of the 6 networks was largest among controls compared to patients. About 50% fewer responsive patients showed early theta connectivity within the networks compared to controls, save for within VAN and DAN networks in either condition and VANODD network to pattern changes. The proportion of unresponsive patients that evinced connectivity within each of the networks was less than responsive patients, save for the VANODD network in either condition. This is most likely because the VANODD network had the largest number of possible IC pairs, and, therefore, had the greatest chance to produce meaningful connectivity. Nonetheless, the fact that several unresponsive patients did produce meaningful connectivity within the attention and auditory change detection networks suggests that they may indeed have been trying to count the rare tone runs. Furthermore, connectivity between frontal (VAN) and parietal (ODD) regions may be critical to support consciousness (Baars, 2005; Boly et al., 2012; Dehaene & Naccache, 2001; U. Lee et al., 2009).

The results of this analysis showed that the neural activity associated with attention mechanisms involved in detecting auditory oddballs is highly consistent among individual young, healthy, neurotypical control participants. Furthermore, there is evidence that very few responsive hospice patients recruited frontal regions associated with the VAN to perform this task, suggesting most of the responsive patients applied a focused attention strategy to detect the auditory deviants. There is also some evidence that one patient may have been engaging in endogenous attention processes while they were unresponsive. Finally, given the highly

consistent results of identifying neural sources in auditory tasks and then exploring local regional power and intra- and inter-regional connectivity for controls, it seems justified to attempt this approach for patients. Unfortunately, because of age, illness, and medication, responsive patients in the hospice do not produce results from this analysis that are at this level of consistency, and seem also to differ in strategy for accomplishing the task, making the changes in unresponsive patients difficult to interpret. Nevertheless, evidence of even an inconsistent level of responsiveness in attention and change detection networks among unresponsive patients implies that these networks might still be functioning when a person is only hours from death. These analyses, therefore, may offer an expanded perspective on what a patient might be experiencing while unresponsive.

Chapter 5: Electrophysiological evidence of default mode activation at the end of life

Recently, there has been growing interest in characterising pathological changes in cortical network activity in the so-called "resting state," where the participant simply relaxes with no task to perform, with the goal of adding to the diagnostic criteria for disorders of consciousness (J. S. Crone et al., 2011; Fernández-Espejo et al., 2012). The benefit of investigating resting state activity is that it does not require that unresponsive patients engage in challenging cognitive tasks that make considerable demands on limited cognitive resources. The most commonly studied resting state network is the brain's default mode network (DMN), a collection of medial fronto-parietal regions (Raichle et al., 2001) that are thought to support stimulus-independent thought (Buckner et al., 2008b). Preserved, yet altered, activation within DMN is associated with pathologic decrease in conscious state, such as loss of consciousness due to epileptic seizure (Danielson et al., 2011), and particularly among DOC patients (Hannawi et al., 2015). Decreased functional connectivity between nodes within the DMN has been associated with states of decreased consciousness, including during deep sleep, (Horovitz et al., 2009), anesthesia (Deshpande et al., 2010), and again among DOC patients (Boly, Phillips, et al., 2008; Vanhaudenhuyse et al., 2010). Long-range connectivity within DMN is also known to decrease with age (D. Tomasi & Volkow, 2012), particularly among connections that include the ventral PCC and dorso-medial PFC (Campbell et al., 2013; Wu et al., 2011). Changes in DMN connectivity may be associated with impaired consciousness among DOC patients (J. S. Crone et al., 2015), and measuring DMN activation and functional connectivity could be a beneficial complement to current methods of consciousness assessment (Fernández-Espejo et al., 2012; Vanhaudenhuyse et al., 2010).

While the specific function of the DMN remains unclear, the conventional view is that it supports internally-directed thought (Buckner et al., 2008a), which can include (but is not limited to) mind-wandering (Christoff et al., 2016; Kucyi et al., 2012), autobiographical planning (Spreng et al., 2008), internal mentation (Buckner et al., 2008a), scene construction (Hassabis & Maguire, 2007), and awareness of the self (Davey et al., 2016). The DMN may also be involved in aspects of externally-oriented cognition, such as passive surveillance of one's external environment (Hahn et al., 2007), spatial navigation (Spreng et al., 2008), and theory of mind (Spreng et al., 2008). Because there is currently no unified theory of DMN function, DMN activation and connectivity among unresponsive patients could support a variety of different conscious experiences. Low levels of of DMN connectivity, on the other hand, would most likely signal a pathological decrease in consciousness (Noirhomme et al., 2010).

Here I report activation of, and functional connectivity between, regions associated with DMN among young neurotypical controls and patients at rest. I expected that responsive patients would show patterns of DMN activation and connectivity similar to those of controls. In line with cited work with DOC patients, I expected that unresponsive patients would show reduced activation and reduced functional connectivity within DMN compared to responsive patients. The results of this study provide insight into whether or not unresponsive hospice patients at the end of life show residual signs of cortical function associated with internally-directed thought.

5.1 Materials and Methods

5.1.1. Controls and Ethics statement

A total of 30 participants were recruited through the community via posting at the Paid Participants Study List hosted by Psychology Graduate Student Council website, and remunerated $20 (CAD) for their participation (23 females; M = 24.5 years old, SD = 7.98; 28 were right-handed). All had no history of neurological problems and had normal or corrected-to-normal vision. Participants provided written informed consent to the experimental procedure, and the UBC Behavioral Review Ethics Board approved all procedures and protocols of this experiment.

5.1.2 Patients and Ethics Statement

Patients and ethics statement are the same as those described in Chapter 3.

5.1.3 Procedure

Data from all participants (controls and patients) were collected using a 64-electrode portable EEG system (Biosemi Active 2). Control data were sampled at 256 Hz, patient data sampled at 2048 Hz, downsampled to 256 Hz. Approximately 3 minutes of resting state data were collected from controls, 2 minutes from patients (thus about 46,080 data points per control, 30,720 per patient). Control data were collected at the end of another study (data not reported here), and patient data were collected in an interval between other parts of the protocol. Participants were asked to close their eyes and let their mind wander during rest. All other aspects of data collection pertaining to patients are the same as those described in previous chapters.

5.1.4 Artefact rejection and source localization

High-pass (3Hz) and low-pass (50Hz) FIR filters were applied to patient channel data only. All other aspects of artefact rejections and source localization pertain to both controls and

patients. Noisy channels and clear single-instance artefacts were removed. As in previous chapters, rejection of EMG and eyeblink artefacts, source localization, and functional connectivity analyses were all conducted on independent components (ICs). As in Chapter 4, only ICs classified as "brain" (ICLabel in EEGLAB) (Pion-Tonachini et al., 2019) and with good single dipole scalp map fits (> 85% scalp map variance accounted for by a single equivalent-current dipole model) were retained for further analysis (see Chapter 4 for complete details).

5.1.5 ROI clustering

Regions of interest (ROIs) within DMN were defined as those areas of significant BOLD activation that were consistent across the first two experiments reported in Raichle et al. (2001). These included dorso-medial prefrontal cortex (dMPFC), ventro-medial prefrontal cortex (vMPFC), posterior cingulate cortex (PCC), and inferior parietal lobule (IPL) (see Table 5.1 for seed locations). Although Raichle et al. (2001) only found left IPL and left-biased dMPFC, I also seeded these areas on the right. I converted the MNI coordinates reported in Raichle et al. (2001) to Talairach space and calculated the Euclidean distance between Talairach coordinates of the dipoles fitted to each patient's valid ICs and those of the seed regions. An IC dipole was grouped into an ROI if its distance from the ROI seed location was less than 35mm. If an IC dipole was within 35mm of more than one ROI, it was grouped into the nearest ROI.

Region	Abbreviation	Seed Talairach Coordinates (x, y, z)
Ventral-medial prefrontal cortex	vMPFC	-1, 42, -4
Left dorsal-medial prefrontal cortex	L dMPFC	-15, 53, 23
Right dorsal-medial prefrontal cortex	R dMPFC	15, 53, 23
Posterior cingulate cortex	PCC	-4, -46, 37
Left inferior parietal lobule	L IPL	-49, -50, 37

Right inferior parietal lobule	R IPL	49, -50, 37

Table 5.1. DMN regions and their seed coordinates in Talairach space.

Seed coordinates of the first four regions were taken from Raichle et al (2001). L IPL coordinates represent the mean between two regions within L IPL found by Raichle and colleagues. Coordinates for R IPL are equal and opposite to the L IPL coordinates.

5.1.6 Phase-locking Values (PLVs)

Phase synchrony analyses were conducted to determine the degree to which neural regions active during rest share information. First, valid IC activations were divided into 1000ms epochs. Because there were no pre-stimulus periods to act as a baseline, epochs were not baseline corrected. Second, a wavelet analysis generated a time-frequency decomposition of the activations of each valid IC for each participant (Makeig, 1993). This wavelet analysis produced a wavelet coefficient, which comprises a measure of instantaneous amplitude and phase, for each time point of IC activation at each frequency. To compute wavelet coefficients for the low frequencies, duplicates of each epoch were concatenated along the time dimension to generate 4000s epochs, where every 1000s was identical. After wavelet analyses were completed, only 1000ms from the middle (1500 to 2500 ms from the onset of the epoch) of each epoch were retained for further analysis. Third, phase locking values (PLV) (Lachaux et al., 1999) were computed for all possible combinations of valid IC pairs. Only PLVs for IC pairs that came from the same participant were computed. Non-significant PLVs within IC pairs were masked using a surrogate distribution (N = 200 permutations) generated for each time-frequency point ($p < 0.005$, 1 - tailed). The largest significant PLV value at each timepoint was extracted for four frequency bands (theta: 3 to < 8 Hz; alpha: 8 to < 12 Hz; beta: 15 to < 30 Hz; gamma: 30 to < 50 Hz). This resulted in 4 frequency vectors for each IC pair. Connectivity between two ICs at a

frequency band was considered meaningful if at least 50% of the timepoints within that frequency vector were significant (Bayesian probability of making a type I error reported in results). Only meaningful connectivity was retained for further analysis. Finally, meaningful connectivity between two ICs at a frequency band is represented by the mean PLV of all significant timepoints within that frequency vector. This resulted in a single PLV value for each IC pair at each meaningfully connected frequency band.

Connectivity between ICs that were localized to the same neural region are not reported. For example, if both IC A and B were localized to the PCC, then any meaningful connectivity between those regions was not reported. In cases where connectivity between two neural regions was represented by multiple pairs of ICs, only the largest PLV value at each frequency band was retained. For example, if IC C was localized to the vMPFC, then connectivity between IC pairs A-C and B-C both represent connectivity between PCC and vMPFC. In such cases, connectivity between PCC and vMPFC was represented by whichever IC pair (A-C or B-C) generated the largest PLV value for each frequency band. In other words, if A-C had a larger PLV than B-C at gamma, then gamma connectivity between PCC and vMPFC was represented by A-C. If B-C had a larger PLV than A-C at theta, then theta connectivity between PCC and vMPFC was represented by B-C.

5.2 Results

5.2.1 Controls

A total of 507 valid ICs were localized within brain space, and 207 were localized within DMN according to the seed locations described in Table 5.1. The mean number of DMN ICs per participant was 6.9, ranging from 2 to 17 ICs.

5.2.1.1 Sources localized to DMN

Most controls had at least one valid IC localized to PCC (97%) or IPL (77%) (see Table 5.2). Fewer than half of the controls had ICs localized to dMPFC (40%) or vMPFC (47%).

ROI	BA	% Part Cont	PVAF	% Brain	Coords
vMPFC	24	46.7	92.7	73.5	2, 31, -2
L dMPFC	9	26.7	93.3	76.5	-18, 33, 24
R dMPFC	9	23.3	96.3	97.6	18, 29, 21
PCC	31	96.7	93.5	93.7	-1, -47, 34
L IPL	n/a	50.0	91.5	95.6	-40, -45, 25
R IPL	39	66.7	93.7	94.5	36, -49, 26

Table 5.2. Details of seeded ROIs within DMN.

ROI = Region of interest. BA = Brodmann Area. Part Cont: proportion of patients who contributed at least one IC to each region. PVAF = mean percentage of variance accounted for by single dipole fits of ICs localized to each ROI. % Brain % = mean probability of IC being classified as brain. Coords = mean Talairach coordinates of all ICs localized to each ROI. vMPFC = Ventral-Medial Prefrontal Cortex, dMPFC = Dorsal-Medial Prefrontal Cortex, PCC = Posterior Cingulate Cortex, IPL = Inferior Parietal Lobule.

Cochran's Q tests (IC contributions to each region were treated as binary: participant score =1 if at least 1 IC localized to that region, = 0 if none), performed on all DMN regions separated by hemisphere (i.e. vMPFC, PCC, R dMPFC, L dMPFC, R IPL, L IPL), revealed that ICs localized to DMN were not evenly distributed among all regions within the DMN ($Q(5) = 182.32$, $p < .00001$). McNemar's tests were performed to determine if the regions with the largest proportion of patient IC contribution (PCC and RIPL) were significantly larger than other regions within DMN. IC contribution to PCC was larger than all other ROIs, and IC contribution to RIPL was larger than bilateral dMPFC only (see Table 5.3 for a complete list of p values from McNemar's tests).

Control	vMPFC	R dMPFC	L dMPFC	PCC	R IPL	L IPL

PCC	0.0002	2.38×10^{-07}	4.77×10^{-07}	--	0.005	0.0002
RIPL	0.09	0.0005	0.002	0.005	--	0.08

Table 5.3. p values of McNemar's test to compare the IC contributions of PCC and RIPL to other ROIs withing DMN.

5.2.1.2 Connectivity between neural sources at rest

PLV analyses were conducted on controls with valid ICs in two or more DMN ROIs (n_{con} = 25). This resulted in a total of 824 IC pairs. Recall that IC pairs were meaningfully connected at a given frequency band if at least 50% of the time points within that frequency band were significant at $p < 0.005$ (binomial probability of getting 128 or more successes in 256 trials, with binomial $p = 0.005$ and binomial $q = 1 - p = 0.995$, is less than 0.000001; experiment-wise probability of making a type I error is 824 IC pairs x 4 frequency bands x 0.000001 < 0.003). All controls had meaningful connectivity between every ROI localized to DMN within at least one frequency band. The proportion of participants with connectivity between ROIs within DMN were, therefore, proportional to the number of ICs they had in those ROIs (see Figure 5.1).

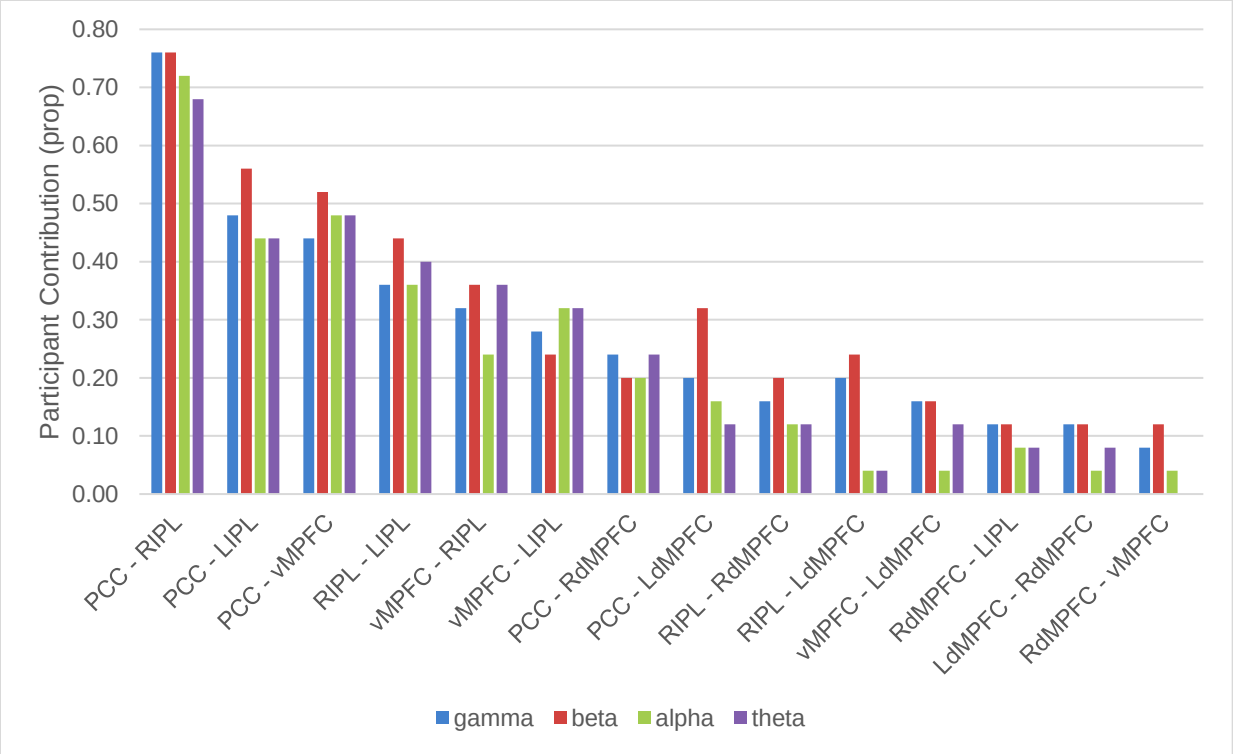

Figure 5.1. Proportion of controls with at least one meaningful connection between each ROI for each frequency band.

5.2.2 Patients

A total of 106 valid ICs were localized within brain space for both responsive and unresponsive patients (see Appendix D for list of all valid ICs, their locations, and single dipole fits). Fifty-eight valid ICs were localized within DMN, 40 from eight responsive patients, and 18 from five unresponsive patients. The mean number of valid DMN ICs per patient was 4.46, ranging from 0 to 9 ICs. One patient (P002) generated no valid ICs when responsive, and only one when unresponsive (see Discussion for more details about this specific patients' results).

5.2.2.1 Sources localized to DMN

For most responsive and unresponsive patients (88%), sources were localized to one of vMPFC or PCC (see Table 5.4). Only P002 had no sources localized to either of these regions (or any region within the DMN). Fewer (40-50%) patients contributed ICs to dMPFC and IPL.

Patient ID	vMPFC	PCC	dMPFC	IPL	**Total**
Responsive					
P002*					**0**
P003	1	3			**4**
P004*	6	2			**8**
P005	6		1		**7**
P006		1		1	**2**
P007*	2	2	2	3	**9**
P008*	1	3	1		**5**
P009	3	1		1	**5**
Total ICs	***19***	***12***	***4***	***6***	***40***
% Pat Cont	**0.75**	**0.75**	**0.38**	**0.38**	
Unresponsive					
P001	1	3		4	**8**
P002*					**0**
P004*	1	1	2		**4**
P007*	1	2	1	1	**5**
P008*		1			**1**
Total ICs	***3***	***7***	***3***	***5***	***18***
% Pat Cont	**0.6**	**0.8**	**0.4**	**0.4**	

Table 5.4. The number of ICs localized to regions within the DMN (either hemisphere) per patient.

Starred patients contributed data both when responsive and when unresponsive. "% Pat Cont" refers to the proportion of patients with ICs localized to an ROI.

Cochran's Q tests (IC contributions to each region were treated as binary: patient score =1 if at least 1 IC localized to that region, = 0 if none), performed on all DMN regions separated by hemisphere, revealed that ICs localized to DMN were not evenly distributed among all regions within the DMN (responsive ($Q(5) = 16.77$, $p = .005$; unresponsive ($Q(5) = 19.38$, $p =$

.002). McNemar's tests to determine if the regions with the largest proportion of patient IC contribution (vMPFC and PCC) were significantly larger than other regions within DMN were not significant (Bonferroni corrected α = .003) (see Table 5.5 for a complete list of p values from McNemar's tests). There was no significant difference in the number of active DMN regions between patient groups (M_{res} = 2.5, M_{unres} = 2.4, $t(11) = 0.11$, $p = 0.91$, equal variances assumed, $F(4,7) = 1.44$, $p = 0.31$), nor the distribution of active DMN regions between patient groups (Md_{res} = 2, Md_{unres} = 3, Mann-Whitney $U = 40$, $n_{res} = 8$, $n_{unres} = 5$, $p > .05$). Of the four patients who contributed data to both the responsive and unresponsive sessions (highlighted with asterisks in Table 5.4), the number of ICs per unresponsive patient localized to DMN (3.6) was nearly three-quarters of the number of ICs per responsive patient localized to DMN (5).

Responsive	vMPFC	R dMPFC	L dMPFC	PCC	R IPL	L IPL
vMPFC	--	.063	.065	1.00	.125	.313
PCC	.500	.094	.031	--	.063	.125
Unresponsive						
vMPFC	--	.500	.250	1.00	1.00	.500
PCC	.500	.250	.063	--	.250	.125

Table 5.5. List of p values for McNemar's tests comparing vMPFC and PCC (rows) to the remaining regions within DMN (columns), for both responsive (top) and unresponsive (bottom) patients.

To determine p values, the number of patients with at least one IC in vMPFC (or PCC) and not in the comparison region (x), to the number of patients who had no ICs in vMPFC (or PCC) and at least one IC in the comparison region (y). Exact p values represent the probability of obtaining x from a binomial distribution with size equivalent to x + y.

5.2.2.2 Connectivity between neural sources at rest

PLV analyses were conducted on patients with two or more ICs localized to DMN (n_{res} = 7, n_{unres} = 3). This resulted in a total of 152 IC pairs across both patient groups (binomial probability of getting 128 or more successes in 256 trials, with binomial $p = 0.005$ and binomial

$q = 1 - p = 0.995$, is less than 0.000001; experiment-wise probability of making a type I error is 152 IC pairs x 4 frequency bands x 0.000001 < 0.0006). All 10 patients had meaningful connectivity between every IC localized to DMN within at least one frequency band (Figure 5.2). vMPFC and PCC were the most commonly connected regions within the DMN for both responsive (mean degree across all four frequency bands 4.25 and 3.72, respectively) and unresponsive (mean degree 3.25 and 3.75, respectively) patients.

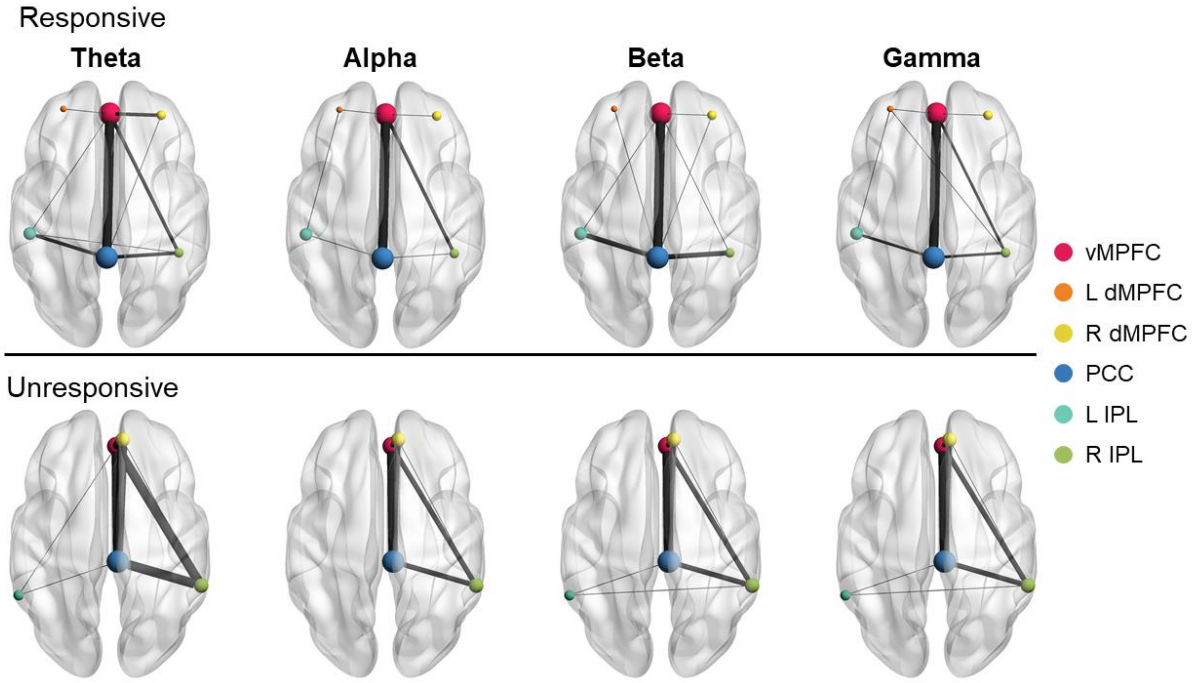

Figure 5.2. Functional connectivity between regions within the DMN between responsive and unresponsive patients.

Node location represents the average position in Talairach space of all ICs localized to that region. The size of the nodes is scaled by the proportion of participants who have activation in that neural region. A line connecting two nodes means that at least one patient had connectivity between those two regions. The thickness of the lines is scaled by the proportion of patients who had connectivity between those two regions.

5.3 Discussion

Near-ubiquitous activation of PCC at rest among controls

All controls had at least one IC localized to DMN, most commonly PCC. And while not all controls had ICs localized to more than one region within the DMN, those that did showed near ubiquitous connectivity between those regions. The PCC is part of the "core" DMN (Christoff et al., 2016; Kabbara et al., 2017; Smallwood et al., 2012), it is the most highly connected node within the DMN (Fransson & Marrelec, 2008; Leech et al., 2011, 2012; Dardo Tomasi & Volkow, 2011), and within the cortex in general (Heuvel & Sporns, 2013). Furthermore, PCC connectivity may play a pivotal role in maintaining internal (Fransson & Marrelec, 2008) and external (Herbet et al., 2014) awareness. While cortical activity within nodes of the DMN varied considerably between neurotypical controls, a near-constant was activation within PCC. Should an unresponsive patient only generate activation within the PCC at rest, this can, therefore, be taken as a positive sign of DMN activity that is consistent with patterns of cortical activation among healthy neurotypical brains at rest.

The DMN is active among unresponsive end of life patients

Most patients had at least one IC localized to either vMPFC or PPC. These regions are considered members of the "core" DMN, and associated with internally oriented cognition (Christoff et al., 2016; Smallwood et al., 2012). Furthermore, the number of ICs within these regions was about 28% lower for unresponsive than for responsive patients, consistent with previous research on DOC patients, where activation within the DMN is preserved, though altered, among most such patients (J. S. Crone et al., 2011), and particularly among patients with more severe clinical conditions (Cauda et al., 2009). There was no clear difference between the

distribution of activation among regions within the DMN between responsive and unresponsive patients. Finally, all patients (responsive and unresponsive) with more than one active region within DMN showed meaningful functional connectivity within DMN. This suggests that unresponsive end-of-life patients have the functional architecture to sustain internally-directed cognition.

The results from P002 are anomalous, as they generated no valid ICs when they were responsive, and only one when they were unresponsive. This patient informally reported to me that they practiced Buddhist meditation. Meditators are known to show decreased activity in DMN during meditation practice (Danielson et al., 2011; Hannawi et al., 2015; Hassabis & Maguire, 2007). Because the task instructions did not specifically preclude patients from meditating during the recording, it is possible that P002 chose to do so. It is, therefore, conceivable that P002 was meditating during the recording both when they were responsive and when they became unresponsive. The same might be said of P008. Over several conversations with P008 I observed that they would frequently enter a meditative-like state. While P008 never identified themselves as an experienced meditator, it is conceivable that they too could have been in such a state when they became unresponsive. Meditation is a possible explanation for the reduced DMN activation among these patients.

This study shows that some unresponsive hospice patients at the end of life evidence DMN activation and within-DMN functional connectivity. Whether neurotypical levels of DMN activation or connectivity imply conscious internally-oriented mental activity per se is currently unknown, although it is likely a necessary, and potentially a sufficient, property of consciousness (Boly, Phillips, et al., 2008). Although these results do not speak to these patients' capacity to sustain awareness of their external environment while they were unresponsive, they do support

the possibility that even unresponsive patients were experiencing something akin to mind-wandering (Christoff et al., 2016) or mental imagery (Hassabis & Maguire, 2007).

Chapter 6: Electrophysiological evidence of music listening at the end of life

In this chapter I report exploratory analyses of local power underlying music listening among controls and patients. These data were initially intended as a distractor task associated with an EEG adaptation of a mental imagery paradigm previously used to assess awareness among DOC patients (Owen et al., 2006, 2007). Whereas the data from the imagery task did not yield interpretable results (and are therefore not reported in this dissertation), the music data were surprisingly informative. The study of music as a diagnostic or therapeutic tool for use among DOC patients is relatively new, but has produced some promising results (Castro et al., 2015; Heine et al., 2015; Magee et al., 2016; O'Kelly et al., 2013; Okumura et al., 2014; Rollnik & Altenmüller, 2014; Varotto et al., 2012; Verger et al., 2014). For example, Castro and colleagues (2015) found that more DOC patients could generate an N2 or P3 (although I have concerns about how the authors defined N2 and P3 in this study) to their own name (subject's own name, SON) after they heard 1 minute of music, compared to hearing 1 minute of noise. Those that responded to SON after passive music listening (responders) showed positive outcomes at 6 months follow-up, while those that did not respond to SON (non-responders) had not changed or had negative outcomes. Moreover, only about 30% of responders, and none of the non-responders, generated an MMN in a classic oddball task. The authors attribute these results to the emotional and arousal effects of music listening (Rickard, 2004; Salimpoor et al., 2009), as DOC patients have been shown to produce responses to emotionally salient or self-referential stimuli, such as their own name (Fischer et al., 2008; Laureys et al., 2004; Perrin et al., 2006; Qin et al., 2008) or a familiar voice (H. B. Di et al., 2007). Furthermore, neurotypical responses to one's own name are stronger compared to neutral stimuli (Holeckova et al., 2006), and can be detected during sleep (Perrin et al., 1999).

Others have explored ERSP (O'Kelly et al., 2013) and functional connectivity responses to music (Heine et al., 2015) among DOC patients, but results were difficult to interpret. Specifically, O'Kelly and colleagues (2013) reported increased frontal alpha ERS among neurotypical and MCS patients, but not UWS patients, in response to each participants' preferred music compared to control conditions (such as baseline silence, disliked music, and live improvisation), but it's unclear what cognitive processes might be underlying this response. Using fMRI, Heine and colleagues (2015) reported increased frontal-parietal connectivity among DOC patients during preferred music listening compared to a baseline condition, but found no difference between music and baseline conditions among neurotypical control participants. Because these studies all involved only passive music listening, it's difficult to infer whether any of these signals are indicative of awareness of the musical stimuli.

This chapter comprises two experiments. In Experiment 1 I describe neurotypical electrophysiological signals that distinguish control participants who were actively engaged in music listening (active condition) from participants who were asked to ignore music stimuli (passive condition). In Experiment 2 I report the prevalence of these signals among responsive and unresponsive hospice patients when they're asked to actively engage in music listening. I expected the responsive patients' EEGs to resemble the actively engaged neurotypicals', although I also expected that the medications they were taking would dull this response to some extent. If unresponsive patients were actively engaging in the music listening, in spite of being unresponsive to requests from caregivers, then their electrophysiological signals should resemble those of the actively engaged neurotypical controls and/or responsive patients. For these experiments I have limited the analyses to local spectral power (ERSPs), rather than other electrophysiological measures such as ERPs and functional connectivity. ERPs are not an

appropriate signal to measure for this paradigm because the music trials are very long (7 seconds) and do not contain a time-locked event for participants to respond to. Given the heterogeneity of individual intracortical connectivity within attention networks reported in Chapter 4, connectivity analyses will not be reported in this chapter either. To my knowledge, this chapter describes a novel approach to evaluating attention and awareness among behaviourally unresponsive patients.

6.1. Experiment 6.1-Neurotypical Control Participants

6.1.1. Materials and Methods

6.1.1.1. Ethics Statement

All aspects of the experimental protocol, including the recruitment and consent procedures, were approved by the University of British Columbia Behavioural Research Ethics Board in accordance with the provisions of the World Medical Association Declaration of Helsinki. Participants gave written informed consent by reading and signing the approved consent document.

6.1.1.2. Participants

Data were collected initially from 22 participants. From 15–25 participants has been shown in previous studies in our lab and others to yield reliable EEG data for source localization and ERSP analysis given the numbers of stimulus trials in the study design. Data collection was stopped after the indicated number of participants had been included. Data from the Passive condition were not collected for two participants. Data from one participant were excluded from the Passive condition because of excessive noise in their EEG. The analysis to be described is based on 22 participants (16 female, age 18 to 30 years, mean age 23.14 years) in the Active Condition and 19 participants in the Passive Condition participants (14 female, age 18 to 30

years, mean age 23.52 years). Participants were offered monetary compensation ($10/hr) for their participation. Participants reported no hearing or neurological difficulties.

6.1.1.3. Stimuli

Stimuli consisted of excerpts from classical concertos featuring one of three solo instruments: piano, trumpet, or violin. Excerpts were 6 seconds-long and were selected for the prominence of the featured instrument and, when possible, contained most or all of a melodic line. There were 9 music excerpts in all, 3 for each solo instrument. Stimuli were administered binaurally at 70 dB through insert earphones (EAR 3A) in a sound-attenuating chamber. Stimuli were presented and responses registered using Presentation software (Neurobehavioral Systems Berkeley CA USA).

6.1.1.4. Procedure

Music stimuli were presented as part of a mental imagery task, where participants were asked to perform alternating visuo-spatial and auditory imagery. While electrophysiological responses associated with mental imagery will not be reported in this dissertation, the entire protocol, including both mental imagery and music trials, will be described here.

Data were recorded in a sound-attenuating chamber. Each participant heard 4 blocks of trials comprised of alternating imagery and music excerpts. Each block consisted of alternating imagery trials beginning with “birthday”, with randomly selected music excerpt trials between each imagery trial (see Figure 6.1). In the Active condition, participants were instructed to imagine themselves singing happy birthday to themselves whenever they heard the “birthday” cue. Similarly, they were instructed to imagine themselves walking from room to room in their own home whenever they heard the “room” cue. Participants were instructed to identify the featured music instrument, either piano, trumpet, or violin, and name it silently whenever they

heard a music excerpt. The inter-stimulus interval between imagery and music trials was 1 second (1000 ms). Participants were familiarized with the imagery and music stimuli before the experiment began. In the Passive condition, participants were asked to ignore the imagery cues and music excerpts while they watched a subtitled movie. Subtitles were always in English. Each participant performed both Active and Passive conditions; the order with which each condition was presented was counter-balanced. Each block was identical (save for the music excerpts), lasted approximately 4 minutes (224 seconds), and consisted of 32 trials; 8 birthday trials, 8 room trials, and 16 music excerpts. Each participant, therefore, performed 64 music trials over four blocks. Participants were given 2 minutes of rest between every block. The total time for this experiment was approximately 21 minutes.

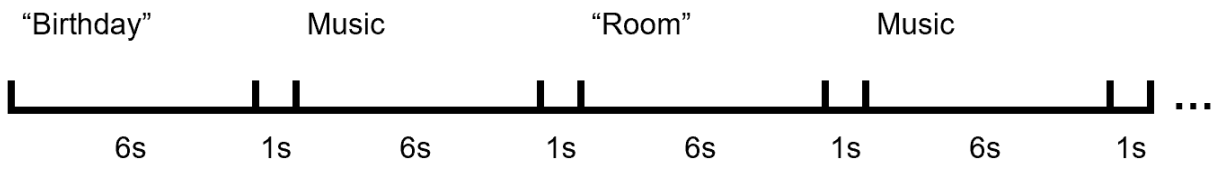

Figure 6.1. Study 2 consisted of 4 blocks of alternating imagery and music trials, where imagery trials also alternated between auditory ("Birthday") and visual-spatial ("Room") trials.

Music excerpts were randomly chosen from 9 possible excerpts from a variety of concertos featuring either a piano, trumpet, or violin. Each trial lasted for 6 seconds, with a 1 second ISI in between.

6.1.1.5. Artefact rejection and source localization

Artefact rejection and source localization analyses were the same as those described in Chapter 2. ICA was performed on music data epoched from 1 second before to 7 seconds after each music stimulus. All ICs that were classified as either eye-blinks or EMG artefacts were removed from each participants' EEG recording. The neural source of each remaining IC was

localized using the EEGLAB dipfit algorithm. Electrode locations were co-registered to the Montreal Neurological Institute (MNI) average brain, allowing for IC sources to be visualized in Talairach space. ICs were only included for further analysis if their power spectra followed a *1/f* shape (which is characteristic of a single dipole neural source), if their source was fitted to a single dipole that accounted for at least 80% of the variance of the IC's electrode weights, and if their source was fitted inside of MNI brain space.

6.1.1.6. IC Source Clustering

The retained ICs (hereafter referred to as "valid ICs") were grouped into spatially similar clusters based on the MNI coordinate estimate of each IC's single equivalent current dipole (hereafter referred to as a valid IC's "dipole location"). Grouping of spatially similar dipoles (hereafter referred to as "clustering") was performed using the *k*-means clustering method used in EEGLAB (Delorme & Makeig, 2004). As in Chapter 2, "stable" clusters were chosen by determining which clusters appear repeatedly over multiple iterations of the *k*-means algorithm. Since *k*-means requires the number of output clusters to be determined a priori, the number of output clusters varied across these iterations.

A stable cluster was retained for further analysis (hereafter referred to as a "valid cluster") if it contained ICs from at least 50% of the participants in the study (minimum 11 participants in the Active condition, and minimum 10 participants in the Passive condition). Only a single IC per participant was permitted into any single cluster to avoid biasing the contribution of a subset of participants to the cluster. If more than one valid IC per participant was within a cluster, only the IC closest to the cluster centroid was kept in the cluster.

Cluster analyses were performed twice, once separately between Active and Passive conditions (between-subjects analysis), and again, using the seeding algorithm described in chapter 2, by combining Active and Passive ICs (within-subjects analysis).

6.1.1.7. Event Related Spectral Perturbations (ERSPs)

Oscillatory power in each epoch at every timepoint, and at each frequency between 0 Hz and 60 Hz, was computed from a time-frequency (wavelet) decomposition of all ROI cluster IC activations in the time window immediately following the onset of each music stimulus. Recall that data were epoched from 1s before to 7s after the onset of each music stimulus. ERSPs were normalized to a baseline between 150 and 50 ms before the onset of each music stimulus. Thus, ERSP in decibels at each timepoint equals 10 log (timepoint power/baseline power). Differences in ERSPs averaged over epochs were computed between Active and Passive conditions. Significant differences between conditions were masked at $p < 0.01$ by EEGLAB's permutation test.

6.1.2. Results

6.1.2.1. Between-Subjects Cluster Results

K-means clustering generated seven valid clusters common to both Active and Passive conditions (see Table 6.1). These clusters were localized to the Middle Cingulate Cortex (Cing), Right Visual Cortex (R Vis), Left Auditory Cortex (L Aud), bilateral Motor Cortices (L/R Mtr), precuneus (PCU), and Orbital Frontal Cortex (OFC). Six additional clusters were found in either the Active or Passive condition. In the Active condition, 2 additional clusters were found in the Posterior Cingulate Cortex (PCC) and Left Inferior Frontal Gyrus (L IFG). In the Passive condition, 4 additional clusters were found in the Anterior Cingulate Cortex (ACC), the Right Inferior Frontal Gyrus (R IFG), Left Visual Cortex (L Vis), and Right Insula (R Ins).

	Active (22 participants)					*Passive (19 participants)*			
ROI	BA	# Participants (%)	Tal Coords	PVAF		BA	# Participants (%)	Tal Coords	PVAF
OFC	11	59.09	-2, 42, -26	89.89		11	78.94	-5, 21, -21	90.14
RIFG	N/A					47	63.16	17, 9, -17	88.41
LIFG	47	77.27	-10, 14, -13	89.60		N/A			
RIns	N/A					13	73.68	26, -25, 16	88.94
ACC	N/A					32	84.21	7, 23, 20	89.46
Cing	24	90.90	-6, -1, 23	90.59		24	89.47	1, -15, 38	91.26
LAud	22	68.18	-31, -60, 13	92.83		22	68.42	-40, -48, 13	89.66
PCC	23	86.36	-4, -35, 17	92.59		N/A			
PCU	7	68.18	1, -48, 45	92.81		7	63.16	0, -37, 43	90.96
RMtr	6	86.36	26, -10, 52	91.30		6	68.42	35, -10, 53	94.02
LMtr	6	81.81	-29, -12, 44	91.75		6	63.16	-37, -13, 49	94.30
RVis	18	86.36	24, -73, 26	94.38		18	63.16	14, -67, 1	90.54
LVis	N/A					18	73.68	-6, -75, 22	91.44

Table 6.1. Clusters uncovered in between-subjects comparisons of Active and Passive conditions separately.

Of particular interest are the clusters localized to Orbital Frontal Cortex, bilateral Motor Cortices and L Auditory Cortex. The Orbital Frontal cluster in the Passive condition contained a larger proportion of the total participants (approx. 20% more) than the Orbital Frontal cluster in the Active condition. A similar but opposite pattern was observed in motor clusters, where motor clusters in the Active condition contained ICs from a larger proportion of the total participants (approx. 20% more) than motor clusters in the Passive Condition.

In addition, whereas motor clusters in both the Active and Passive conditions were localized to the same ROI and Brodmann Area, clusters in the Active condition were more medial than those in the Passive condition. Similarly, the Left Auditory cluster in the Passive Condition was localized closer to the primary Auditory Cortex, whereas the same cluster in the Active Condition was localized more medially and posteriorally, closer to angular gyrus and temporo-parietal junction. These spatial differences may be within the margin of error associated with source-estimation using EEG (see Michel et al., 2004 for a review). They may also be

related to the nature of the task participants were instructed to perform, as in the Active Condition participants were told to actively name (but silently) the featured instrument (piano, violin, or trumpet), whereas participants in the Passive condition were told to ignore the music stimuli.

6.1.2.2. Pooled Clusters Results

Clusters were pooled across Active and Passive conditions so that ERSPs could be compared between conditions using spatially-similar ICs (see Table 6.2). Only those participants who had recordings of both Active and Passive conditions were included in the following analysis (N = 19). All valid ICs from both Active and Passive conditions were combined for this clustering analysis. Talairach centroids of *k*-means clusters from both Active and Passive conditions were seeded (seed locations are described in Table 6.1), resulting in clusters that contained ICs from both Active and Passive conditions. If an ROI appeared in both Active and Passive conditions, the midpoint between the Talairach centroids of the two clusters was seeded. For example, because both Active and Passive conditions generated a valid cluster in the mid Cingulate Cortex (Cing), the midpoint between the Active cluster (tal: -6, -1, 23) and the Passive cluster (tal: 1, -15, 38) was seeded (tal: -3, -8, 31). Each cluster contained a maximum of two ICs per participant, one IC from the Active condition and one IC from the Passive condition.

ROI	**BA**	**Total Active ICs (%)**	**Total Passive ICs (%)**	**Tal Coords**	**PVAF**
ACC	24	78.9	84.2	6, 20, 19	90.0
Cing	24	84.2	89.5	-4, -10, 32	90.7
PCC	23	89.4	89.4	-4, -38, 18	91.6
RVis	18	84.2	78.9	15, -68, 19	92.1
LVis	18	42.1	36.8	-14, -74, 25	91.1
LAud	N/A	42.1	47.4	-36, -49, 10	90.7
RMtr	6	89.5	73.7	27, -11, 51	91.7
LMtr	6	78.9	57.9	-34, -14, 46	93.4
PCU	7	63.2	42.1	0, -38, 48	91.7
RIFG	11	68.4	84.2	12, 10, -18	89.8

LIFG	11	57.9	52.6	-13, 22, -18	89.7
OFC	11	42.1	21.1	-3, 41, -27	89.3
RIns	N/A	68.4	68.4	25, -24, 12	88.9

Table 6.2. Clusters containing ICs from both Active and Passive conditions.

The percentage of total Active and Passive ICs refers to the percentage of participants who contributed Active and Passive ICs to the cluster. Note that some ROIs listed here were not found using k-means clustering (e.g. ACC in Active condition).

6.1.2.3. ERSP results

ERSPs were compared between Active and Passive conditions for each pooled cluster reported in Table 6.2. Figure 6.2 shows clusters with ICs from at least 50% of participants from both Active and Passive conditions (at least 10 Active ICs and 10 Passive ICs).

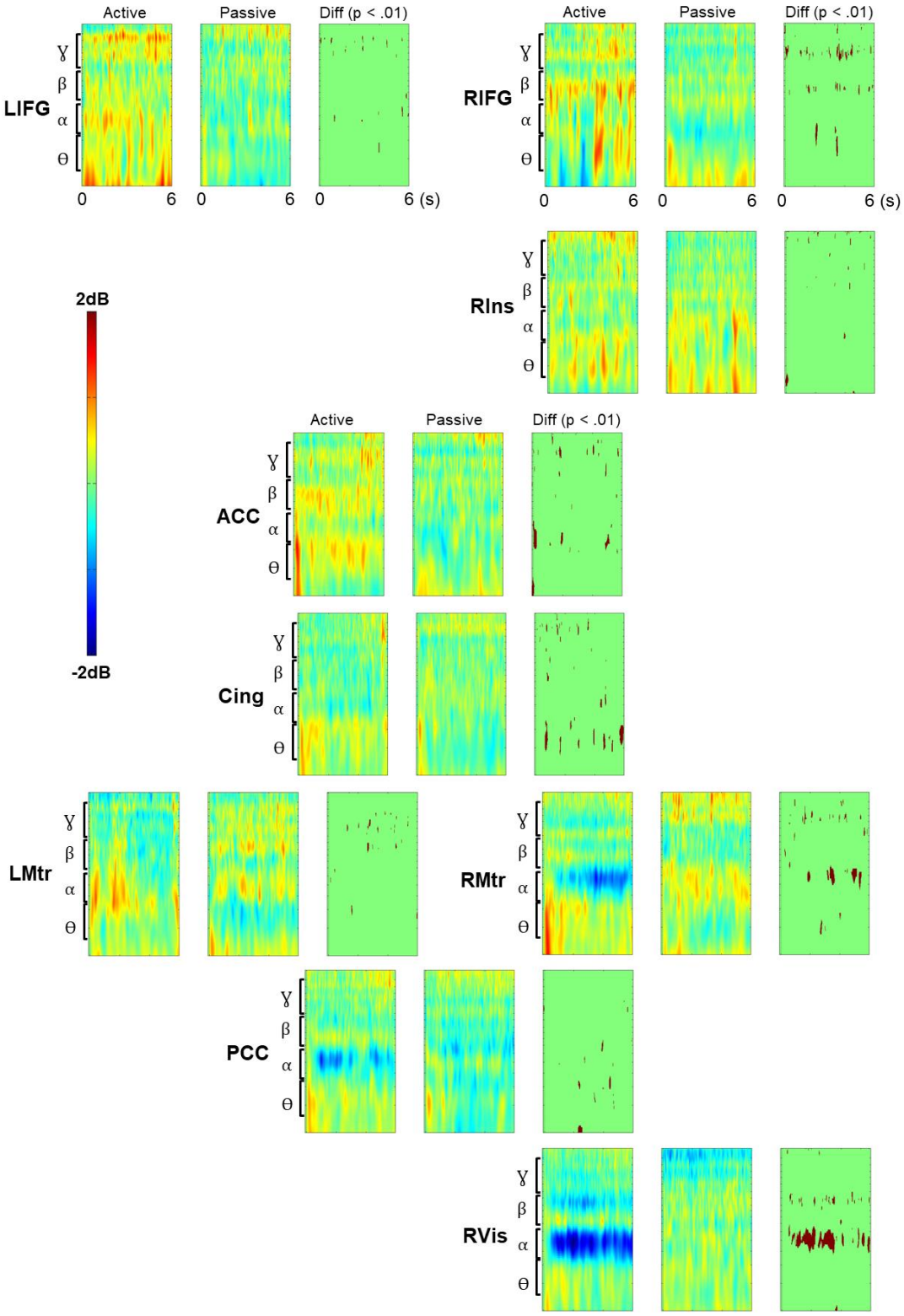

Figure 6.2. Clusters with at least 10 Active and 10 Passive ICs.

Notice that the x-axis in each figure covers 6 sec after music onset, in which there are 1500 data points. Thus, only the most prominent and sustained differences between conditions are apparent in the figure.

Key differences between conditions include greater gamma and beta ERS in frontal ROIs (IFG), theta ERS in central ROIs (ACC and Cing), and alpha ERD in posterio-parietal ROIs (R Mtr and R Vis) in the Active condition compared to the Passive condition. This pattern of increased theta/gamma and decreased alpha power is frequently seen during auditory discrimination and sustained attention tasks (see Ribary et al., 2017 for a review). While this pattern of local theta/gamma synchronization and alpha desynchronization is a indicative of sustained attention to an auditory stimulus at the group level, hereafter I will focus on the most salient difference between the conditions: posterio-parietal alpha ERD.

In R Vis and R Mtr clusters, there was sustained alpha suppression (ERD) in the Active condition that is absent in the Passive condition (this pattern also appears to be present in the PCC, but the difference between conditions isn't significant). Upon visual inspection of the individual ICs contained in these clusters, I found several posterio-parietal ICs that showed a similar pattern of sustained alpha suppression in the Active condition that was absent in the Passive condition. This observation served as the inspiration for the following analysis of individual differences in which neural regions may be associated with active engagement in music stimuli.

6.1.2.4. ERSP analysis-individual differences

The subsequent analyses were performed on individual valid Active and Passive ICs. Source classification for each individual IC was based on which cluster they were assigned to in the group analysis. Significant Event-Related Desynchronization (ERD, negative ERSP values

indicating lower power than at baseline) within the alpha frequency band (8-15Hz) was computed for each valid IC from 0 to 6 seconds after the onset of the music stimulus using bootstrap statistics (200 permutations, masked at $p < .01$). A large frequency band was used to define alpha to accommodate variation in individual peak alpha frequency (c.f. Klimesch, 1999). To compute ERD, ERSP values were compared against the average baseline for each IC (i.e. the average baseline from 150 to 50 ms before the onset of each music trial). Since the amplitude of the ERD was not relevant for this analysis, significant ERD values (i.e. more negative than the most negative number within each bootstrap distribution) were coded as 1, and all other ERSP values were coded as 0. This resulted in a frequency x time matrix of 0's and 1's for each valid Active and Passive IC. Each timepoint was reclassified as significant (coded as a 1) if at least 50% of the frequency points at that timepoint was significant. In other words, a timepoint was considered to contain significant alpha suppression if at least 50% of the frequency points between 8 and 15Hz at that timepoint were also significant as per the previous bootstrap analysis. This resulted in a 1 frequency x 1500 timepoint vector of significant alpha suppression for each valid IC. To determine if the alpha suppression was sustained from 0 to 6 seconds after the onset of the music trial for each IC, each vector was further reduced to 6 x 1000ms bins (250 timepoints each). A time *bin* was deemed meaningful if at least 75% of the timepoints within the bin were significant (i.e. if at least 188/250 timepoints had a value of 1). An IC was considered to have sustained alpha suppression if over half those 1000 ms time bins (at least 4/6) were considered meaningful.

Figure 6.3 shows the proportion of participants that had sustained alpha suppression over all ROIs in both active and passive conditions. Alpha suppression was far more prevalent in the active condition than in the passive condition, as there were twice as many ICs with sustained

alpha suppression in the Active condition (52 ICs) than in the Passive (26 ICs). The proportion of participants with at least one IC with sustained alpha suppression in frontal ROIs (OFC, IFG, Ins, ACC, and Cing) was the same in both active and passive conditions (52.6%). There were, however, nearly 50% more participants with some evidence of sustained alpha suppression in posterio-parietal ROIs (Aud, PCC, Par, Mtr, and Vis) in the active condition (84.2%) compared to the passive condition (36.8%).

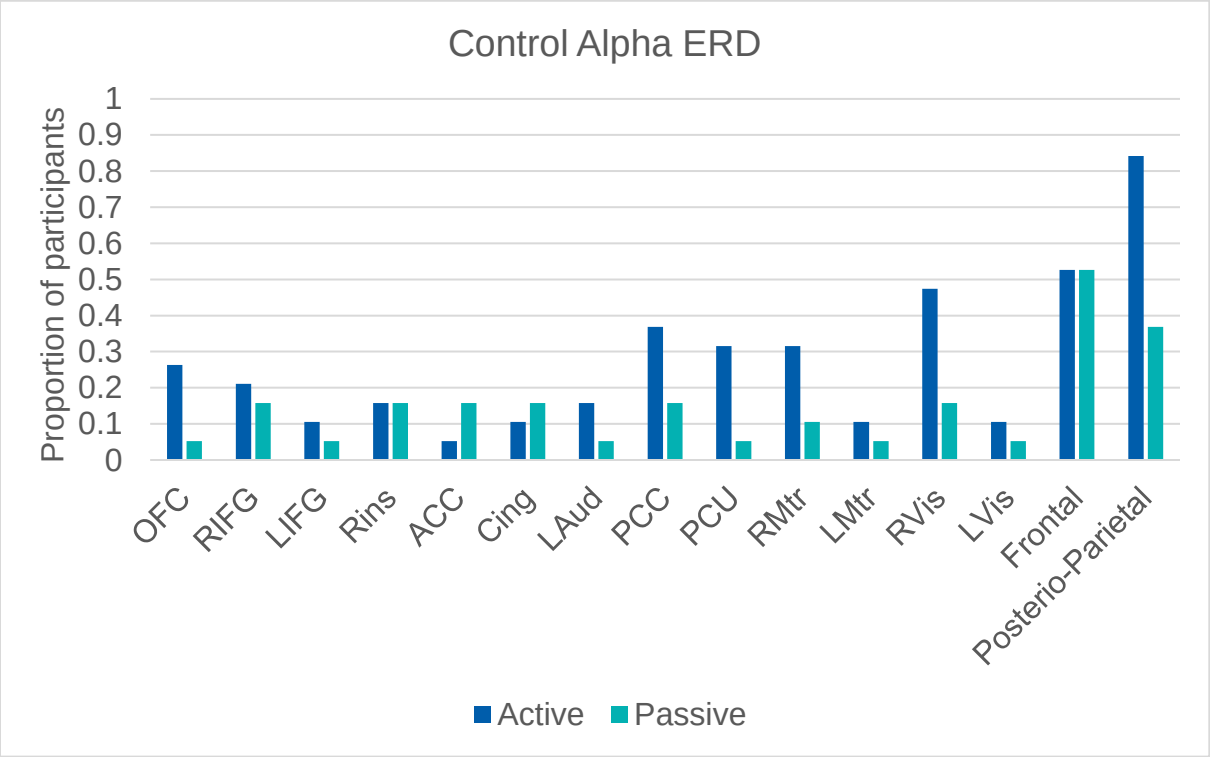

Figure 6.3. The proportion of controls with alpha suppression in each ROI.

The first 6 ROIs (OFC through Cing) were classified as frontal regions, whereas the last 7 (LAud through LVis) were classified as posterio-parietal regions. "Frontal" and "Posterio-parietal" columns represent the proportion of participants with sustained alpha suppression in at least one frontal ROI and at least one posterio-parietal ROI, respectively.

6.1.3. Discussion

Given the results of this study, sustained posterio-parietal alpha ERD could be a promising neural marker of attention and memory processes associated with attention to, and identification of, the instrument featured in each music excerpt. Alpha ERD is generally observed among brain regions recruited during an attention-demanding task (Klimesch, 2012; Pfurtscheller & Lopes da Silva, 1999), and the spatio-temporal dynamics of alpha ERD correlate with the locus of attention. In visual-spatial cueing tasks, alpha ERD is found over the posterio-parietal cortex contralateral to the attended visual field, and alpha ERS over ipsilateral parietaloccipital cortex (Doesburg et al., 2008; Rihs et al., 2007; P. Sauseng et al., 2005; Worden et al., 2000). This effect is observed even when visual stimuli are presented continuously to bilateral visual fields (Kelly et al., 2006). In both auditory and visual oddball tasks, alpha ERD is commonly generated after stimulus presentation (Klimesch, 2012; Klimesch et al., 1998; Yordanova et al., 2001), and the strength and duration of post stimulus alpha ERD is longer after target identification (Klimesch et al., 1998; Yordanova et al., 2001). The role of alpha ERD in cognitive processes varies across the frequency band; lower alpha (approx. 7 – 10 Hz) is involved with attentional processes and arousal in general (Klimesch et al., 1997), whereas upper alpha (approx. 10 – 14 Hz) is involved in semantic processing and memory retrieval (Başar & Güntekin, 2012; Klimesch, 2012; Klimesch et al., 1997, 2006). Moreover, sustained alpha ERD has been observed during the timeframe where participants retrieve a target from memory (Klimesch et al., 1999), often over posterio-parietal cortex (Pfurtscheller et al., 1994), and can persist for up to 3000 ms (Krause et al., 1996). Although none of these studies described the relationship between alpha ERD and attention or memory processes among individual

participants, the prevalence of posterio-parietal alpha ERD during the active condition of Experiment 1 may reflect attention to the music stimuli, and even retrieval from memory the instrument featured in each excerpt. This is further supported by the fact that far fewer participants evinced alpha ERD to the music stimuli when they were told to ignore the excerpts during the passive condition. Evidence of posterio-parietal ERD does not, however, distinguish active from passive participants in all cases in Experiment 1, as nearly 40% of participants in the passive condition also generated posterio-parietal alpha ERD to music stimuli, and about 15% of participants in the active condition did not. This could be because EEG does not always separate weak signals from noise, or it could be because of a lack of incentive for participants to engage in the music and distractor tasks when told to. In a future replication I intend to include behavioural measures to confirm that participants were a) actively engaged in the music task during the active condition, and b) actively engaged in the distractor task in the passive condition, in order to correlate posterio-parietal alpha ERD with task performance, rather than condition instructions.

6.2. Experiment 6.2-Hospice Patients

6.2.1. Materials and Methods

6.2.1.1. Patients, Stimuli, Procedure, and EEG recording

Hospice patients are the same as those described in Chapters 3-5. Stimuli and procedure were identical to those described in Experiment 6.1, apart from aspects of the protocol specific to the hospice that are described in Chapter 3. Both responsive and unresponsive patients participated only in the Active version of the task. One unresponsive patient's data were not included in this analysis due to excessive noise in the EEG.

6.2.1.2. Artefact Rejection, IC source clustering, and ERSP analysis

IC artefact rejection was performed using the same machine-learning classification system described in Chapters 3 and 5. Valid ICs were classified according to the same criteria described in Chapter 5 (spectra was *1/f* shape, dipole fit accounting for at least 85% of scalp variance, highest probability classification was "brain"). The ROI centroids identified in Experiment 6.1 were used as seed locations. ERSP analyses were identical to those described in Experiment 6.1. Briefly, vectors of alpha ERD were computed for each valid IC, which were then divided into 1000 ms time bins. A time bin was deemed meaningful if at least 75% of the timepoints within the bin were significantly larger than 0 (200 permutation, $p < .01$). An IC was considered to have sustained alpha suppression if over half those 1000 ms time bins (at least 4/6) were considered meaningful.

6.2.2. Results

6.2.2.1. Patient Cluster Results

The same cluster centroids were seeded for both responsive and unresponsive participants, but results were reported separately (see Table 6.3). Recall that ROIs identified in Experiment 6.1 were seeded, and details of the resulting responsive and unresponsive clusters are reported in Table 6.1. Some ROIs were different from the seed coordinates. For example, the unresponsive cluster that was seeded as PCU resulted in a cluster whose centroid was localized to SMA. The clusters with the largest proportion of participants with IC contribution among both responsive and unresponsive patients were ACC (62.5% – 75 %) and L Mtr (75% – 100%). IC contributions to all other clusters varied between responsive and unresponsive patients.

	Responsive (8 participants)		***Unresponsive (5 participants)***

ROI	BA	# Parts. (%)	Tal Coords	PVAF	% Cat.		BA	# Parts. (%)	Tal Coords	PVAF	% Cat.
OFC	11	4 (50.0)	4, 50, -25	93.49	72.98		11	4 (100)	3, 34, -20	98.03	67.60
LIFG							11	1 (25.0)	-2, 14, -23	99.20	63.03
RIns							13	2 (50.0)	37, -22, 16	92.68	82.06
ACC	32	5 (62.5)	2, 33, 21	93.02	80.63		32	3 (75.0)	-6, 39, 14	94.33	94.13
Cing	24	6 (75.0)	-5, -16, 39	94.48	97.84		24	1 (25.0)	-1, -8, 34	96.12	94.85
SMA							6	3 (75.0)	-1, -27, 63	93.69	98.70
RTPJ							39	1 (25.0)	36, -60, 31	87.92	87.11
LAud	19	3 (37.5)	-32, -65, 4	93.24	80.00		22	2 (50.0)	-49, -43, 5	92.94	93.90
PCC	23	2 (25.0)	4, -43, 20	95.47	94.46		30	1 (25.0)	-23, -77, 2	91.67	55.70
PCU	7	5 (62.5)	1, -35, 44	94.99	92.19						
RMtr	6	3 (37.5)	30, -8, 48	94.38	81.85		6	3 (75.0)	22, -16, 62	94.81	90.69
LMtr	6	6 (75.0)	-32, -17, 58	89.61	95.54		6	4 (100)	-37, -10, 39	92.68	93.60
RVis	17	5 (62.5)	21, -79, 14	94.37	84.84		18	1 (25.0)	6, -70, -7	97.46	74.95
LVis	18	4 (50.0)	-19, -66, 23	94.36	92.74						

Table 6.3. Clusters containing ICs from both Responsive and Unresponsive patients.

Clusters are the result of seeding ROIs reported in Experiment 6.1. The percentage of total ICs refers to the percentage of Participants who contributed Active and Passive ICs to the cluster. PVAF refers to the average percentage of scalp variance accounted for by all ICs within a cluster. Percent category (% Cat.) is the average probability of cluster ICs being classified as "brain".

6.2.2.2. Individual Patient ERSPs

Figure 6.4 shows the proportion of responsive and unresponsive patients that had sustained alpha suppression across all ROIs. For both responsive and unresponsive patients, alpha suppression was more prevalent in posterio-parietal ICs (75% and 100%, respectively) compared to frontal ICs (25% and 50%, respectively). Frontal ROIs included OFC, IFG, R Ins, ACC, Cing, and SMA, whereas posterio-parietal ROIs included R TPJ, L Aud, PCC, PCU, Mtr and Vis. The ratio of posterio-parietal to frontal ICs with sustained alpha suppression was 3 among responsive patients, and 2 among unresponsive patients.

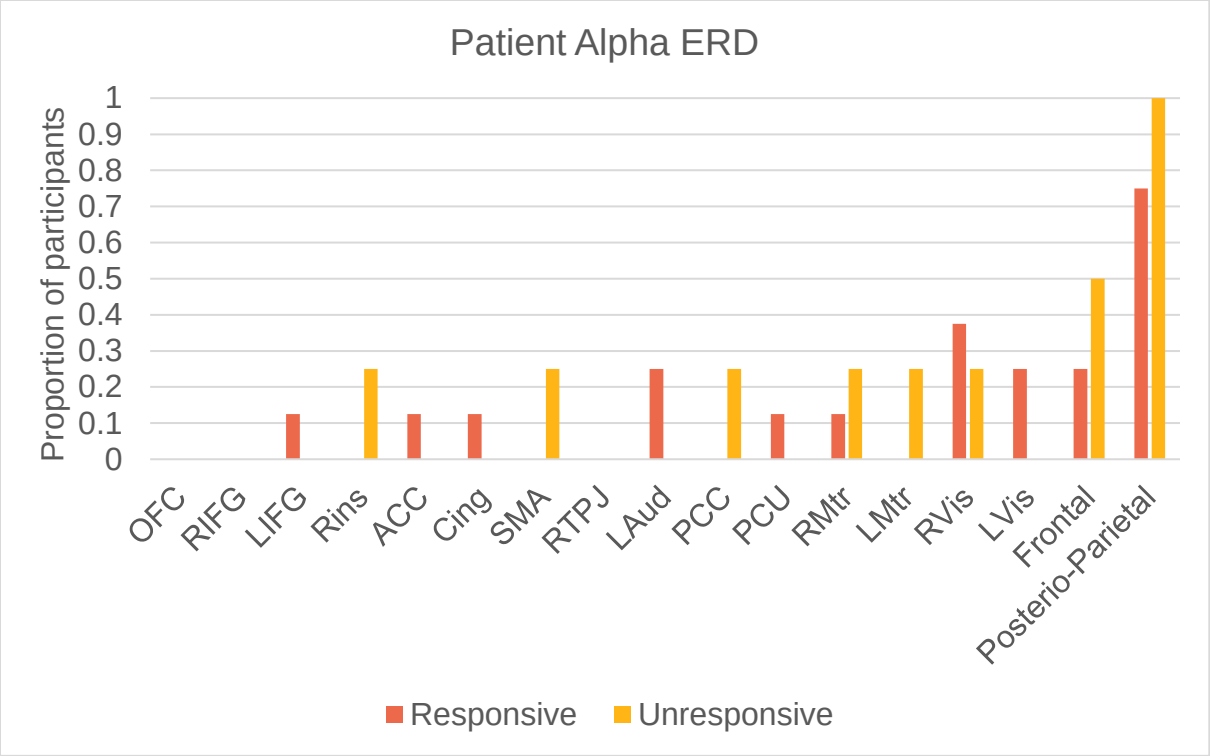

Figure 6.4. The proportion of patients with alpha suppression in each ROI.

The first 7 ROIs (OFC through SMA) were classified as frontal regions, whereas the last 8 (R TPJ through LVis) were classified as posterio-parietal regions. "Frontal" and "Posterio-parietal" columns represent the proportion of patients with sustained alpha suppression in at least one frontal ROI and at least one posterio-parietal ROI, respectively.

This pattern is more similar to that of controls in the Active condition than that of controls in the Passive condition (see Figure 6.5). Overall, participants assigned to the Active condition, which includes both patient groups, had more ICs with sustained alpha suppression localized to posterio-parietal areas compared to frontal areas, than those neurotypical controls assigned to the Passive condition.

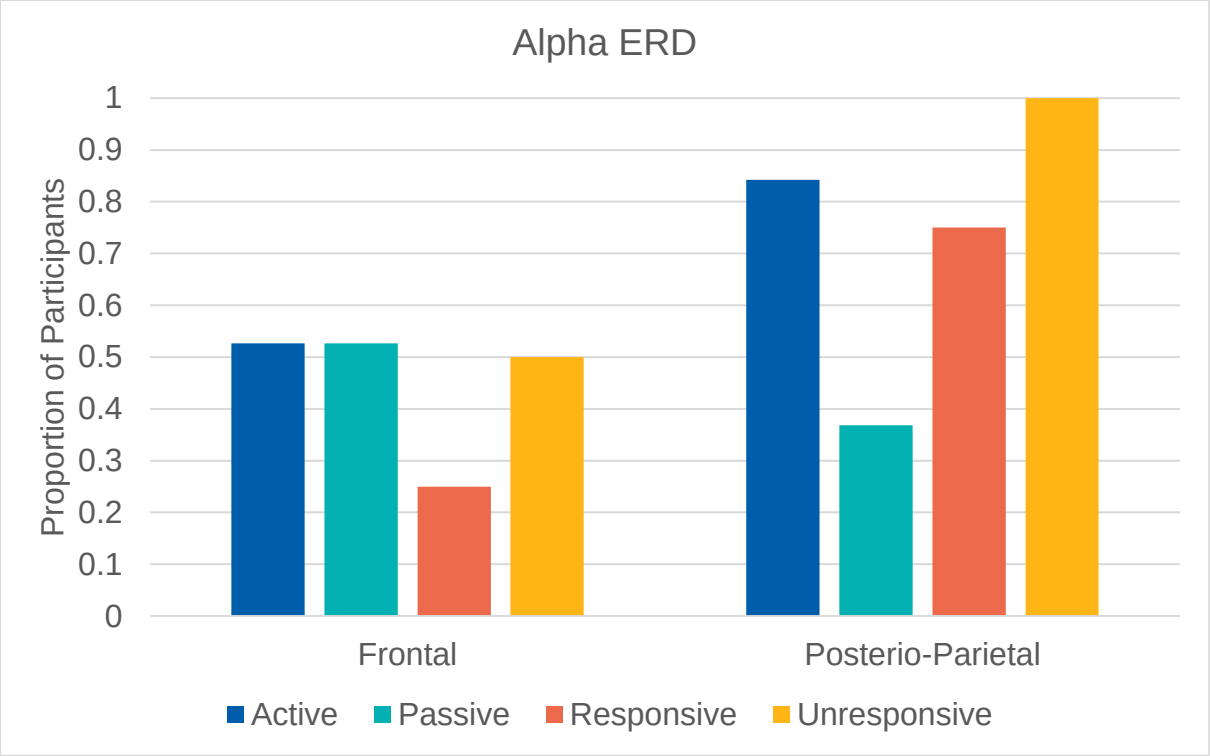

Figure 6.5. The proportion of participants with at least one IC with sustained alpha suppression in frontal and posterio-parietal ROIs.

Unfortunately, not all individual participants followed this pattern. Table 6.4 reports the number of posterio-parietal and frontal ICs with sustained alpha suppression for each participant. Because 50% of participants had no frontal ICs with alpha suppression, to calculate the ratio of posterio-parietal to frontal ICs I added 1 to both the numerator and denominator.

	Active			Passive		
	Frontal	Posterio-parietal	Ratio	Frontal	Posterio-parietal	Ratio
N018	0	2	3	1	2	1.5
N019	0	1	2	2	1	0.67
N020	0	1	2	2	2	1
N021	0	2	3	2	2	1
N022	3	2	0.75	0	0	1
N023	1	1	1	0	0	1
N024	0	0	1	0	1	2
N025	2	3	1.33	1	0	0.5

N026	0	0	1	0	0	1
N027	1	5	3	0	1	2
N028	1	3	2	1	0	0.5
N029	0	2	3	2	0	0.33
N030	0	0	1	1	0	0.5
N031	1	1	1	1	3	2
N032	5	5	1	0	0	1
N033	1	1	1	1	0	0.5
N034	0	1	2	0	0	1
N035	1	4	2.5	0	0	1
N036	1	1	1	0	0	1
	Responsive			Unresponsive		
	Frontal	Posterio-parietal	Ratio	Frontal	Posterio-parietal	Ratio
P001				1	1	1
P002	0	2	3	0	1	2
P003	0	2	3			
P004	2	1	0.67	1	1	1
P005	1	1	1			
P006	0	0	1			
P007	0	2	3	0	1	2
P008	0	1	2			
P009	0	0	1			

Table 6.4. The number of posterio-parietal and frontal ICs with sustained alpha suppression for each participant.

Control IDs start at 18 so as not to confuse them with control data from Chapters 3 and 4.

Only 52.6% of Active controls had a posterio-parietal to frontal alpha suppression ratio of greater than 1, and only 31.6% of Passive controls had a ratio of less than 1. 50% of responsive and 50% of unresponsive patients had ratios of greater than 1, but only one responsive (and no unresponsive) patient had a ratio of less than 1.

6.2.3. Discussion

The results of Experiment 6.2 imply that some (and perhaps all) of the unresponsive patients may have been attending to the music stimuli while they were unresponsive. The case for attention is stronger for the unresponsive patients with ERD ratios of greater than 1, as only 4/19 (21%) of passive controls had ERD ratios of greater than 1. While it is indeed possible that, in the absence of competing stimuli, alpha ERD to music stimuli may be pre-attentive (or even pre-conscious), this is highly unlikely. Recently, Fellinger et al. (2011) compared parietal alpha ERD responses to oddball targets between neurotypical control, MCS, and UWS patients. They found that the magnitude of neurotypical alpha ERD was 4 times stronger when participants were asked to count their own name compared to a passive condition with no distractor task. Alpha ERD was even weaker when controls were asked to count an unfamiliar name, further supporting the interpretation that the magnitude of alpha ERD is modulated by how well integrated the target is in long-term memory (Fellinger et al., 2011; Klimesch et al., 1997). Critically, UWS patients generated no parietal alpha ERD in either the active or passive condition, despite having shown some evidence of stimulus response (frontal theta ERS) to their own name in both active and passive conditions. The presence of alpha ERD could, therefore, indicate preserved attention mechanisms to the external environment, and may imply consciousness among behaviourally unresponsive patients at the end of life.

Chapter 7: General Discussion

The last hours of a loved one's life can be a deeply spiritual time for families and friends. Given anecdotal reports from those who've had near-death experiences, there is a persistent belief that "hearing is the last to go," implying that patients who become unresponsive at the end of their lives may retain some awareness. The goal of this thesis was to test that hypothesis directly, and in so doing shed light on the spatio-temporal network dynamics underlying neural signals that have been used to demonstrate both externally-oriented, and internally-oriented, cognition among behaviourally unresponsive patients.

7.1. Relation of current results to other work

In Chapter 2 I described the spatio-temporal dynamics underlying two subcomponents of the P300 ERP, the fronto-central P3a, and the parietal P3b, generated in an auditory serial search task. In this chapter I showed that the primary neural generators of the P3a are most likely fronto-central neural sources associated with the Ventral Attention Network (VAN), the ACC, Cingulate, and SMA. Projections from ICs localized to these regions account for the largest percentage of power (45%) recorded at central electrodes during the P3a timeframe (about 300 ms post stimulus onset). They also exhibit post-stimulus theta and low alpha event-related synchronization (ERS) to rare, salient tone deviants, consistent with attention (Missonnier et al., 2006) and working memory (Klimesch et al., 2005) processes associated with frontal theta ERS. Moreover, regions localized to the VAN were more functionally connected with each other, and with other neural regions responsive to auditory deviations, immediately following detection of rare deviant tones compared to pattern deviants. The P3a is, therefore, a strong indication of exogenous attention orienting to highly salient tone deviants, even when such deviants are task-relevant, as was the case in this study.

In Chapters 3 and 4 I showed that most, but not all, neurotypical control participants generated P3a and/or early frontal theta ERS to tone deviants, but instances of these responses were not significantly correlated with one another. Furthermore, most, but not all, controls showed evidence of early frontal theta ERS to *pattern* changes as well, despite there being no evidence of such a response at the group level. Similarly, the proportion of participants with meaningful VAN connectivity was similar in both tone and pattern change conditions (save for VANDAN connectivity). This implies that endogenous attention mechanisms are involved in both diffuse and focused attention strategies, even if neural signatures of such activity were only measurable to salient tone changes at the group level. The discrepancy between individual and group results is most likely due to differences in the temporal dynamics of spectral activity, as early frontal theta ERS appeared to be entrained to the salient tone changes, resulting in a more temporally consistent response across participants, whereas individual early frontal theta ERS to pattern changes was more temporally varied.

The precise neural generators of the P3b, by contrast, were less clear, and varied depending on the features of the target run. Projections from ICs localized to R SPC and PCC accounted for the largest percentage of power recorded at parietal electrodes during the P3b timeframe (about 300 ms) to both tone and pattern changes, albeit their contributions to P3b power was no more than 30%. Theta ERS was distributed among R SPC and L PreCG to tone changes, and L MFG and L PreCG to pattern changes. In addition, significant ERD in the beta band was found in R SPC, L PreCG, and SMA/Cing during the P3b timeframe (and beyond) to tone changes only. There was no significant ERSP response to either target among ICs localized to the PCC. The neural generators of the P3b were, therefore, predominantly parietal regions (R SPC, PCC, and L PreCG) when the target was highly salient, whereas a left-dominant fronto-

parietal distribution (L MFG, PCC, and L PreCG) was associated with detection of less salient targets. These regions were associated with the Dorsal Attention Network (DAN) and a network of regions commonly active during detection of auditory oddball targets (ODD). Connectivity within DAN was greater to tone than to pattern changes at the group level (Chapter 2), but this pattern was not evident at the individual level (Chapter 4).

Chapters 3 and 4 revealed that most controls exhibited P3b responses and centro-parietal beta ERD to both tone and pattern changes, but there was no clear relationship between the presence of a P3b and parietal beta ERD among individual participants. Later centro-parietal beta ERD is most likely a movement signal associated with the button press that controls were asked to make whenever they heard a rare run (see Pfurtscheller & Lopes da Silva, 1999 for a review). The fact that centro-parietal beta ERD was only found in tone change group analyses in Chapter 2 is also most likely because of the faster response latency to tone changes than to pattern changes (see Figure 3.1 for individual reaction times).

Chapter 3 also revealed that P3a prevalence among responsive patients was similar to that of controls. In contrast, Chapter 4 revealed that frontal theta ERS to tone changes was much less prominent among responsive patients compared to controls. Because theta ERS in fronto-central regions is associated with exogenous attention processes, this overall decrease in activity could suggest that fewer responsive patients engaged in a passive, exogenous attention strategy to identify the salient tone changes. The prevalence of the P3a among responsive patients, however, could indicate that cortical activation in response to salient events may have remained intact. By contrast, over half of the responsive patients generated either a P3b or parietal beta ERD to tone changes, but those measures also were not correlated with one another. Some unresponsive patients too generated centro-parietal beta ERD to both tone and pattern changes. Because

patients weren't asked to press a button when they heard rare runs, the prevalence of beta ERD may be a result of covert finger counting, either on fingers or in their imagination (McFarland et al., 2000). These results imply that many responsive, and perhaps too some unresponsive, patients were actively attending to both tone and pattern changes, and mentally tracking the target runs.

The most striking result from Chapter 3 was that most unresponsive patients showed evidence of MMN activity to tone changes. The conventional view of the MMN is that it operates on pre-attentive processes, as it is frequently elicited when participant attention is engaged in a distractor task (see Näätänen et al., 2007 for a review). It is also conventionally considered a *pre-conscious* process, primarily because it can be elicited during certain stages of sleep (Sculthorpe et al., 2009) and under anesthesia (van Hooff et al., 1997). In a recent study, however, Dykstra and Gutschalk (2015) used informational masking to directly manipulate awareness of an auditory oddball stream, and revealed that participants only generated an MMN when they were aware of the stream. This raises the possibility that for unresponsive patients to generate an MMN to auditory irregularities (different final tone in change runs), they must have been aware of the established auditory *regularity* (same final tone in flat runs). Given that an MMN was measured from most unresponsive patients, this could be taken as a (tentative) positive sign of awareness of the tone changes among many unresponsive patients.

Some contradictory results were also revealed in Chapters 3 and 4. First, two unresponsive patients appeared to generate P3a responses to tone changes, which is a positive sign of active exogenous attention processes. None of them, however, generated frontal theta ERS in the same condition, which is a negative sign of active exogenous attention processes. Instead, over half of the unresponsive patients generated frontal theta ERS to pattern changes,

which implies a passive attention strategy to pattern changes but not to tone changes. Second, one unresponsive patient generated a P3b to the less salient pattern changes, but not to the more salient tone changes. Further research is required to understand these unexpected results.

Chapter 5 demonstrated the prevalence of PCC activation during a period of rest among neurotypical controls (measured from 97% of controls). It also showed that connectivity between other regions within DMN is equivalent across all frequency bands. Chapter 5 further revealed that almost all patients, both responsive and unresponsive, had ICs localized to one of the two "core" regions within the DMN, the PPC and the vMPFC, while they were at rest. Of the patients with ICs localized to DMN, most showed meaningful connectivity between core regions, and many with other regions within DMN, within at least one frequency band. This could be taken as a positive sign of internally-oriented cognition for three unresponsive patients.

Finally, Chapter 6 revealed that most neurotypical control participants generated sustained posterio-parietal alpha ERD when they were asked to attend to the music excerpts, but few controls generated this response when they were asked to ignore the excerpts. Because posterio-parietal post-stimulus alpha ERD is associated with attention and memory retrieval (Klimesch et al., 1997), detection of alpha ERD could be a positive sign of identification of the instrument featured in the music excerpt (Klimesch, 1999). Interestingly, most responsive, and all unresponsive, patients showed this positive sign of attention to the music excerpts. The ubiquity of this response among patients, compared to other measures described in this dissertation, may be because of the arousing affects of music (Castro et al., 2015; Rickard, 2004; Salimpoor et al., 2009), or because emotionally-relevant stimuli are particularly effective at capturing attention (Lang, 1995; Öhman et al., 2001; Schupp et al., 2006).

7.2. Is hearing the last to go?

Whereas it is beyond the scope of this dissertation to prove definitively whether unresponsive patients at the end of life were capable of sustaining awareness, there is evidence of all unresponsive patients engaging in either cortical auditory processing (MMN to tone changes), exogenous attention orienting (P3a or frontal theta ERS to tone changes), endogenous attention and context updating (P3b to tone or pattern changes), motor imagery (parietal beta ERD to tone or pattern changes), internally-oriented thought (connectivity between core regions within DMN), and music listening (sustained posterio-parietal alpha ERD). Table 7.1 describes the evidence of each of these processes for both responsive and unresponsive patients. Evidence is characterized as either strong (++) or weak (+) based on different metrics. Evidence of auditory cortical processing was strong if the response to change runs was significantly more negative than to flat runs (MMN) at $p < 0.01$ for some timepoints, and evidence was weak if all timepoints were at $p < 0.05$. Evidence of exogenous attention processes was considered to be weak if a participant generated either a P3a *or* early frontal theta ERS to tone changes, and to be strong if they generated both. Evidence of endogenous attention processes was considered to be weak if a participant generated a P3b to either tone *or* to pattern changes, and strong if to both. Evidence of motor imagery was considered to be weak if a patient generated later beta ERD to either tone or pattern changes, and to be strong if they generated both. Evidence of internally-oriented thought was considered to be strong if a participant had an IC localized to PCC, and had meaningful connectivity between core members of the DMN, and weak if no connectivity. Evidence of music listening was considered to be weak if a patient generated sustained posterio-parietal alpha ERD to music excerpts, and strong if the ratio of posterio-parietal to frontal alpha ERD was greater than 1.

ID	Aud Proc.	Exog. Attn	Endo. Attn	Mot. Im.	Intern. Tht.	Mus. List.	++	+++

Responsive								
P002		+		++		++	2	3
P003	++		+	++	++	++	4	5
P004		+		++	++	+	2	4
P005	++	+	+			+	1	4
P006	++	+	++	++			3	4
P007	++	+	+	+	++	++	3	6
P008	++	+	+		++	++	3	5
P009	+	++		++	++		3	4
Unresponsive								
P001	++		+		++	+	2	4
P002	++					++	2	2
P004	+			+	++	+	1	4
P007		+	+		++	++	2	4
P008	++	+		++	+	n/a	2	4

Table 7.1. Strong (++) and weak (+) evidence of 6 different potential biomarkers of cognition among responsive (top) and unresponsive (bottom) palliative care patients.

The final two columns represent the total number of strong signals (++) and both strong and weak signals (+++) for each patient. Empty cells indicate the absence of the signal for that patient. N/A means that the analysis was not performed for that patient.

Regarding the number of strong and weak signals of cognition among patients, responsive and unresponsive patients are virtually indistinguishable, although there are some obvious categorical differences between the groups. The largest proportion of patients with strong signals is for auditory cortical processing, motor imagery, internally-oriented thought, and music listening among responsive patients. Cortical auditory processing and music listening, by contrast, had the strongest evidence overall among unresponsive patients. The fact that the P3b was not the most prevalent potential biomarker among palliative patients casts doubt on whether this measure is the most appropriate for eventual clinical adaptation for this particular patient population (cf. Bekinschtein et al, 2009). For one, these patients are quite ill, and the auditory oddball paradigm that was used in Chapters 2-4 was, quite frankly, too difficult for many

responsive patients to perform. It was my impression that many of the patients had memory impairment (though I have no clinical measures of this), and found counting the rare runs, particularly rare flat runs, both challenging and discouraging. This is the most likely reason for why none of the responsive patients generated a P3b to pattern changes. Second, the task is quite boring (and unpleasant after too long), and whereas I trust that patients were initially motivated to perform the task to the best of their ability, after a few blocks I suspect some minds may have wandered. Finally, low-frequency signals such as ERPs are vulnerable to contamination from low-frequency noise, which might be particularly prevalent among this patient population. For example, one unresponsive patient (P008) exhibited laboured breathing (Cheyne-Stokes breathing) throughout the recording of the music data, causing their whole upper body to move in time with the breathing. This induced high amplitude low frequency noise made analysis of the music data for that patient untenable.

By contrast, measures of induced cortical responses to external stimulation, such as ERSPs, may be a beneficial complement to awareness assessment among unresponsive TBI patients. For one, mid-range oscillations, such as alpha and beta oscillations, are less susceptible to sources of noise such as small muscle artefacts (high frequency noise), and large movement artefacts (low frequency noise). Second, they can provide a measure of ongoing cognitive processing, such as sustained attention (Klimesch, 1999) or motor-planning (McFarland et al., 2000). Third, unlike ERPs, ERSPs do not have a specific morphology that requires visual inspection to make a positive identification. Detection of ERS or ERD can, therefore, be done more objectively than detection of an ERP from an individual participant.

The fact that most unresponsive patients generated MMNs to tone changes and alpha ERD to music is evidence that patients may have been capable of hearing their environment

when they were unresponsive. These results lend credence to the belief that "hearing is the last to go" and supports the recommendation that families and loved ones should continue to communicate with patients even when they become unresponsive. The results also allow me to speculate about *what* the patients may have been hearing. The fact that most patients could generate an MMN to tone changes, but few could generate P3b responses to those tone changes, suggests that the patients may have been aware of the standard stream of tones, and perhaps too the salient deviant tones of the change runs, but did not ascribe any meaning to those tone deviants. They may have either forgotten the task instructions or lacked the cognitive resources to keep the instructions in mind while they were unresponsive. Listening to music, on the other hand, is a far more engaging and pleasant activity, and requires minimal resources from working memory. Even if unresponsive patients weren't mentally naming the featured instrument of the music excerpts, it's plausible that music provided sufficient emotional arousal to allow for the unresponsive patients to engage with their environment. This is also observed among patients with dementia (Foster & Valentine, 2001; Hirokawa, 2004; Holmes et al., 2006; Särkämö et al., 2012).

7.3. How do neural network dynamics change at the end of life?

This dissertation sheds some light on how spatial and connectivity characteristics of so-called "canonical" neural networks change at the end of life. By canonical here I mean groups of neural regions whose activation and within-network connectivity have been consistently associated with a specific cognitive function; examples of canonical networks are the VAN, DAN, and DMN (Fox et al., 2005; Mantini et al., 2007). Recently, it was shown that networks become increasingly differentiated (the number of nodes within some networks increases, and decreases within others) from infancy to young adulthood (Gu et al., 2015) but become

dedifferentiated (the number of nodes within networks become more similar) in later adulthood (Dennis & Cabeza, 2011; Grady et al., 2016; Meunier et al., 2009). Age-related changes in network differentiation, however, were not observed in these data, as there were no significant difference in the number of ICs localized to any of the task-positive networks (VAN, DAN, or ODD) (the 2 condition x 3 network interaction was not significant, $F(2,46) = 1.04$, $p = 0.36$, Hyunh-Feldt corrected) nor to the DMN ($t(35) = 0.74$, $p = 0.47$, equal variances assumed) between controls and responsive patients. Similarly, no further dedifferentiation was observed when patients became unresponsive in either task-positive networks (3 condition x 3 network interaction was not significant, $F(4,54) = 1.77$, $p = 0.15$, Huynh-Feldt corrected) nor in the DMN (one-way ANOVA comparing all 3 conditions was not significant, $F(2,38) = 1.03$, $p = 0.37$). This discrepancy could result from the small size of the palliative samples, but could also result from differences in how the networks were defined (networks reported in the cited literature were defined using data-driven graph-theoretical algorithms, whereas the networks reported here were defined a-priori).

Within-network connectivity among so-called “higher order” cognitive networks, such as VAN and DAN, as assessed from fMRI resting state data, appears to decrease from infancy to young adulthood, as also does between-network connectivity (Gu et al., 2015). Importantly, both within- and between-network connectivity in the DMN increase with age through young adulthood (Gu, et al., 2015). Such patterns are less consistent during the transition to older adulthood, where changes in within- and between-network connectivity vary depending on network and study conditions (task-positive vs at rest) (Grady et al., 2016). For example, Grady and colleagues (2016) showed that both within- and between-network connectivity for the DAN were similar among younger and older adults at rest, but between-network connectivity was

larger among older adults when participants were engaged in behavioural tasks that involved visual memory and self-referential associations (but within-network connectivity remained the same). Patterns of connectivity reported in Chapter 4, however, based on our EEG phase synchronization data, are different from those results, as about 50% fewer responsive patients had meaningful between-network connectivity (VANDAN, VANODD, and DANODD) compared to controls (save for VANODD connectivity to pattern changes), but within-network connectivity (VAN and DAN) remained fairly consistent with that of controls. ODD connectivity, by contrast, was considerably reduced among responsive patients, but since ODD is not a "canonical" network, there's no reason to expect that patterns of connectivity within ODD would be similar to those of the VAN and DAN. It's important to reiterate that the ODD label was simply applied to regions identified in Chapter 2 that have been frequently implicated in oddball tasks but have not been established as a "canonical" network implicated in a specific cognitive function. Connectivity within ODD could represent connectivity between different canonical networks that share the same neural regions, such as DMN (PCC), sensorimotor (LPreCG), and visual (Occ) networks (Fox et al., 2005; Gu et al., 2015; Heuvel & Sporns, 2013; Mantini et al., 2007; Meunier et al., 2009; van den Heuvel & Hulshoff Pol, 2010).

Unresponsive patients, by contrast, showed decreases in both within- and between-network connectivity. About 50% fewer unresponsive patients had meaningful connectivity within VAN compared to controls and responsive patients in the tone change condition (VAN connectivity to patterns changes was similar across all 3 groups), and no unresponsive patients showed any evidence of within-DAN connectivity in either condition (though recall that this is because no unresponsive patients had ICs localized to more than one region within the DAN). Between-network connectivity was also decreased compared to the other participant groups,

particularly in VANDAN where no unresponsive patients had any meaningful connectivity in either condition. A comparison of the number of IC pairs with meaningful early theta connectivity both within (VAN, DAN, and ODD) and between (VANDAN, VANODD, DANODD) networks in either condition revealed a main effect of participant group ($F(2,27) = 5.63$, $p = 0.01$). Post hoc comparisons using Tukey HSD showed that connectivity among controls was significantly larger than that of unresponsive patients (*Mdiff* = 5.81), whereas all main effects of group on connectivity were not significant (although the difference between controls and responsive patients was nearly significant and $p = 0.052$). Furthermore, there was a significant group x connectivity type (within-network or between-network) interaction ($F(2,27) = 4.60$, $p = 0.02$, Huynh-Feldt corrected), where between-network connectivity among controls was significantly larger than that of the two patient groups (see Figure 7.1). These data show that between-network connectivity appears to decrease considerably over the lifespan, whereas within-network connectivity also decreases, but to a lesser extent. Interestingly, while both within and between-network connectivity decreased once patients became unresponsive, particularly connectivity that included the DAN, this decrease was not significant.

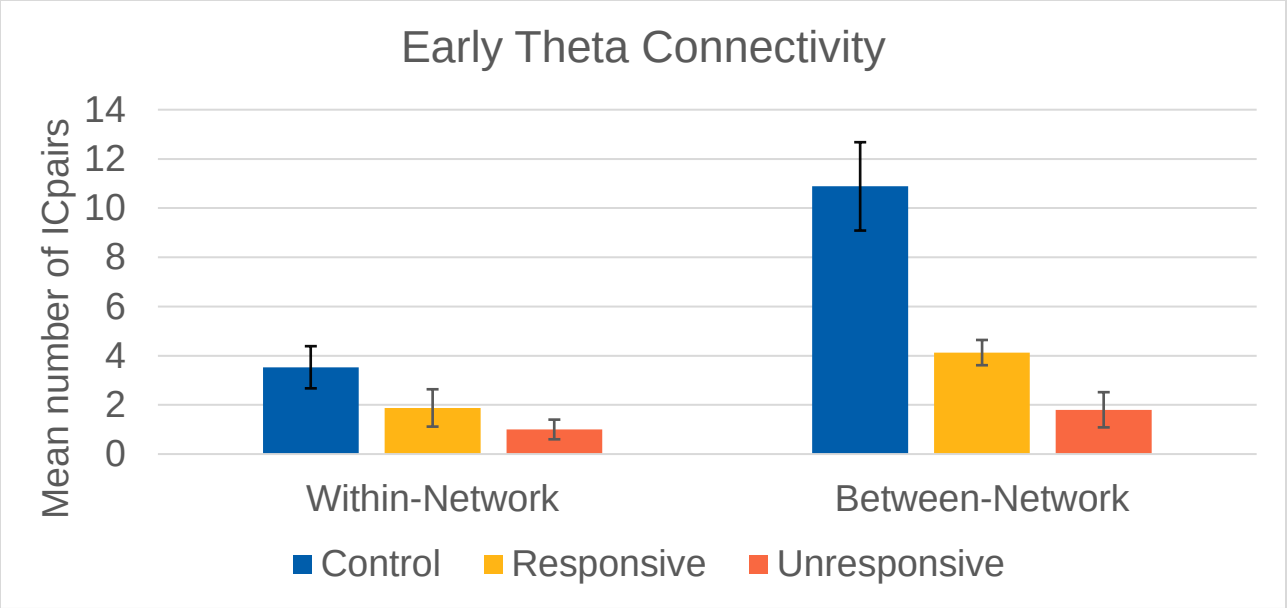

Figure 7.1. Comparison of within-network (VAN, DAN, ODD) and between-network (VANDAN, VANODD, DANODD) connectivity for all patient groups reported in Chapter 4.

The vertical axis represents the mean number of IC pairs with meaningful connectivity within the first 500 ms post stimulus. Total IC pairs were summed across both tone and pattern change conditions. Error bars represent one standard error.

By contrast, it has been shown, based on fMRI data, that both within and between-network connectivity within DMN increase considerably from infancy to young adulthood (Gu et al., 2015), yet within-network connectivity drops from younger to older adulthood (between-network connectivity remain the same) (Grady et al., 2016). This is inconsistent with the data reported in Chapter 5, since connectivity measured by EEG phase synchronization, was nearly ubiquitous among all ICs localized to DMN for all participant groups, and there was no significant decrease in ICs localized to DMN among groups (see above). Connectivity within DMN, therefore, at least as measured by EEG phase synchronization, does not appear to decrease over the lifespan, nor does it decrease as patients become unresponsive. Overall these data show that network differentiation, and within-network connectivity, appear to remain

relatively stable over the lifespan, whereas between-network connectivity is significantly reduced. Interestingly, there is very little difference in the spatial and connectivity characteristics of the reported neural networks between responsive and unresponsive patients (save for the decrease in DAN connectivity). Recently it was shown that patterns of cortical network connectivity may not be correlated with levels of consciousness in the rat brain (Pal et al., 2020). In this study rats were exposed to ongoing general anesthesia, but had their wakefulness restored by carbachol injection to the frontal cortex. While the rats were in this state of wakefulness while being anesthetized, their patterns of cortical connectivity were more similar to when they were unresponsive and anesthetized, than when they were awake and not anesthetized. This suggests that the suppression in cortical connectivity (among other potential biomarkers of unconsciousness) that is typically associated with unconsciousness from anesthesia may be a result of the anesthetic medication, but separable from the conscious state of the patient. The data reported in Chapters 4 and 5 are consistent with this interpretation, as there is very little difference in overall levels of cortical connectivity between responsive and unresponsive palliative patients. Patterns of network connectivity may offer greater insight into the contents of an unresponsive patients' experience (c.f. Block, 2005; Bor & Seth, 2012; Revonsuo, 1999; Smallwood et al., 2012), rather than into their level of consciousness.

7.4. Strengths, limitations, future directions, and clinical recommendations

A key feature of this work is that it employs sensitive, sophisticated, and nuanced measures to characterize cortical activity associated with cognitive processes amongst a clinical population that has never been studied in this depth. These nuanced measures allowed me to characterize the network activity of individual neurotypical and palliative patients, which has also rarely been attempted. One major contribution of this dissertation is, therefore, that it clearly

demonstrates the variability of neurotypical cortical activity associated with certain cognitive processes. In Chapter 3 I demonstrate that not all neurotypical participants generate a P3b to auditory oddballs, despite showing near-perfect accuracy in behaviourally identifying those oddballs. This task would, therefore, fail to detect awareness in 6% (1/17) of conscious, young, healthy, neurotypical people. One can only assume the failure rate would increase among older, unwell people, many of whom will have suffered neurological damage. The primary reason for such a failure rate is unlikely to be an instrument error, but rather variability in neurological responding to external stimulation. Chapters 2 and 4 show that, whereas there are clear commonalities with respect to the neural generators of P300 ERPs (Chapter 2), they are by no means uniform across participants (Chapter 4). In addition, Chapter 5 shows that whereas most neurotypical controls show activation within the PCC at rest, activation within other ROIs that are associated with the DMN varies greatly across participants (c.f. Meindl et al., 2010). Such variability in neurotypical cortical activity means that simple binary questions pertaining to unresponsive palliative patients, such as "is my loved one aware," cannot be met with simple binary answers. As shown in Table 7.1, the strength of evidence of awareness can vary, and can depend on the type of task from which awareness is inferred. While providing such a nuanced picture of cortical processing may not be ideal for predicting prognosis, as is essential for treating DOC patients, it can offer insight into what an unresponsive patient at the end of life may be capable of experiencing.

One major limitation of this work is that it does not make use of age-matched controls. There are age-related changes in most measures employed in this dissertation that should be taken into consideration in future replications of this work (Campbell et al., 2013; Grady et al., 2016; Meunier et al., 2009; Näätänen et al., 2012; Polich, 1996; Spreng & Schacter, 2012; D.

Tomasi & Volkow, 2012; Tsolaki et al., 2015; Vesco et al., 1993). Because one of the goals of this dissertation was to characterize individual variability in the spatio-temporal dynamics underlying potential biomarkers of awareness previously studied in the context of disorders of consciousness, it seemed appropriate to do so using control data that were similar in demographics to the controls commonly featured in the DOC literature. Since palliative care, however, typically serves an older population, it's important to establish age-appropriate norms for these potential biomarkers for future study of awareness at the end of life.

Incorporating music could greatly improve current methods of awareness assessment, as it shares features of many of the most promising neuroimaging assessment tools that have been developed for DOC patients and improves on some of their weaknesses. First, music not only engages cortical auditory processing and auditory attention (c.f. Bekinschtein et al., 2009; Cruse et al., 2012; Fischer et al., 2010; Kotchoubey et al., 2005; Morlet & Fischer, 2014; Real et al., 2016), but also emotional processing that can enhance arousal and encourage externally-oriented attention (c.f. Castro et al., 2015; Chennu & Bekinschtein, 2012; Lang, 1995; Öhman et al., 2001; Salimpoor et al., 2009; Schupp et al., 2006). Using a patients' preferred music can also engage in self-referential processes that are known to encourage engagement from TBI patients (c.f. Eichenlaub et al., 2012; Holeckova et al., 2006, 2008; Perrin et al., 2006). Second, it's possible to detect a sustained neural response that is easily measurable by EEG. Measuring a sustained neural response, as opposed to a short-latency response that relies on cortical entrainment to a given stimulus (ERPs), can accommodate increased latencies or temporal variability in cognitive responses that may be seen in patients who are brain injured (Lew et al., 2007; Segalowitz et al., 1997), cognitively impaired (Ball et al., 1989; Polich et al., 1986), or taking medications with psychoactive effects (Barker et al., 2004; Buffett-Jerrott & Stewart,

2002; Engelhardt et al., 1992; Milligan et al., 1989). Furthermore, EEG is one of the few neuroimaging methods that can allow for bedside assessment (Laureys et al., 2006). And finally, listening to music is an easy and pleasurable experience for patients. This is one of the most important features of any study to be performed in a hospice setting, as it is consistent with the mandate of all palliative care facilities; to maximize the quality of life of the patients. It is my hope that future studies of awareness assessment consider incorporating music into their battery of assessments, as music-centered paradigms may be both scientifically useful and enjoyable for patients.

References

Alegre, M., Labarga, A., Gurtubay, I. G., Iriarte, J., Malanda, A., & Artieda, J. (2002). Beta electroencephalograph changes during passive movements: Sensory afferences contribute to beta event-related desynchronization in humans. *Neuroscience Letters*, *331*(1), 29–32. https://doi.org/10.1016/S0304-3940(02)00825-X

Anderer, P., Semlitsch, H. V., & Saletu, B. (1996). Multichannel auditory event-related brain potentials: Effects of normal aging on the scalp distribution of N1, P2, N2 and P300 latencies and amplitudes. *Electroencephalography and Clinical Neurophysiology*, *99*(5), 458–472. https://doi.org/10.1016/S0013-4694(96)96518-9

Andrews, K., Murphy, L., Munday, R., & Littlewood, C. (1996). Misdiagnosis of the vegetative state: Retrospective study in a rehabilitation unit. *BMJ*, *313*(7048), 13–16. https://doi.org/10.1136/bmj.313.7048.13

Andrews-Hanna, J. R., Reidler, J. S., Sepulcre, J., Poulin, R., & Buckner, R. L. (2010). Functional-Anatomic Fractionation of the Brain's Default Network. *Neuron*, *65*(4), 550–562. https://doi.org/10.1016/j.neuron.2010.02.005

Atienza, M., Cantero, J. L., & Escera, C. (2001). Auditory information processing during human sleep as revealed by event-related brain potentials. *Clinical Neurophysiology*, *112*(11), 2031–2045. https://doi.org/10.1016/S1388-2457(01)00650-2

Baars, B. J. (2005). Global workspace theory of consciousness: Toward a cognitive neuroscience of human experience. In S. Laureys (Ed.), *Progress in Brain Research* (Vol. 150, pp. 45–53). Elsevier. https://doi.org/10.1016/S0079-6123(05)50004-9

Ball, S. S., Marsh, J. T., Schubarth, G., Brown, W. S., & Strandburg, R. (1989). Longitudinal P300 Latency Changes in Alzheimer's Disease. *Journal of Gerontology*, *44*(6), M195–M200. https://doi.org/10.1093/geronj/44.6.M195

Barker, M. J., Greenwood, K. M., Jackson, M., & Crowe, S. F. (2004). Cognitive Effects of Long-Term Benzodiazepine Use. *CNS Drugs*, *18*(1), 37–48. https://doi.org/10.2165/00023210-200418010-00004

Başar, E., & Güntekin, B. (2012). A short review of alpha activity in cognitive processes and in cognitive impairment. *International Journal of Psychophysiology*, *86*(1), 25–38. https://doi.org/10.1016/j.ijpsycho.2012.07.001

Başar, E., Tülay, E., & Güntekin, B. (2015). Multiple gamma oscillations in the brain: A new strategy to differentiate functional correlates and P300 dynamics. *International Journal of Psychophysiology*, *95*(3), 406–420. https://doi.org/10.1016/j.ijpsycho.2015.01.013

Bauer, L. O. (2001). CNS recovery from cocaine, cocaine and alcohol, or opioid dependence: A P300 study. *Clinical Neurophysiology*, *112*(8), 1508–1515. https://doi.org/10.1016/S1388-2457(01)00583-1

Bedo, N., Ribary, U., & Ward, L. M. (2014). Fast Dynamics of Cortical Functional and Effective Connectivity during Word Reading. *PLOS ONE*, *9*(2), e88940. https://doi.org/10.1371/journal.pone.0088940

Bekinschtein, T. A., Dehaene, S., Rohaut, B., Tadel, F., Cohen, L., & Naccache, L. (2009). Neural signature of the conscious processing of auditory regularities. *Proceedings of the National Academy of Sciences*, *106*(5), 1672–1677. https://doi.org/10.1073/pnas.0809667106

Bernat, E. M., Malone, S. M., Williams, W. J., Patrick, C. J., & Iacono, W. G. (2007). Decomposing delta, theta, and alpha time–frequency ERP activity from a visual oddball task using PCA. *International Journal of Psychophysiology*, *64*(1), 62–74. https://doi.org/10.1016/j.ijpsycho.2006.07.015

Bledowski, C., Prvulovic, D., Hoechstetter, K., Scherg, M., Wibral, M., Goebel, R., & Linden, D. E. J. (2004). Localizing P300 Generators in Visual Target and Distractor Processing: A Combined Event-Related Potential and Functional Magnetic Resonance Imaging Study. *Journal of Neuroscience*, *24*(42), 9353–9360. https://doi.org/10.1523/JNEUROSCI.1897-04.2004

Block, N. (2005). Two neural correlates of consciousness. *Trends in Cognitive Sciences*, *9*(2), 46–52. https://doi.org/10.1016/j.tics.2004.12.006

Blume, C., del Giudice, R., Wislowska, M., Lechinger, J., & Schabus, M. (2015). Across the consciousness continuum—From unresponsive wakefulness to sleep. *Frontiers in Human Neuroscience*, *9*. https://doi.org/10.3389/fnhum.2015.00105

Blundon, E. G., Rumak, S. P., & Ward, L. M. (2017). Sequential search asymmetry: Behavioral and psychophysiological evidence from a dual oddball task. *PLOS ONE*, *12*(3), e0173237. https://doi.org/10.1371/journal.pone.0173237

Blundon, E. G., & Ward, L. M. (2019). Search asymmetry in a serial auditory task: Neural source analyses of EEG implicate attention strategies. *Neuropsychologia*, *134*, 107204. https://doi.org/10.1016/j.neuropsychologia.2019.107204

Boly, M., Faymonville, M.-E., Schnakers, C., Peigneux, P., Lambermont, B., Phillips, C., Lancellotti, P., Luxen, A., Lamy, M., Moonen, G., Maquet, P., & Laureys, S. (2008). Perception of pain in the minimally conscious state with PET activation: An

observational study. *The Lancet Neurology*, *7*(11), 1013–1020. https://doi.org/10.1016/S1474-4422(08)70219-9

Boly, M., Garrido, M. I., Gosseries, O., Bruno, M.-A., Boveroux, P., Schnakers, C., Massimini, M., Litvak, V., Laureys, S., & Friston, K. (2011). Preserved Feedforward But Impaired Top-Down Processes in the Vegetative State. *Science*, *332*(6031), 858–862. https://doi.org/10.1126/science.1202043

Boly, M., Moran, R., Murphy, M., Boveroux, P., Bruno, M.-A., Noirhomme, Q., Ledoux, D., Bonhomme, V., Brichant, J.-F., Tononi, G., Laureys, S., & Friston, K. (2012). Connectivity Changes Underlying Spectral EEG Changes during Propofol-Induced Loss of Consciousness. *Journal of Neuroscience*, *32*(20), 7082–7090. https://doi.org/10.1523/JNEUROSCI.3769-11.2012

Boly, M., Phillips, C., Tshibanda, L., Vanhaudenhuyse, A., Schabus, M., Dang-Vu, T. T., Moonen, G., Hustinx, R., Maquet, P., & Laureys, S. (2008). Intrinsic Brain Activity in Altered States of Consciousness. *Annals of the New York Academy of Sciences*, *1129*, 119–129. https://doi.org/10.1196/annals.1417.015

Bor, D., & Seth, A. K. (2012). Consciousness and the Prefrontal Parietal Network: Insights from Attention, Working Memory, and Chunking. *Frontiers in Psychology*, *3*. https://doi.org/10.3389/fpsyg.2012.00063

Borjigin, J., Lee, U., Liu, T., Pal, D., Huff, S., Klarr, D., Sloboda, J., Hernandez, J., Wang, M. M., & Mashour, G. A. (2013). Borjigin, J., Lee, U., Liu, T., Pal, D., Huff, S., Klarr, D., ... & Mashour, G. A. (2013). Surge of neurophysiological coherence and connectivity in the dying brain. *Proceedings of the National Academy of Sciences*, *110*(35), 14432–14437.

Bressler, S. L. (1995). Large-scale cortical networks and cognition. *Brain Research Reviews*, *20*(3), 288–304. https://doi.org/10.1016/0165-0173(94)00016-I

Buckner, R. L., Andrews-Hanna, J. R., & Schacter, D. L. (2008a). The brain's default network: Anatomy, function, and relevance to disease. In *The year in cognitive neuroscience 2008* (pp. 1–38). Blackwell Publishing.

Buckner, R. L., Andrews-Hanna, J. R., & Schacter, D. L. (2008b). The brain's default network: Anatomy, function, and relevance to disease. In *The year in cognitive neuroscience 2008.* (pp. 1–38). Blackwell Publishing.

Buffett-Jerrott, S. E., & Stewart, S. H. (2002). Cognitive and sedative effects of benzodiazepine use. *Current Pharmaceutical Design*, *8*(1), 45–58. https://doi.org/info:doi/10.2174/1381612023396654

Buzsáki, G. (2002). Theta Oscillations in the Hippocampus. *Neuron*, *33*(3), 325–340. https://doi.org/10.1016/S0896-6273(02)00586-X

Calhoun, V. D., Liu, J., & Adalı, T. (2009). A review of group ICA for fMRI data and ICA for joint inference of imaging, genetic, and ERP data. *NeuroImage*, *45*(1, Supplement 1), S163–S172. https://doi.org/10.1016/j.neuroimage.2008.10.057

Campbell, K. L., Grigg, O., Saverino, C., Churchill, N., & Grady, C. L. (2013). Age differences in the intrinsic functional connectivity of default network subsystems. *Frontiers in Aging Neuroscience*, *5*, 73. https://doi.org/10.3389/fnagi.2013.00073

Casali, A. G., Gosseries, O., Rosanova, M., Boly, M., Sarasso, S., Casali, K. R., Casarotto, S., Bruno, M.-A., Laureys, S., Tononi, G., & Massimini, M. (2013). A Theoretically Based Index of Consciousness Independent of Sensory Processing and Behavior. *Science*

Translational Medicine, *5*(198), 198ra105-198ra105. https://doi.org/10.1126/scitranslmed.3006294

Castro, M., Tillmann, B., Luauté, J., Corneyllie, A., Dailler, F., André-Obadia, N., & Perrin, F. (2015). Boosting Cognition With Music in Patients With Disorders of Consciousness. *Neurorehabilitation and Neural Repair*, *29*(8), 734–742. https://doi.org/10.1177/1545968314565464

Cauda, F., Micon, B. M., Sacco, K., Duca, S., D'Agata, F., Geminiani, G., & Canavero, S. (2009). Disrupted intrinsic functional connectivity in the vegetative state. *Journal of Neurology, Neurosurgery & Psychiatry*, *80*(4), 429–431. https://doi.org/10.1136/jnnp.2007.142349

Cavinato, M., Freo, U., Ori, C., Zorzi, M., Tonin, P., Piccione, F., & Merico, A. (2009). Post-acute P300 predicts recovery of consciousness from traumatic vegetative state. *Brain Injury*, *23*(12), 973–980. https://doi.org/10.3109/02699050903373493

Charland-Verville, V., Jourdan, J.-P., Thonnard, M., Ledoux, D., Donneau, A.-F., Quertemont, E., & Laureys, S. (2014). Near-death experiences in non-life-threatening events and coma of different etiologies. *Frontiers in Human Neuroscience*, *8*. https://doi.org/10.3389/fnhum.2014.00203

Chennu, S., & Bekinschtein, T. A. (2012). Arousal Modulates Auditory Attention and Awareness: Insights from Sleep, Sedation, and Disorders of Consciousness. *Frontiers in Psychology*, *3*. https://doi.org/10.3389/fpsyg.2012.00065

Childs, N. L., Mercer, W. N., & Childs, H. W. (1993). Accuracy of diagnosis of persistent vegetative state. *Neurology*, *43*(8), 1465–1465.

Chou, R., Fanciullo, G. J., Fine, P. G., Adler, J. A., Ballantyne, J. C., Davies, P., Donovan, M. I., Fishbain, D. A., Foley, K. M., Fudin, J., Gilson, A. M., Kelter, A., Mauskop, A., O'Connor, P. G., Passik, S. D., Pasternak, G. W., Portenoy, R. K., Rich, B. A., Roberts, R. G., … Miaskowski, C. (2009). Clinical Guidelines for the Use of Chronic Opioid Therapy in Chronic Noncancer Pain. *The Journal of Pain*, *10*(2), 113-130.e22. https://doi.org/10.1016/j.jpain.2008.10.008

Christoff, K., Irving, Z. C., Fox, K. C. R., Spreng, R. N., & Andrews-Hanna, J. R. (2016). Mind-wandering as spontaneous thought: A dynamic framework. *Nature Reviews Neuroscience*, *17*(11), 718–731. https://doi.org/10.1038/nrn.2016.113

Cole, M. W., Reynolds, J. R., Power, J. D., Repovs, G., Anticevic, A., & Braver, T. S. (2013). Multi-task connectivity reveals flexible hubs for adaptive task control. *Nature Neuroscience*, *16*(9), 1348–1355. https://doi.org/10.1038/nn.3470

Coleman, M. R., Rodd, J. M., Davis, M. H., Johnsrude, I. S., Menon, D. K., Pickard, J. D., & Owen, A. M. (2007). Do vegetative patients retain aspects of language comprehension? Evidence from fMRI. *Brain*, *130*(10), 2494–2507. https://doi.org/10.1093/brain/awm170

Comerchero, M. D., & Polich, J. (1999). P3a and P3b from typical auditory and visual stimuli. *Clinical Neurophysiology*, *110*(1), 24–30. https://doi.org/10.1016/S0168-5597(98)00033-1

Conroy, M. A., & Polich, J. (2007). Normative Variation of P3a and P3b from a Large Sample. *Journal of Psychophysiology*, *21*(1), 22–32. https://doi.org/10.1027/0269-8803.21.1.22

Corbetta, M., Kincade, J. M., & Shulman, G. L. (2002). Neural Systems for Visual Orienting and Their Relationships to Spatial Working Memory. *Journal of Cognitive Neuroscience*, *14*(3), 508–523. https://doi.org/10.1162/089892902317362029

Corbetta, M., Patel, G., & Shulman, G. L. (2008). The Reorienting System of the Human Brain: From Environment to Theory of Mind. *Neuron*, *58*(3), 306–324. https://doi.org/10.1016/j.neuron.2008.04.017

Corbetta, M., & Shulman, G. L. (2002). Control of goal-directed and stimulus-driven attention in the brain. *Nature Reviews Neuroscience*, *3*(3), 201–215. https://doi.org/10.1038/nrn755

Cote, K. A. (2002). Probing awareness during sleep with the auditory odd-ball paradigm. *International Journal of Psychophysiology*, *46*(3), 227–241. https://doi.org/10.1016/S0167-8760(02)00114-9

Coyle, D., Stow, J., McCreadie, K., McElligott, J., & Carroll, Á. (2015). Sensorimotor Modulation Assessment and Brain-Computer Interface Training in Disorders of Consciousness. *Archives of Physical Medicine and Rehabilitation*, *96*(3, Supplement), S62–S70. https://doi.org/10.1016/j.apmr.2014.08.024

Crone, J. S., Ladurner, G., Höller, Y., Golaszewski, S., Trinka, E., & Kronbichler, M. (2011). Deactivation of the Default Mode Network as a Marker of Impaired Consciousness: An fMRI Study. *PLOS ONE*, *6*(10), e26373. https://doi.org/10.1371/journal.pone.0026373

Crone, J. S., Schurz, M., Höller, Y., Bergmann, J., Monti, M., Schmid, E., Trinka, E., & Kronbichler, M. (2015). Impaired consciousness is linked to changes in effective connectivity of the posterior cingulate cortex within the default mode network. *NeuroImage*, *110*, 101–109. https://doi.org/10.1016/j.neuroimage.2015.01.037

Crone, N. E., Miglioretti, D. L., Gordon, B., & Lesser, R. P. (1998). Functional mapping of human sensorimotor cortex with electrocorticographic spectral analysis. II. Event-related synchronization in the gamma band. *Brain*, *121*(12), 2301–2315. https://doi.org/10.1093/brain/121.12.2301

Cruse, D., Chennu, S., Chatelle, C., Bekinschtein, T. A., Fernández-Espejo, D., Pickard, J. D., Laureys, S., & Owen, A. M. (2011). Bedside detection of awareness in the vegetative state: A cohort study. *The Lancet*, *378*(9809), 2088–2094. https://doi.org/10.1016/S0140-6736(11)61224-5

Cruse, D., Chennu, S., Fernández-Espejo, D., Payne, W. L., Young, G. B., & Owen, A. M. (2012). Detecting Awareness in the Vegetative State: Electroencephalographic Evidence for Attempted Movements to Command. *PLOS ONE*, *7*(11), e49933. https://doi.org/10.1371/journal.pone.0049933

Curley, W. H., Forgacs, P. B., Voss, H. U., Conte, M. M., & Schiff, N. D. (2018). Characterization of EEG signals revealing covert cognition in the injured brain. *Brain*, *141*(5), 1404–1421. https://doi.org/10.1093/brain/awy070

Danielson, N. B., Guo, J. N., & Blumenfeld, H. (2011). The Default Mode Network and Altered Consciousness in Epilepsy. *Behavioural Neurology*, *24*(1), 55–65. https://doi.org/10.3233/BEN-2011-0310

Davey, C. G., Pujol, J., & Harrison, B. J. (2016). Mapping the self in the brain's default mode network. *NeuroImage*, *132*, 390–397. https://doi.org/10.1016/j.neuroimage.2016.02.022

David, O., Kilner, J. M., & Friston, K. J. (2006). Mechanisms of evoked and induced responses in MEG/EEG. *NeuroImage*, *31*(4), 1580–1591. https://doi.org/10.1016/j.neuroimage.2006.02.034

Dehaene, S., & Naccache, L. (2001). Towards a cognitive neuroscience of consciousness: Basic evidence and a workspace framework. *Cognition*, *79*(1), 1–37. https://doi.org/10.1016/S0010-0277(00)00123-2

Delorme, A., & Makeig, S. (2004). EEGLAB: An open source toolbox for analysis of single-trial EEG dynamics including independent component analysis. *Journal of Neuroscience Methods*, *134*(1), 9–21. https://doi.org/10.1016/j.jneumeth.2003.10.009

Delorme, A., Palmer, J., Onton, J., Oostenveld, R., & Makeig, S. (2012). Independent EEG Sources Are Dipolar. *PLOS ONE*, *7*(2), e30135. https://doi.org/10.1371/journal.pone.0030135

Delorme, A., Sejnowski, T., & Makeig, S. (2007). Enhanced detection of artifacts in EEG data using higher-order statistics and independent component analysis. *NeuroImage*, *34*(4), 1443–1449. https://doi.org/10.1016/j.neuroimage.2006.11.004

Demertzi, A., Soddu, A., Faymonville, M.-E., Bahri, M. A., Gosseries, O., Vanhaudenhuyse, A., Phillips, C., Maquet, P., Noirhomme, Q., Luxen, A., & Laureys, S. (2011). Chapter 20—Hypnotic modulation of resting state fMRI default mode and extrinsic network connectivity. In E. J. W. Van Someren, Y. D. Van Der Werf, P. R. Roelfsema, H. D. Mansvelder, & F. H. Lopes Da Silva (Eds.), *Progress in Brain Research* (Vol. 193, pp. 309–322). Elsevier. https://doi.org/10.1016/B978-0-444-53839-0.00020-X

Demiralp, T., Ademoglu, A., Comerchero, M., & Polich, J. (2001). Wavelet Analysis of P3a and P3b. *Brain Topography*, *13*(4), 251–267. https://doi.org/10.1023/A:1011102628306

Dennis, N. A., & Cabeza, R. (2011). Age-related dedifferentiation of learning systems: An fMRI study of implicit and explicit learning. *Neurobiology of Aging*, *32*(12), 2318.e17-2318.e30. https://doi.org/10.1016/j.neurobiolaging.2010.04.004

Deshpande, G., Kerssens, C., Sebel, P. S., & Hu, X. (2010). Altered Local Coherence in the Default Mode Network due to Sevoflurane Anesthesia. *Brain Research*, *1318*, 110–121. https://doi.org/10.1016/j.brainres.2009.12.075

Di, H. B., Yu, S. M., Weng, X. C., Laureys, S., Yu, D., Li, J. Q., Qin, P. M., Zhu, Y. H., Zhang, S. Z., & Chen, Y. Z. (2007). Cerebral response to patient's own name in the vegetative and minimally conscious states. *Neurology*, *68*(12), 895–899.

Di, H., Boly, M., Weng, X., Ledoux, D., & Laureys, S. (2008). Neuroimaging activation studies in the vegetative state: Predictors of recovery? *Clinical Medicine*, *8*(5), 502–507. https://doi.org/10.7861/clinmedicine.8-5-502

Di Perri, C., Bahri, M. A., Amico, E., Thibaut, A., Heine, L., Antonopoulos, G., Charland-Verville, V., Wannez, S., Gomez, F., Hustinx, R., Tshibanda, L., Demertzi, A., Soddu, A., & Laureys, S. (2016). Neural correlates of consciousness in patients who have emerged from a minimally conscious state: A cross-sectional multimodal imaging study. *The Lancet Neurology*, *15*(8), 830–842. https://doi.org/10.1016/S1474-4422(16)00111-3

Di Perri, C., Stender, J., Laureys, S., & Gosseries, O. (2014). Functional neuroanatomy of disorders of consciousness. *Epilepsy & Behavior*, *30*, 28–32. https://doi.org/10.1016/j.yebeh.2013.09.014

Doeller, C. F., Opitz, B., Mecklinger, A., Krick, C., Reith, W., & Schröger, E. (2003). Prefrontal cortex involvement in preattentive auditory deviance detection: Neuroimaging and electrophysiological evidence. *NeuroImage*, *20*(2), 1270–1282. https://doi.org/10.1016/S1053-8119(03)00389-6

Doesburg, S. M., Green, J. J., McDonald, J. J., & Ward, L. M. (2009). Rhythms of Consciousness: Binocular Rivalry Reveals Large-Scale Oscillatory Network Dynamics Mediating Visual Perception. *PLOS ONE*, *4*(7), e6142. https://doi.org/10.1371/journal.pone.0006142

Doesburg, S. M., Green, J. J., McDonald, J. J., & Ward, L. M. (2012). Theta modulation of inter-regional gamma synchronization during auditory attention control. *Brain Research*, *1431*, 77–85. https://doi.org/10.1016/j.brainres.2011.11.005

Doesburg, S. M., Roggeveen, A. B., Kitajo, K., & Ward, L. M. (2008). Large-Scale Gamma-Band Phase Synchronization and Selective Attention. *Cerebral Cortex*, *18*(2), 386–396. https://doi.org/10.1093/cercor/bhm073

Doesburg, S. M., Ward, L. M., & Ribary, U. (2015). The alpha-theta-gamma (ATG) switch: Toward unified principles of cortical processing. *Current Trends in Neurology*, *9*, 1–12.

Downar, J., Crawley, A. P., Mikulis, D. J., & Davis, K. D. (2000). A multimodal cortical network for the detection of changes in the sensory environment. *Nature Neuroscience*, *3*(3), 277–283. https://doi.org/10.1038/72991

Droney, J., & Hall, E. (2008). Status Epilepticus in a Hospice Inpatient Setting. *Journal of Pain and Symptom Management*, *36*(1), 97–105. https://doi.org/10.1016/j.jpainsymman.2007.08.009

Dykstra, A. R., & Gutschalk, A. (2015). Does the mismatch negativity operate on a consciously accessible memory trace? | Science Advances. *Sciences Advances*, *1*(10), e1500677. https://doi.org/10.1126/sciadv.1500677

Eichenlaub, J.-B., Ruby, P., & Morlet, D. (2012). What is the specificity of the response to the own first-name when presented as a novel in a passive oddball paradigm? An ERP study. *Brain Research*, *1447*, 65–78. https://doi.org/10.1016/j.brainres.2012.01.072

Engel, A. K., & Fries, P. (2010). Beta-band oscillations—Signalling the status quo? *Current Opinion in Neurobiology*, *20*(2), 156–165. https://doi.org/10.1016/j.conb.2010.02.015

Engelhardt, W., Friess, K., Hartung, E., Sold, M., & Dierks, T. (1992). EEG and auditory evoked potential P300 compared with psychometric tests in assessing vigilance after benzodiazepine sedation and antagonism. *BJA: British Journal of Anaesthesia*, *69*(1), 75–80. https://doi.org/10.1093/bja/69.1.75

Evans, D. W. (2009). Neuropathology of Brain Death in the Modern Transplant Era. *Neurology*, *72*(7), 677–678. https://doi.org/10.1212/01.wnl.0000339390.48966.e2

Facco, E., & Agrillo, C. (2012). Near-death experiences between science and prejudice. *Frontiers in Human Neuroscience*, *6*. https://doi.org/10.3389/fnhum.2012.00209

Fainsinger, R., Miller, M. J., Bruera, E., Hanson, J., & Maceachern, T. (1991). Symptom Control during the Last Week of Life on a Palliative Care Unit. *Journal of Palliative Care*, *7*(1), 5–11. https://doi.org/10.1177/082585979100700102

Fell, J., Fernández, G., Klaver, P., Elger, C. E., & Fries, P. (2003). Is synchronized neuronal gamma activity relevant for selective attention? *Brain Research Reviews*, *42*(3), 265–272. https://doi.org/10.1016/S0165-0173(03)00178-4

Fell, J., Hinrichs, H., & Röschke, J. (1997). Time course of human 40 Hz EEG activity accompanying P3 responses in an auditory oddball paradigm. *Neuroscience Letters*, *235*(3), 121–124. https://doi.org/10.1016/S0304-3940(97)00730-1

Fellinger, R., Klimesch, W., Schnakers, C., Perrin, F., Freunberger, R., Gruber, W., Laureys, S., & Schabus, M. (2011). Cognitive processes in disorders of consciousness as revealed by EEG time–frequency analyses. *Clinical Neurophysiology*, *122*(11), 2177–2184. https://doi.org/10.1016/j.clinph.2011.03.004

Fernández-Espejo, D., Norton, L., & Owen, A. M. (2014). The Clinical Utility of fMRI for Identifying Covert Awareness in the Vegetative State: A Comparison of Sensitivity

between 3T and 1.5T. *PLOS ONE*, *9*(4), e95082. https://doi.org/10.1371/journal.pone.0095082

Fernández-Espejo, D., & Owen, A. M. (2013). Detecting awareness after severe brain injury. *Nature Reviews Neuroscience*, *14*(11), 801–809. https://doi.org/10.1038/nrn3608

Fernández-Espejo, D., Soddu, A., Cruse, D., Palacios, E. M., Junque, C., Vanhaudenhuyse, A., Rivas, E., Newcombe, V., Menon, D. K., Pickard, J. D., Laureys, S., & Owen, A. M. (2012). A role for the default mode network in the bases of disorders of consciousness. *Annals of Neurology*, *72*(3), 335–343. https://doi.org/10.1002/ana.23635

Fingelkurts, A. A., Fingelkurts, A. A., Bagnato, S., Boccagni, C., & Galardi, G. (2013). Chapter 5—The value of spontaneous EEG oscillations in distinguishing patients in vegetative and minimally conscious states. In E. Başar, C. Başar-Eroĝlu, A. Özerdem, P. M. Rossini, & G. G. Yener (Eds.), *Supplements to Clinical Neurophysiology* (Vol. 62, pp. 81–99). Elsevier. https://doi.org/10.1016/B978-0-7020-5307-8.00005-3

Fischer, C., Dailler, F., & Morlet, D. (2008). Novelty P3 elicited by the subject's own name in comatose patients. *Clinical Neurophysiology*, *119*(10), 2224–2230. https://doi.org/10.1016/j.clinph.2008.03.035

Fischer, C., Luaute, J., & Morlet, D. (2010). Event-related potentials (MMN and novelty P3) in permanent vegetative or minimally conscious states. *Clinical Neurophysiology*, *121*(7), 1032–1042. https://doi.org/10.1016/j.clinph.2010.02.005

Fitzgibbon, S. P., DeLosAngeles, D., Lewis, T. W., Powers, D. M. W., Grummett, T. S., Whitham, E. M., Ward, L. M., Willoughby, J. O., & Pope, K. J. (2016). Automatic determination of EMG-contaminated components and validation of independent

component analysis using EEG during pharmacologic paralysis. *Clinical Neurophysiology*, *127*(3), 1781–1793. https://doi.org/10.1016/j.clinph.2015.12.009

Foster, N. A., & Valentine, E. R. (2001). The Effect of Auditory Stimulation on Autobiographical Recall in Dementia. *Experimental Aging Research*, *27*(3), 215–228. https://doi.org/10.1080/036107301300208664

Fox, M. D., Snyder, A. Z., Vincent, J. L., Corbetta, M., Essen, D. C. V., & Raichle, M. E. (2005). The human brain is intrinsically organized into dynamic, anticorrelated functional networks. *Proceedings of the National Academy of Sciences*, *102*(27), 9673–9678. https://doi.org/10.1073/pnas.0504136102

Fransson, P., & Marrelec, G. (2008). The precuneus/posterior cingulate cortex plays a pivotal role in the default mode network: Evidence from a partial correlation network analysis. *NeuroImage*, *42*(3), 1178–1184. https://doi.org/10.1016/j.neuroimage.2008.05.059

French, C. C. (2005). Near-death experiences in cardiac arrest survivors. In S. Laureys (Ed.), *Progress in Brain Research* (Vol. 150, pp. 351–367). Elsevier. https://doi.org/10.1016/S0079-6123(05)50025-6

Friedman, D., Cycowicz, Y. M., & Gaeta, H. (2001). The novelty P3: An event-related brain potential (ERP) sign of the brain's evaluation of novelty. *Neuroscience & Biobehavioral Reviews*, *25*(4), 355–373. https://doi.org/10.1016/S0149-7634(01)00019-7

Fries, P. (2005). A mechanism for cognitive dynamics: Neuronal communication through neuronal coherence. *Trends in Cognitive Sciences*, *9*(10), 474–480. https://doi.org/10.1016/j.tics.2005.08.011

Fries, P. (2009). Neuronal Gamma-Band Synchronization as a Fundamental Process in Cortical Computation. *Annual Review of Neuroscience*, *32*(1), 209–224. https://doi.org/10.1146/annurev.neuro.051508.135603

Garrison, K. A., Zeffiro, T. A., Scheinost, D., Constable, R. T., & Brewer, J. A. (2015). Meditation leads to reduced default mode network activity beyond an active task. *Cognitive, Affective, & Behavioral Neuroscience*, *15*(3), 712–720. https://doi.org/10.3758/s13415-015-0358-3

Gerlach, K. D., Spreng, R. N., Madore, K. P., & Schacter, D. L. (2014). Future planning: Default network activity couples with frontoparietal control network and reward-processing regions during process and outcome simulations. *Social Cognitive and Affective Neuroscience*, *9*(12), 1942–1951. https://doi.org/10.1093/scan/nsu001

Giacino, J. T., Fins, J. J., Laureys, S., & Schiff, N. D. (2014). Disorders of consciousness after acquired brain injury: The state of the science. *Nature Reviews Neurology*, *10*(2), 99–114. https://doi.org/10.1038/nrneurol.2013.279

Giacino, J. T., Kalmar, K., & Whyte, J. (2004). The JFK Coma Recovery Scale-Revised: Measurement characteristics and diagnostic utility1. *Archives of Physical Medicine and Rehabilitation*, *85*(12), 2020–2029. https://doi.org/10.1016/j.apmr.2004.02.033

Giacino, J. T., Schnakers, C., Rodriguez-Moreno, D., Kalmar, K., Schiff, N., & Hirsch, J. (2009). Behavioral assessment in patients with disorders of consciousness: Gold standard or fool's gold? In S. Laureys, N. D. Schiff, & A. M. Owen (Eds.), *Progress in Brain Research* (Vol. 177, pp. 33–48). Elsevier. https://doi.org/10.1016/S0079-6123(09)17704-X

Giani, A. S., Belardinelli, P., Ortiz, E., Kleiner, M., & Noppeney, U. (2015). Detecting tones in complex auditory scenes. *NeuroImage*, *122*, 203–213. https://doi.org/10.1016/j.neuroimage.2015.07.001

Gibson, R. M., Chennu, S., Fernández-Espejo, D., Naci, L., Owen, A. M., & Cruse, D. (2016). Somatosensory attention identifies both overt and covert awareness in disorders of consciousness. *Annals of Neurology*, *80*(3), 412–423. https://doi.org/10.1002/ana.24726

Gibson, R. M., Fernández-Espejo, D., Gonzalez-Lara, L. E., Kwan, B. Y., Lee, D. H., Owen, A. M., & Cruse, D. (2014). Multiple tasks and neuroimaging modalities increase the likelihood of detecting covert awareness in patients with disorders of consciousness. *Frontiers in Human Neuroscience*, *8*. https://doi.org/10.3389/fnhum.2014.00950

Goldfine, A. M., Bardin, J. C., Noirhomme, Q., Fins, J. J., Schiff, N. D., & Victor, J. D. (2013). Reanalysis of "Bedside detection of awareness in the vegetative state: A cohort study." *The Lancet*, *381*(9863), 289–291. https://doi.org/10.1016/S0140-6736(13)60125-7

Goldman-Rakic, P. S. (1988). Topography of cognition: Parallel distributed networks in primate association cortex. *Annual Review of Neuroscience*, *11*(1), 137–156.

Goncharova, I. I., McFarland, D. J., Vaughan, T. M., & Wolpaw, J. R. (2003). EMG contamination of EEG: Spectral and topographical characteristics. *Clinical Neurophysiology*, *114*(9), 1580–1593. https://doi.org/10.1016/S1388-2457(03)00093-2

Gott, P. S., Rabinowicz, A. L., & DeGiorgio, C. M. (1991). P300 Auditory Event-Related Potentials in Nontraumatic Coma: Association With Glasgow Coma Score and Awakening. *Archives of Neurology*, *48*(12), 1267–1270. https://doi.org/10.1001/archneur.1991.00530240071024

Grady, C., Sarraf, S., Saverino, C., & Campbell, K. (2016). Age differences in the functional interactions among the default, frontoparietal control, and dorsal attention networks. *Neurobiology of Aging*, *41*, 159–172. https://doi.org/10.1016/j.neurobiolaging.2016.02.020

Greicius, M. D., Kiviniemi, V., Tervonen, O., Vainionpää, V., Alahuhta, S., Reiss, A. L., & Menon, V. (2008). Persistent default-mode network connectivity during light sedation. *Human Brain Mapping*, *29*(7), 839–847. https://doi.org/10.1002/hbm.20537

Greyson, B. (2000). Dissociation in people who have near-death experiences: Out of their bodies or out of their minds? *The Lancet*, *355*(9202), 460–463. https://doi.org/10.1016/S0140-6736(00)82013-9

Greyson, B., Holden, J. M., & Lommel, P. van. (2012). 'There is nothing paranormal about near-death experiences' revisited: Comment on Mobbs and Watt. *Trends in Cognitive Sciences*, *16*(9), 445. https://doi.org/10.1016/j.tics.2012.07.002

Greyson, B., Kelly, E. F., & Dunseath, W. J. R. (2013). Surge of neurophysiological activity in the dying brain. *Proceedings of the National Academy of Sciences*, *110*(47), E4405–E4405. https://doi.org/10.1073/pnas.1316937110

Gu, S., Satterthwaite, T. D., Medaglia, J. D., Yang, M., Gur, R. E., Gur, R. C., & Bassett, D. S. (2015). Emergence of system roles in normative neurodevelopment. *Proceedings of the National Academy of Sciences*, *112*(44), 13681–13686. https://doi.org/10.1073/pnas.1502829112

Güntekin, B., & Başar, E. (2010). A new interpretation of P300 responses upon analysis of coherences. *Cognitive Neurodynamics*, *4*(2), 107–118. https://doi.org/10.1007/s11571-010-9106-0

Gurtubay, I. G., Alegre, M., Labarga, A., Malanda, A., & Artieda, J. (2004). Gamma band responses to target and non-target auditory stimuli in humans. *Neuroscience Letters*, *367*(1), 6–9. https://doi.org/10.1016/j.neulet.2004.05.104

Gurtubay, I. G., Alegre, M., Labarga, A., Malanda, A., Iriarte, J., & Artieda, J. (2001). Gamma band activity in an auditory oddball paradigm studied with the wavelet transform. *Clinical Neurophysiology*, *112*(7), 1219–1228. https://doi.org/10.1016/S1388-2457(01)00557-0

Hahn, B., Ross, T. J., & Stein, E. A. (2007). Cingulate Activation Increases Dynamically with Response Speed under Stimulus Unpredictability. *Cerebral Cortex*, *17*(7), 1664–1671. https://doi.org/10.1093/cercor/bhl075

Hannawi, Y., Lindquist, M. A., Caffo, B. S., Sair, H. I., & Stevens, R. D. (2015). Resting brain activity in disorders of consciousness. *Neurology*, *84*(12), 1272–1280. https://doi.org/10.1212/WNL.0000000000001404

Hassabis, D., & Maguire, E. A. (2007). Deconstructing episodic memory with construction. *Trends in Cognitive Sciences*, *11*(7), 299–306. https://doi.org/10.1016/j.tics.2007.05.001

Heine, L., Castro, M., Martial, C., Tillmann, B., Laureys, S., & Perrin, F. (2015). Exploration of Functional Connectivity During Preferred Music Stimulation in Patients with Disorders of Consciousness. *Frontiers in Psychology*, *6*, 1704. https://doi.org/10.3389/fpsyg.2015.01704

Heinke, W., & Koelsch, S. (2005). The effects of anesthetics on brain activity and cognitive function. *Current Opinion in Anesthesiology*, *18*(6), 625. https://doi.org/10.1097/01.aco.0000189879.67092.12

Herbet, G., Lafargue, G., de Champfleur, N. M., Moritz-Gasser, S., le Bars, E., Bonnetblanc, F., & Duffau, H. (2014). Disrupting posterior cingulate connectivity disconnects consciousness from the external environment. *Neuropsychologia*, *56*, 239–244. https://doi.org/10.1016/j.neuropsychologia.2014.01.020

Heuvel, M. P. van den, & Sporns, O. (2013). Network hubs in the human brain. *Trends in Cognitive Sciences*, *17*(12), 683–696. https://doi.org/10.1016/j.tics.2013.09.012

Hipp, J. F., Engel, A. K., & Siegel, M. (2011). Oscillatory Synchronization in Large-Scale Cortical Networks Predicts Perception. *Neuron*, *69*(2), 387–396. https://doi.org/10.1016/j.neuron.2010.12.027

Hirokawa, E. (2004). Effects of Music Listening and Relaxation Instructions on Arousal Changes and the Working Memory Task in Older Adults. *Journal of Music Therapy*, *41*(2), 107–127. https://doi.org/10.1093/jmt/41.2.107

Holeckova, I., Fischer, C., Giard, M.-H., Delpuech, C., & Morlet, D. (2006). Brain responses to a subject's own name uttered by a familiar voice. *Brain Research*, *1082*(1), 142–152. https://doi.org/10.1016/j.brainres.2006.01.089

Holeckova, I., Fischer, C., Morlet, D., Delpuech, C., Costes, N., & Mauguière, F. (2008). Subject's own name as a novel in a MMN design: A combined ERP and PET study. *Brain Research*, *1189*, 152–165. https://doi.org/10.1016/j.brainres.2007.10.091

Holmes, C., Knights, A., Dean, C., Hodkinson, S., & Hopkins, V. (2006). Keep music live: Music and the alleviation of apathy in dementia subjects. *International Psychogeriatrics*, *18*(4), 623–630. https://doi.org/10.1017/S1041610206003887

Horovitz, S. G., Braun, A. R., Carr, W. S., Picchioni, D., Balkin, T. J., Fukunaga, M., & Duyn, J. H. (2009). Decoupling of the brain's default mode network during deep sleep.

Proceedings of the National Academy of Sciences, *106*(27), 11376–11381. https://doi.org/10.1073/pnas.0901435106

Hui, D., Nooruddin, Z., Didwaniya, N., Dev, R., De La Cruz, M., Kim, S. H., Kwon, J. H., Hutchins, R., Liem, C., & Bruera, E. (2014). Concepts and Definitions for "Actively Dying," "End of Life," "Terminally Ill," "Terminal Care," and "Transition of Care": A Systematic Review. *Journal of Pain and Symptom Management*, *47*(1), 77–89. https://doi.org/10.1016/j.jpainsymman.2013.02.021

Jääskeläinen, I. P., Hirvonen, J., Saher, M., Pekkonen, E., Sillanaukee, P., Näätänen, R., & Tiitinen, H. (1999). Benzodiazepine temazepam suppresses the transient auditory 40-Hz response amplitude in humans. *Neuroscience Letters*, *268*(2), 105–107. https://doi.org/10.1016/S0304-3940(99)00393-6

Jensen, O., Kaiser, J., & Lachaux, J.-P. (2007). Human gamma-frequency oscillations associated with attention and memory. *Trends in Neurosciences*, *30*(7), 317–324. https://doi.org/10.1016/j.tins.2007.05.001

Jung, T.-P., Makeig, S., Humphries, C., Lee, T.-W., McKEOWN, M. J., Iragui, V., & Sejnowski, T. J. (2000). Removing electroencephalographic artifacts by blind source separation. *Psychophysiology*, *37*(2), 163–178. https://doi.org/10.1111/1469-8986.3720163

Kabbara, A., El-Falou, W., Khalil, M., Wendling, F., & Hassan, M. (2017). The dynamic functional core network of the human brain at rest. *Scientific Reports*, *7*(1), 1–16. https://doi.org/10.1038/s41598-017-03420-6

Kabbara, A., Khalil, M., El-Falou, W., Eid, H., & Hassan, M. (2016). Functional Brain Connectivity as a New Feature for P300 Speller. *PLOS ONE*, *11*(1), e0146282. https://doi.org/10.1371/journal.pone.0146282

Karamzadeh, N., Medvedev, A., Azari, A., Gandjbakhche, A., & Najafizadeh, L. (2013). Capturing dynamic patterns of task-based functional connectivity with EEG. *NeuroImage*, *66*, 311–317. https://doi.org/10.1016/j.neuroimage.2012.10.032

Katayama, J., & Polich, J. (1998). Stimulus context determines P3a and P3b. *Psychophysiology*, *35*(1), 23–33. https://doi.org/10.1111/1469-8986.3510023

Kehl, K. A., & Kowalkowski, J. A. (2013). A Systematic Review of the Prevalence of Signs of Impending Death and Symptoms in the Last 2 Weeks of Life. *American Journal of Hospice and Palliative Medicine*, *30*(6), 601–616. https://doi.org/10.1177/1049909112468222

Kelly, S. P., Lalor, E. C., Reilly, R. B., & Foxe, J. J. (2006). Increases in Alpha Oscillatory Power Reflect an Active Retinotopic Mechanism for Distracter Suppression During Sustained Visuospatial Attention. *Journal of Neurophysiology*, *95*(6), 3844–3851. https://doi.org/10.1152/jn.01234.2005

Kim, H. (2014). Involvement of the dorsal and ventral attention networks in oddball stimulus processing: A meta-analysis. *Human Brain Mapping*, *35*(5), 2265–2284. https://doi.org/10.1002/hbm.22326

Kim, J.-W., Kim, P.-J., Kim, H.-G., & Shin, T. J. (2019). Changes of auditory stimulus processing in sevoflurane-induced sedation. *Neuroscience Letters*, *698*, 121–125. https://doi.org/10.1016/j.neulet.2019.01.018

King, J.-R., Bekinschtein, T., & Dehaene, S. (2011). Comment on “Preserved Feedforward But Impaired Top-Down Processes in the Vegetative State.” *Science*, *334*(6060), 1203–1203. https://doi.org/10.1126/science.1210012

Kivisaari, R., Lehtinen, R., Autti, T., Puuskari, V., Jokela, O., Ahveninen, J., Rapeli, P., & Kähkönen, S. (2007). Impaired pre-attentive auditory processing in opioid dependence with and without benzodiazepine co-dependence revealed by combined magnetoencephalography and electroencephalography. *Progress in Neuro-Psychopharmacology and Biological Psychiatry*, *31*(7), 1378–1386. https://doi.org/10.1016/j.pnpbp.2007.06.001

Klimesch, W. (1999). EEG alpha and theta oscillations reflect cognitive and memory performance: A review and analysis. *Brain Research Reviews*, *29*(2), 169–195. https://doi.org/10.1016/S0165-0173(98)00056-3

Klimesch, W. (2012). Alpha-band oscillations, attention, and controlled access to stored information. *Trends in Cognitive Sciences*, *16*(12), 606–617. https://doi.org/10.1016/j.tics.2012.10.007

Klimesch, W., Doppelmayr, M., & Hanslmayr, S. (2006). Upper alpha ERD and absolute power: Their meaning for memory performance. In C. Neuper & W. Klimesch (Eds.), *Progress in Brain Research* (Vol. 159, pp. 151–165). Elsevier. https://doi.org/10.1016/S0079-6123(06)59010-7

Klimesch, W., Doppelmayr, M., Pachinger, T., & Russegger, H. (1997). Event-related desynchronization in the alpha band and the processing of semantic information. *Cognitive Brain Research*, *6*(2), 83–94. https://doi.org/10.1016/S0926-6410(97)00018-9

Klimesch, W., Doppelmayr, M., Russegger, H., Pachinger, T., & Schwaiger, J. (1998). Induced alpha band power changes in the human EEG and attention. *Neuroscience Letters*, *244*(2), 73–76. https://doi.org/10.1016/S0304-3940(98)00122-0

Klimesch, W., Doppelmayr, M., Schwaiger, J., Auinger, P., & Winkler, Th. (1999). `Paradoxical' alpha synchronization in a memory task. *Cognitive Brain Research*, *7*(4), 493–501. https://doi.org/10.1016/S0926-6410(98)00056-1

Klimesch, W., Schack, B., & Sauseng, P. (2005). The Functional Significance of Theta and Upper Alpha Oscillations. *Experimental Psychology*, *52*(2), 99–108. https://doi.org/10.1027/1618-3169.52.2.99

Koch, C., Massimini, M., Boly, M., & Tononi, G. (2016). Neural correlates of consciousness: Progress and problems. *Nature Reviews Neuroscience*, *17*(5), 307–321. https://doi.org/10.1038/nrn.2016.22

Koelsch, S., Heinke, W., Sammler, D., & Olthoff, D. (2006). Auditory processing during deep propofol sedation and recovery from unconsciousness. *Clinical Neurophysiology*, *117*(8), 1746–1759. https://doi.org/10.1016/j.clinph.2006.05.009

Kolev, V., Demiralp, T., Yordanova, J., Ademoglu, A., & Isoglu-Alkaç, Ü. (1997). Time–frequency analysis reveals multiple functional components during oddball P300. *NeuroReport*, *8*(8), 2061.

Kotchoubey, B., Lang, S., Mezger, G., Schmalohr, D., Schneck, M., Semmler, A., Bostanov, V., & Birbaumer, N. (2005). Information processing in severe disorders of consciousness: Vegetative state and minimally conscious state. *Clinical Neurophysiology*, *116*(10), 2441–2453. https://doi.org/10.1016/j.clinph.2005.03.028

Krause, C. M., Heikki Lang, A., Laine, M., Kuusisto, M., & Pörn, B. (1996). Event-related. EEG desynchronization and synchronization during an auditory memory task. *Electroencephalography and Clinical Neurophysiology*, *98*(4), 319–326. https://doi.org/10.1016/0013-4694(96)00283-0

Kucyi, A., Hodaie, M., & Davis, K. D. (2012). Lateralization in intrinsic functional connectivity of the temporoparietal junction with salience- and attention-related brain networks. *Journal of Neurophysiology*, *108*(12), 3382–3392. https://doi.org/10.1152/jn.00674.2012

Lachaux, J.-P., Rodriguez, E., Martinerie, J., & Varela, F. J. (1999). Measuring phase synchrony in brain signals. *Human Brain Mapping*, *8*(4), 194–208. https://doi.org/10.1002/(SICI)1097-0193(1999)8:4<194::AID-HBM4>3.0.CO;2-C

Lake, J. (2017). The near-death experience: A testable neural model. *Psychology of Consciousness: Theory, Research, and Practice*, *4*(1), 115–134. https://doi.org/10.1037/cns0000099

Lang, P. J. (1995). The emotion probe: Studies of motivation and attention. *American Psychologist*, *50*(5), 372–385. https://doi.org/10.1037/0003-066X.50.5.372

Laureys, S. (2005). The neural correlate of (un)awareness: Lessons from the vegetative state. *Trends in Cognitive Sciences*, *9*(12), 556–559. https://doi.org/10.1016/j.tics.2005.10.010

Laureys, S., Celesia, G. G., Cohadon, F., Lavrijsen, J., León-Carrión, J., Sannita, W. G., Sazbon, L., Schmutzhard, E., von Wild, K. R., Zeman, A., Dolce, G., & the European Task Force on Disorders of Consciousness. (2010). Unresponsive wakefulness syndrome: A new name for the vegetative state or apallic syndrome. *BMC Medicine*, *8*(1), 68. https://doi.org/10.1186/1741-7015-8-68

Laureys, S., Giacino, J. T., Schiff, N. D., Schabus, M., & Owen, A. M. (2006). How should functional imaging of patients with disorders of consciousness contribute to their clinical rehabilitation needs? *Current Opinion in Neurology*, *19*(6), 520–527. https://doi.org/10.1097/WCO.0b013e3280106ba9

Laureys, S., Goldman, S., Phillips, C., Van Bogaert, P., Aerts, J., Luxen, A., Franck, G., & Maquet, P. (1999). Impaired Effective Cortical Connectivity in Vegetative State: Preliminary Investigation Using PET. *NeuroImage*, *9*(4), 377–382. https://doi.org/10.1006/nimg.1998.0414

Laureys, S., Perrin, F., Faymonville, M.-E., Schnakers, C., Boly, M., Bartsch, V., Majerus, S., Moonen, G., & Maquet, P. (2004). Cerebral processing in the minimally conscious state. *Neurology*, *63*(5), 916–918.

Laureys, S., Perrin, F., Schnakers, C., Boly, M., & Majerus, S. (2005). Residual cognitive function in comatose, vegetative and minimally conscious states. *Current Opinion in Neurology*, *18*(6), 726. https://doi.org/10.1097/01.wco.0000189874.92362.12

Lee, B., Park, K. S., Kang, D.-H., Kang, K. W., Kim, Y. Y., & Kwon, J. S. (2007). Generators of the gamma-band activities in response to rare and novel stimuli during the auditory oddball paradigm. *Neuroscience Letters*, *413*(3), 210–215. https://doi.org/10.1016/j.neulet.2006.11.066

Lee, U., Kim, S., Noh, G.-J., Choi, B.-M., Hwang, E., & Mashour, G. A. (2009). The directionality and functional organization of frontoparietal connectivity during consciousness and anesthesia in humans. *Consciousness and Cognition*, *18*(4), 1069–1078. https://doi.org/10.1016/j.concog.2009.04.004

Leech, R., Braga, R., & Sharp, D. J. (2012). Echoes of the Brain within the Posterior Cingulate Cortex. *Journal of Neuroscience*, *32*(1), 215–222. https://doi.org/10.1523/JNEUROSCI.3689-11.2012

Leech, R., Kamourieh, S., Beckmann, C. F., & Sharp, D. J. (2011). Fractionating the Default Mode Network: Distinct Contributions of the Ventral and Dorsal Posterior Cingulate

Cortex to Cognitive Control. *Journal of Neuroscience*, *31*(9), 3217–3224. https://doi.org/10.1523/JNEUROSCI.5626-10.2011

Lemaire, J.-J., Sontheimer, A., Nezzar, H., Pontier, B., Luauté, J., Roche, B., Gillart, T., Gabrillargues, J., Rosenberg, S., Sarret, C., Feschet, F., Vassal, F., Fontaine, D., & Coste, J. (2014). Electrical modulation of neuronal networks in brain-injured patients with disorders of consciousness: A systematic review. *Annales Françaises d'Anesthésie et de Réanimation*, *33*(2), 88–97. https://doi.org/10.1016/j.annfar.2013.11.007

Lew, H. L., Gray, M., & Poole, J. H. (2007). Temporal Stability of Auditory Event-Related Potentials in Healthy Individuals and Patients With Traumatic Brain Injury. *Journal of Clinical Neurophysiology*, *24*(5), 392. https://doi.org/10.1097/WNP.0b013e31814a56e3

Li, F., Chen, B., Li, H., Zhang, T., Wang, F., Jiang, Y., Li, P., Ma, T., Zhang, R., Tian, Y., Liu, T., Guo, D., Yao, D., & Xu, P. (2016). The Time-Varying Networks in P300: A Task-Evoked EEG Study. *IEEE Transactions on Neural Systems and Rehabilitation Engineering*, *24*(7), 725–733. https://doi.org/10.1109/TNSRE.2016.2523678

Linden, D. E. J. (2005). The P300: Where in the Brain Is It Produced and What Does It Tell Us? *The Neuroscientist*, *11*(6), 563–576. https://doi.org/10.1177/1073858405280524

Lopez-Calderon, J., & Luck, S. J. (2014). ERPLAB: An open-source toolbox for the analysis of event-related potentials. *Frontiers in Human Neuroscience*, *8*. https://doi.org/10.3389/fnhum.2014.00213

Luck, S. J., & Hillyard, S. A. (1994). Electrophysiological correlates of feature analysis during visual search. *Psychophysiology*, *31*(3), 291–308. https://doi.org/10.1111/j.1469-8986.1994.tb02218.x

Lutkenhoff, E. S., Chiang, J., Tshibanda, L., Kamau, E., Kirsch, M., Pickard, J. D., Laureys, S., Owen, A. M., & Monti, M. M. (2015). Thalamic and extrathalamic mechanisms of consciousness after severe brain injury. *Annals of Neurology*, *78*(1), 68–76. https://doi.org/10.1002/ana.24423

Machado, C., & Korein, J. (2009). Neuropathology of brain death in the modern transplant era. *Neurology*, *72*(11), 1028–1028. https://doi.org/10.1212/01.wnl.0000339394.33719.76

MacLean, S. E., Blundon, E. G., & Ward, L. M. (2015). Brain regional networks active during the mismatch negativity vary with paradigm. *Neuropsychologia*, *75*, 242–251. https://doi.org/10.1016/j.neuropsychologia.2015.06.019

MacLean, S. E., & Ward, L. M. (2014). Temporo-frontal phase synchronization supports hierarchical network for mismatch negativity. *Clinical Neurophysiology*, *125*(8), 1604–1617. https://doi.org/10.1016/j.clinph.2013.12.109

MacLean, S. E., & Ward, L. M. (2016). Oscillatory power and functional connectivity in the speech change detection network. *Neuropsychologia*, *89*, 320–334. https://doi.org/10.1016/j.neuropsychologia.2016.06.039

Magee, W. L., Tillmann, B., Perrin, F., & Schnakers, C. (2016). Editorial: Music and Disorders of Consciousness: Emerging Research, Practice and Theory. *Frontiers in Psychology*, *7*. https://doi.org/10.3389/fpsyg.2016.01273

Makeig, S. (1993). Auditory event-related dynamics of the EEG spectrum and effects of exposure to tones. *Electroencephalography and Clinical Neurophysiology*, *86*(4), 283–293. https://doi.org/10.1016/0013-4694(93)90110-H

Makeig, S., Debener, S., Onton, J., & Delorme, A. (2004). Mining event-related brain dynamics. *Trends in Cognitive Sciences*, *8*(5), 204–210. https://doi.org/10.1016/j.tics.2004.03.008

Mantini, D., Perrucci, M. G., Gratta, C. D., Romani, G. L., & Corbetta, M. (2007). Electrophysiological signatures of resting state networks in the human brain. *Proceedings of the National Academy of Sciences*, *104*(32), 13170–13175. https://doi.org/10.1073/pnas.0700668104

Maris, E., & Oostenveld, R. (2007). Nonparametric statistical testing of EEG- and MEG-data. *Journal of Neuroscience Methods*, *164*(1), 177–190. https://doi.org/10.1016/j.jneumeth.2007.03.024

Marshall, L., Mölle, M., & Bartsch, P. (1996). Event-related gamma band activity during passive and active oddball tasks. *Neuroreport*, *7*(9), 1517–1520. https://doi.org/10.1097/00001756-199606170-00016

McFarland, D. J., Miner, L. A., Vaughan, T. M., & Wolpaw, J. R. (2000). Mu and Beta Rhythm Topographies During Motor Imagery and Actual Movements. *Brain Topography*, *12*(3), 177–186. https://doi.org/10.1023/A:1023437823106

Meindl, T., Teipel, S., Elmouden, R., Mueller, S., Koch, W., Dietrich, O., Coates, U., Reiser, M., & Glaser, C. (2010). Test–retest reproducibility of the default-mode network in healthy individuals. *Human Brain Mapping*, *31*(2), 237–246. https://doi.org/10.1002/hbm.20860

Menon, V., & Uddin, L. Q. (2010). Saliency, switching, attention and control: A network model of insula function. *Brain Structure and Function*, *214*(5), 655–667. https://doi.org/10.1007/s00429-010-0262-0

Meunier, D., Achard, S., Morcom, A., & Bullmore, E. (2009). Age-related changes in modular organization of human brain functional networks. *NeuroImage*, *44*(3), 715–723. https://doi.org/10.1016/j.neuroimage.2008.09.062

Michel, C. M., Murray, M. M., Lantz, G., Gonzalez, S., Spinelli, L., & Grave de Peralta, R. (2004). EEG source imaging. *Clinical Neurophysiology*, *115*(10), 2195–2222. https://doi.org/10.1016/j.clinph.2004.06.001

Milligan, K. R., Lumsden, J., Howard, R. C., Howe, J. P., & Dundee, J. W. (1989). Use of auditory evoked responses as a measure of recovery from benzodiazepine sedation. *Journal of the Royal Society of Medicine*, *82*(10), 595–597.

Missonnier, P., Deiber, M.-P., Gold, G., Millet, P., Gex-Fabry Pun, M., Fazio-Costa, L., Giannakopoulos, P., & Ibáñez, V. (2006). Frontal theta event-related synchronization: Comparison of directed attention and working memory load effects. *Journal of Neural Transmission*, *113*(10), 1477–1486. https://doi.org/10.1007/s00702-005-0443-9

Mobbs, D., & Watt, C. (2011). There is nothing paranormal about near-death experiences: How neuroscience can explain seeing bright lights, meeting the dead, or being convinced you are one of them. *Trends in Cognitive Sciences*, *15*(10), 447–449. https://doi.org/10.1016/j.tics.2011.07.010

Monti, M. M., Coleman, M. R., & Owen, A. M. (2009). Neuroimaging and the vegetative state: Resolving the behavioral assessment dilemma? *Annals of the New York Academy of Sciences*, *1157*(1), 81–89.

Monti, Martin M., Vanhaudenhuyse, A., Coleman, M. R., Boly, M., Pickard, J. D., Tshibanda, L., Owen, A. M., & Laureys, S. (2010). Willful Modulation of Brain Activity in Disorders of Consciousness. *New England Journal of Medicine*, *362*(7), 579–589. https://doi.org/10.1056/NEJMoa0905370

Morlet, D., & Fischer, C. (2014). MMN and Novelty P3 in Coma and Other Altered States of Consciousness: A Review. *Brain Topography*, *27*(4), 467–479. https://doi.org/10.1007/s10548-013-0335-5

Muller-Gass, A., Macdonald, M., Schröger, E., Sculthorpe, L., & Campbell, K. (2007). Evidence for the auditory P3a reflecting an automatic process: Elicitation during highly-focused continuous visual attention. *Brain Research*, *1170*, 71–78. https://doi.org/10.1016/j.brainres.2007.07.023

Näätänen, R., Paavilainen, P., Rinne, T., & Alho, K. (2007). The mismatch negativity (MMN) in basic research of central auditory processing: A review. *Clinical Neurophysiology*, *118*(12), 2544–2590. https://doi.org/10.1016/j.clinph.2007.04.026

Näätänen, Risto., Kujala, T., Escera, C., Baldeweg, T., Kreegipuu, K., Carlson, S., & Ponton, C. (2012). The mismatch negativity (MMN) – A unique window to disturbed central auditory processing in ageing and different clinical conditions. *Clinical Neurophysiology*, *123*(3), 424–458. https://doi.org/10.1016/j.clinph.2011.09.020

Naccache, L. (2018). Why and how access consciousness can account for phenomenal consciousness. *Philosophical Transactions of the Royal Society B: Biological Sciences*, *373*(1755), 20170357. https://doi.org/10.1098/rstb.2017.0357

Naccache, L., Marti, S., Sitt, J. D., Trübutschek, D., & Berkovitch, L. (2016). *Why the P3b is still a plausible correlate of conscious access? A commentary on Silverstein et al., 2015*. https://hal.sorbonne-universite.fr/hal-01317650

Noirhomme, Q., Lehembre, R., Lugo, Z. del R., Lesenfants, D., Luxen, A., Laureys, S., Oddo, M., & Rossetti, A. O. (2014). Automated Analysis of Background EEG and Reactivity

During Therapeutic Hypothermia in Comatose Patients After Cardiac Arrest. *Clinical EEG and Neuroscience*, *45*(1), 6–13. https://doi.org/10.1177/1550059413509616

Noirhomme, Q., Soddu, A., Lehembre, R., Vanhaudenhuyse, A., Boveroux, P., Boly, M., & Laureys, S. (2010). Brain Connectivity in Pathological and Pharmacological Coma. *Frontiers in Systems Neuroscience*, *4*. https://doi.org/10.3389/fnsys.2010.00160

Nourski, K. V., Steinschneider, M., Rhone, A. E., Kawasaki, H., Howard, M. A., & Banks, M. I. (2018). Auditory Predictive Coding across Awareness States under Anesthesia: An Intracranial Electrophysiology Study. *Journal of Neuroscience*, *38*(39), 8441–8452. https://doi.org/10.1523/JNEUROSCI.0967-18.2018

Nunez, P. L. (1974). The brain wave equation: A model for the EEG. *Mathematical Biosciences*, *21*(3), 279–297. https://doi.org/10.1016/0025-5564(74)90020-0

Öhman, A., Flykt, A., & Esteves, F. (2001). Emotion drives attention: Detecting the snake in the grass. *Journal of Experimental Psychology: General*, *130*(3), 466–478. https://doi.org/10.1037/0096-3445.130.3.466

O'Kelly, J., James, L., Palaniappan, R., Fachner, J., Taborin, J., & Magee, W. L. (2013). Neurophysiological and Behavioral Responses to Music Therapy in Vegetative and Minimally Conscious States. *Frontiers in Human Neuroscience*, *7*, 884. https://doi.org/10.3389/fnhum.2013.00884

Okumura, Y., Asano, Y., Takenaka, S., Fukuyama, S., Yonezawa, S., Kasuya, Y., & Shinoda, J. (2014). Brain activation by music in patients in a vegetative or minimally conscious state following diffuse brain injury. *Brain Injury*, *28*(7), 944–950. https://doi.org/10.3109/02699052.2014.888477

Onton, J., Westerfield, M., Townsend, J., & Makeig, S. (2006). Imaging human EEG dynamics using independent component analysis. *Neuroscience & Biobehavioral Reviews*, *30*(6), 808–822. https://doi.org/10.1016/j.neubiorev.2006.06.007

Ossandón, T., Vidal, J. R., Ciumas, C., Jerbi, K., Hamamé, C. M., Dalal, S. S., Bertrand, O., Minotti, L., Kahane, P., & Lachaux, J.-P. (2012). Efficient "Pop-Out" Visual Search Elicits Sustained Broadband Gamma Activity in the Dorsal Attention Network. *Journal of Neuroscience*, *32*(10), 3414–3421. https://doi.org/10.1523/JNEUROSCI.6048-11.2012

Owen, A. M. (2013). Detecting Consciousness: A Unique Role for Neuroimaging. *Annual Review of Psychology*, *64*(1), 109–133. https://doi.org/10.1146/annurev-psych-113011-143729

Owen, A. M. (2014). Diagnostic accuracy of brain imaging in the vegetative state. *Nature Reviews Neurology*, *10*(7), 370–371. https://doi.org/10.1038/nrneurol.2014.102

Owen, A. M., & Coleman, M. R. (2008). Functional neuroimaging of the vegetative state. *Nature Reviews Neuroscience*, *9*(3), 235–243. https://doi.org/10.1038/nrn2330

Owen, A. M., Coleman, M. R., Boly, M., Davis, M. H., Laureys, S., & Pickard, J. D. (2006). Detecting Awareness in the Vegetative State. *Science*, *313*(5792), 1402–1402. https://doi.org/10.1126/science.1130197

Owen, A. M., Coleman, M. R., Boly, M., Davis, M. H., Laureys, S., & Pickard, J. D. (2007). Using Functional Magnetic Resonance Imaging to Detect Covert Awareness in the Vegetative State. *Archives of Neurology*, *64*(8), 1098–1102. https://doi.org/10.1001/archneur.64.8.1098

Owen, A. M., Coleman, M. R., Menon, D. K., Johnsrude, I. S., Rodd, J. M., Davis, M. H., Taylor, K., & Pickard, J. D. (2005). Residual auditory function in persistent vegetative

state: A combined pet and fmri study. *Neuropsychological Rehabilitation*, *15*(3–4), 290–306. https://doi.org/10.1080/09602010443000579

Pal, D., Li, D., Dean, J. G., Brito, M. A., Liu, T., Fryzel, A. M., Hudetz, A. G., & Mashour, G. A. (2020). Level of Consciousness Is Dissociable from Electroencephalographic Measures of Cortical Connectivity, Slow Oscillations, and Complexity. *Journal of Neuroscience*, *40*(3), 605–618. https://doi.org/10.1523/JNEUROSCI.1910-19.2019

Palva, S. (Ed.). (2016). *Multimodal Oscillation-based Connectivity Theory.* Springer International Publishing.

Palva, S., & Palva, J. M. (2011). Functional Roles of Alpha-Band Phase Synchronization in Local and Large-Scale Cortical Networks. *Frontiers in Psychology*, *2*, 204. https://doi.org/10.3389/fpsyg.2011.00204

Pan, J., Xie, Q., He, Y., Wang, F., Di, H., Laureys, S., Yu, R., & Li, Y. (2014). Detecting awareness in patients with disorders of consciousness using a hybrid brain–computer interface. *Journal of Neural Engineering*, *11*(5), 056007. https://doi.org/10.1088/1741-2560/11/5/056007

Pana, R., Hornby, L., Shemie, S. D., Dhanani, S., & Teitelbaum, J. (2016). Time to loss of brain function and activity during circulatory arrest. *Journal of Critical Care*, *34*, 77–83. https://doi.org/10.1016/j.jcrc.2016.04.001

Parnia, S., & Fenwick, P. (2002). Near death experiences in cardiac arrest: Visions of a dying brain or visions of a new science of consciousness. *Resuscitation*, *52*(1), 5–11. https://doi.org/10.1016/S0300-9572(01)00469-5

Parnia, S., Waller, D. G., Yeates, R., & Fenwick, P. (2001). A qualitative and quantitative study of the incidence, features and aetiology of near death experiences in cardiac arrest

survivors. *Resuscitation*, *48*(2), 149–156. https://doi.org/10.1016/S0300-9572(00)00328-2

Pascual-Marqui, R. D. (2002). Standardized low-resolution brain electromagnetic tomography (sLORETA): Technical details. *Methods & Findings in Experimental & Clinical Pharmacology*, *24*(Suppl D), 5–12.

Penfield, W., & Jasper, H. (1954). *Epilepsy and the functional anatomy of the human brain*. Little, Brown & Co.

Peng, W., Hu, L., Zhang, Z., & Hu, Y. (2012). Causality in the Association between P300 and Alpha Event-Related Desynchronization. *PLOS ONE*, *7*(4), e34163. https://doi.org/10.1371/journal.pone.0034163

Perrin, F., García-Larrea, L., Mauguière, F., & Bastuji, H. (1999). A differential brain response to the subject's own name persists during sleep. *Clinical Neurophysiology*, *110*(12), 2153–2164. https://doi.org/10.1016/S1388-2457(99)00177-7

Perrin, F., Schnakers, C., Schabus, M., Degueldre, C., Goldman, S., Brédart, S., Faymonville, M.-E., Lamy, M., Moonen, G., Luxen, A., Maquet, P., & Laureys, S. (2006). Brain Response to One's Own Name in Vegetative State, Minimally Conscious State, and Locked-in Syndrome. *Archives of Neurology*, *63*(4), 562–569. https://doi.org/10.1001/archneur.63.4.562

Peterson, A., Naci, L., Weijer, C., Cruse, D., Fernández-Espejo, D., Graham, M., & Owen, A. M. (2013). Assessing Decision-Making Capacity in the Behaviorally Nonresponsive Patient With Residual Covert Awareness. *AJOB Neuroscience*, *4*(4), 3–14. https://doi.org/10.1080/21507740.2013.821189

Pfurtscheller, G., & Lopes da Silva, F. H. (1999). Event-related EEG/MEG synchronization and desynchronization: Basic principles. *Clinical Neurophysiology*, *110*(11), 1842–1857. https://doi.org/10.1016/S1388-2457(99)00141-8

Pfurtscheller, G., & Neuper, C. (2006). Future prospects of ERD/ERS in the context of brain–computer interface (BCI) developments. In C. Neuper & W. Klimesch (Eds.), *Progress in Brain Research* (Vol. 159, pp. 433–437). Elsevier. https://doi.org/10.1016/S0079-6123(06)59028-4

Pfurtscheller, G., Neuper, C., & Mohl, W. (1994). Event-related desynchronization (ERD) during visual processing. *International Journal of Psychophysiology*, *16*(2), 147–153. https://doi.org/10.1016/0167-8760(89)90041-X

Pion-Tonachini, L., Kreutz-Delgado, K., & Makeig, S. (2019). ICLabel: An automated electroencephalographic independent component classifier, dataset, and website. *NeuroImage*, *198*, 181–197. https://doi.org/10.1016/j.neuroimage.2019.05.026

Plourde, G., & Boylan, J. F. (1991). The long-latency auditory evoked potential as a measure of the level of consciousness during sufentanil anesthesia. *Journal of Cardiothoracic and Vascular Anesthesia*, *5*(6), 577–583. https://doi.org/10.1016/1053-0770(91)90010-Q

Polich, J. (1986). Normal variation of P300 from auditory stimuli. *Electroencephalography and Clinical Neurophysiology/Evoked Potentials Section*, *65*(3), 236–240. https://doi.org/10.1016/0168-5597(86)90059-6

Polich, J. (1996). Meta-analysis of P300 normative aging studies. *Psychophysiology*, *33*(4), 334–353. https://doi.org/10.1111/j.1469-8986.1996.tb01058.x

Polich, J. (1997). On the relationship between EEG and P300: Individual differences, aging, and ultradian rhythms. *International Journal of Psychophysiology*, *26*(1), 299–317. https://doi.org/10.1016/S0167-8760(97)00772-1

Polich, J. (2007). Updating P300: An integrative theory of P3a and P3b. *Clinical Neurophysiology*, *118*(10), 2128–2148. https://doi.org/10.1016/j.clinph.2007.04.019

Polich, J., & Criado, J. R. (2006). Neuropsychology and neuropharmacology of P3a and P3b. *International Journal of Psychophysiology*, *60*(2), 172–185. https://doi.org/10.1016/j.ijpsycho.2005.12.012

Polich, J., Ehlers, C. L., Otis, S., Mandell, A. J., & Bloom, F. E. (1986). P300 latency reflects the degree of cognitive decline in dementing illness. *Electroencephalography and Clinical Neurophysiology*, *63*(2), 138–144. https://doi.org/10.1016/0013-4694(86)90007-6

Polich, J., & McIsaac, H. K. (1994). Comparison of auditory P300 habituation from active and passive conditions. *International Journal of Psychophysiology*, *17*(1), 25–34. https://doi.org/10.1016/0167-8760(94)90052-3

Power, J. D., Cohen, A. L., Nelson, S. M., Wig, G. S., Barnes, K. A., Church, J. A., Vogel, A. C., Laumann, T. O., Miezin, F. M., Schlaggar, B. L., & Petersen, S. E. (2011). Functional Network Organization of the Human Brain. *Neuron*, *72*(4), 665–678. https://doi.org/10.1016/j.neuron.2011.09.006

Qaseem, A., Snow, V., Shekelle, P., Casey, D. E., Cross, J. T., Owens, D. K., & for the Clinical Efficacy Assessment Subcommittee of the American College of Physicians*. (2008). Evidence-Based Interventions to Improve the Palliative Care of Pain, Dyspnea, and Depression at the End of Life: A Clinical Practice Guideline from the American College

of Physicians. *Annals of Internal Medicine*, *148*(2), 141. https://doi.org/10.7326/0003-4819-148-2-200801150-00009

Qin, P., Di, H., Yan, X., Yu, S., Yu, D., Laureys, S., & Weng, X. (2008). Mismatch negativity to the patient's own name in chronic disorders of consciousness. *Neuroscience Letters*, *448*(1), 24–28. https://doi.org/10.1016/j.neulet.2008.10.029

Rady, M. Y., & Verheijde, J. L. (2016). Neuroscience and awareness in the dying human brain: Implications for organ donation practices. *Journal of Critical Care*, *34*, 121–123. https://doi.org/10.1016/j.jcrc.2016.04.016

Raichle, M. E. (1983). The pathophysiology of brain ischemia. *Annals of Neurology*, *13*(1), 2–10. https://doi.org/10.1002/ana.410130103

Raichle, M. E., MacLeod, A. M., Snyder, A. Z., Powers, W. J., Gusnard, D. A., & Shulman, G. L. (2001). A default mode of brain function. *Proceedings of the National Academy of Sciences*, *98*(2), 676–682.

Rappaport, M., McCandless, K. L., Pond, W., & Krafft, M. C. (1991). Passive P300 response in traumatic brain injury patients. *The Journal of Neuropsychiatry and Clinical Neurosciences*, *3*(2), 180–185. https://doi.org/10.1176/jnp.3.2.180

Real, R. G. L., Veser, S., Erlbeck, H., Risetti, M., Vogel, D., Müller, F., Kotchoubey, B., Mattia, D., & Kübler, A. (2016). Information processing in patients in vegetative and minimally conscious states. *Clinical Neurophysiology*, *127*(2), 1395–1402. https://doi.org/10.1016/j.clinph.2015.07.020

Revonsuo, A. (1999). Binding and the Phenomenal Unity of Consciousness. *Consciousness and Cognition*, *8*(2), 173–185. https://doi.org/10.1006/ccog.1999.0384

Ribary, U., Doesburg, S. M., & Ward, L. M. (2017). Unified principles of thalamo-cortical processing: The neural switch. *Biomedical Engineering Letters*, *7*(3), 229–235. https://doi.org/10.1007/s13534-017-0033-4

Ribary, U., Doesburg, S. M., & Ward, L. M. (2019). Unified Principles of Thalamocortical Network Dynamics: A Framework for Typical/Atypical Functional Connectivity. In S. Supek & C. J. Aine (Eds.), *Magnetoencephalography: From Signals to Dynamic Cortical Networks* (2nd ed., pp. 543–570). Springer Nature.

Rickard, N. S. (2004). Intense emotional responses to music: A test of the physiological arousal hypothesis. *Psychology of Music*, *32*(4), 371–388. https://doi.org/10.1177/0305735604046096

Rihs, T. A., Michel, C. M., & Thut, G. (2007). Mechanisms of selective inhibition in visual spatial attention are indexed by α-band EEG synchronization. *European Journal of Neuroscience*, *25*(2), 603–610. https://doi.org/10.1111/j.1460-9568.2007.05278.x

Rinne, T., Antila, S., & Winkler, I. (2001). Mismatch negativity is unaffected by top-down predictive information. *NeuroReport*, *12*(10), 2209.

Rockstroh, B., Elbert, T., Lutzenberger, W., & Altenmüller, E. (1991). Effects of the anticonvulsant benzodiazepine clonazepam on event-related brain potentials in humans. *Electroencephalography and Clinical Neurophysiology*, *78*(2), 142–149. https://doi.org/10.1016/0013-4694(91)90114-J

Rodriguez, E., George, N., Lachaux, J.-P., Martinerie, J., Renault, B., & Varela, F. J. (1999). Perception's shadow: Long-distance synchronization of human brain activity. *Nature*, *397*(6718), 430–433. https://doi.org/10.1038/17120

Rollnik, J. D., & Altenmüller, E. (2014). Music in disorders of consciousness. *Frontiers in Neuroscience*, *8*. https://doi.org/10.3389/fnins.2014.00190

Rossi Sebastiano, D., Panzica, F., Visani, E., Rotondi, F., Scaioli, V., Leonardi, M., Sattin, D., D'Incerti, L., Parati, E., Ferini Strambi, L., & Franceschetti, S. (2015). Significance of multiple neurophysiological measures in patients with chronic disorders of consciousness. *Clinical Neurophysiology*, *126*(3), 558–564. https://doi.org/10.1016/j.clinph.2014.07.004

Ruzzoli, M., Pirulli, C., Brignani, D., Maioli, C., & Miniussi, C. (2012). Sensory memory during physiological aging indexed by mismatch negativity (MMN). *Neurobiology of Aging*, *33*(3), 625.e21-625.e30. https://doi.org/10.1016/j.neurobiolaging.2011.03.021

Salimpoor, V. N., Benovoy, M., Longo, G., Cooperstock, J. R., & Zatorre, R. J. (2009). The Rewarding Aspects of Music Listening Are Related to Degree of Emotional Arousal. *PLOS ONE*, *4*(10), e7487. https://doi.org/10.1371/journal.pone.0007487

Sanders, R. D., Tononi, G., Laureys, S., & Sleigh, J. (2012). Unresponsiveness ≠ Unconsciousness. *Anesthesiology*, *116*(4), 946–959. https://doi.org/10.1097/ALN.0b013e318249d0a7

Särkämö, T., Laitinen, S., Tervaniemi, M., Numminen, A., Kurki, M., & Rantanen, P. (2012). Music, emotion, and dementia: Insight from neuroscientific and clinical research. *Music and Medicine*, *4*(3), 153–162. https://doi.org/10.1177/1943862112445323

Sauseng, P., Klimesch, W., Stadler, W., Schabus, M., Doppelmayr, M., Hanslmayr, S., Gruber, W. R., & Birbaumer, N. (2005). A shift of visual spatial attention is selectively associated with human EEG alpha activity. *European Journal of Neuroscience*, *22*(11), 2917–2926. https://doi.org/10.1111/j.1460-9568.2005.04482.x

Sauseng, Paul, Klimesch, W., Gruber, W., Hanslmayr, S., & Doppelmayr, M. (2007). Are event-related potential components generated by phase resetting of brain oscillations? A critical discussion. *Neuroscience*, *146*, 1435–1444. https://doi.org/10.1016/j.neuroscience.2007.03.014

Schacter, D. L., Addis, D. R., Hassabis, D., Martin, V. C., Spreng, R. N., & Szpunar, K. K. (2012). The Future of Memory: Remembering, Imagining, and the Brain. *Neuron*, *76*(4), 677–694. https://doi.org/10.1016/j.neuron.2012.11.001

Schiff, N. D., & Plum, F. (1999). Cortical function in the persistent vegetative state. *Trends in Cognitive Sciences*, *3*, 43–44. https://doi.org/10.1016/s1364-6613(98)01268-6

Schiff, N. D., Ribary, U., Moreno, D. R., Beattie, B., Kronberg, E., Blasberg, R., Giacino, J., McCagg, C., Fins, J. J., Llinás, R., & Plum, F. (2002). Residual cerebral activity and behavioural fragments can remain in the persistently vegetative brain. *Brain*, *125*(6), 1210–1234. https://doi.org/10.1093/brain/awf131

Schnakers, C., Vanhaudenhuyse, A., Giacino, J., Ventura, M., Boly, M., Majerus, S., Moonen, G., & Laureys, S. (2009). Diagnostic accuracy of the vegetative and minimally conscious state: Clinical consensus versus standardized neurobehavioral assessment. *BMC Neurology*, *9*(1), 35. https://doi.org/10.1186/1471-2377-9-35

Schupp, H. T., Flaisch, T., Stockburger, J., & Junghöfer, M. (2006). Emotion and attention: Event-related brain potential studies. In S. Anders, G. Ende, M. Junghofer, J. Kissler, & D. Wildgruber (Eds.), *Progress in Brain Research* (Vol. 156, pp. 31–51). Elsevier. https://doi.org/10.1016/S0079-6123(06)56002-9

Sculthorpe, L. D., Ouellet, D. R., & Campbell, K. B. (2009). MMN elicitation during natural sleep to violations of an auditory pattern. *Brain Research*, *1290*, 52–62. https://doi.org/10.1016/j.brainres.2009.06.013

Seel, R. T., Sherer, M., Whyte, J., Katz, D. I., Giacino, J. T., Rosenbaum, A. M., Hammond, F. M., Kalmar, K., Pape, T. L.-B., Zafonte, R., Biester, R. C., Kaelin, D., Kean, J., & Zasler, N. (2010). Assessment Scales for Disorders of Consciousness: Evidence-Based Recommendations for Clinical Practice and Research. *Archives of Physical Medicine and Rehabilitation*, *91*(12), 1795–1813. https://doi.org/10.1016/j.apmr.2010.07.218

Seeley, W. W., Menon, V., Schatzberg, A. F., Keller, J., Glover, G. H., Kenna, H., Reiss, A. L., & Greicius, M. D. (2007). Dissociable Intrinsic Connectivity Networks for Salience Processing and Executive Control. *Journal of Neuroscience*, *27*(9), 2349–2356. https://doi.org/10.1523/JNEUROSCI.5587-06.2007

Segalowitz, S. J., Dywan, J., & Unsal, A. (1997). Attentional factors in response time variability after traumatic brain injury: An ERP study. *Journal of the International Neuropsychological Society*, *3*(2), 95–107. https://doi.org/10.1017/S1355617797000957

Sergent, C., Baillet, S., & Dehaene, S. (2005). Timing of the brain events underlying access to consciousness during the attentional blink. *Nature Neuroscience*, *8*(10), 1391–1400. https://doi.org/10.1038/nn1549

Sharova, E. V., Oknina, L. B., Potapov, A. A., Zaĭtsev, O. S., Masherov, E. L., & Kulikov, M. A. (1998). The P300 component of the auditory evoked potential in the posttraumatic vegetative state. *Zhurnal vysshei nervnoi deiatelnosti imeni I P Pavlova*, *48*(4), 719–730.

Siegel, M., Donner, T. H., & Engel, A. K. (2012). Spectral fingerprints of large-scale neuronal interactions. *Nature Reviews Neuroscience*, *13*(2), 121–134. https://doi.org/10.1038/nrn3137

Silverstein, B. H., Snodgrass, M., Shevrin, H., & Kushwaha, R. (2015). P3b, consciousness, and complex unconscious processing. *Cortex*, *73*, 216–227. https://doi.org/10.1016/j.cortex.2015.09.004

Singer, P. A., Martin, D. K., & Kelner, M. (1999). Quality End-of-Life Care: Patients' Perspectives. *JAMA*, *281*(2), 163–168. https://doi.org/10.1001/jama.281.2.163

Singh, S. M., & Basu, D. (2009). CLINICAL STUDY: The P300 event-related potential and its possible role as an endophenotype for studying substance use disorders: a review. *Addiction Biology*, *14*(3), 298–309. https://doi.org/10.1111/j.1369-1600.2008.00124.x

Singh, S. M., Basu, D., Kohli, A., & Prabhakar, S. (2009). Auditory P300 Event-Related Potentials and Neurocognitive Functions in Opioid Dependent Men and Their Brothers. *American Journal on Addictions*, *18*(3), 198–205. https://doi.org/10.1080/10550490902786975

Smallwood, J., Brown, K., Baird, B., & Schooler, J. W. (2012). Cooperation between the default mode network and the frontal–parietal network in the production of an internal train of thought. *Brain Research*, *1428*, 60–70. https://doi.org/10.1016/j.brainres.2011.03.072

Solano, J. P., Gomes, B., & Higginson, I. J. (2006). A Comparison of Symptom Prevalence in Far Advanced Cancer, AIDS, Heart Disease, Chronic Obstructive Pulmonary Disease and Renal Disease. *Journal of Pain and Symptom Management*, *31*(1), 58–69. https://doi.org/10.1016/j.jpainsymman.2005.06.007

Sporns, O. (2002). Network analysis, complexity, and brain function. *Complexity*, *8*(1), 56–60. https://doi.org/10.1002/cplx.10047

Spreng, R. N., Mar, R. A., & Kim, A. S. N. (2008). The Common Neural Basis of Autobiographical Memory, Prospection, Navigation, Theory of Mind, and the Default Mode: A Quantitative Meta-analysis. *Journal of Cognitive Neuroscience*, *21*(3), 489–510. https://doi.org/10.1162/jocn.2008.21029

Spreng, R. N., & Schacter, D. L. (2012). Default Network Modulation and Large-Scale Network Interactivity in Healthy Young and Old Adults. *Cerebral Cortex*, *22*(11), 2610–2621. https://doi.org/10.1093/cercor/bhr339

Stender, J., Gosseries, O., Bruno, M.-A., Charland-Verville, V., Vanhaudenhuyse, A., Demertzi, A., Chatelle, C., Thonnard, M., Thibaut, A., Heine, L., Soddu, A., Boly, M., Schnakers, C., Gjedde, A., & Laureys, S. (2014). Diagnostic precision of PET imaging and functional MRI in disorders of consciousness: A clinical validation study. *The Lancet*, *384*(9942), 514–522. https://doi.org/10.1016/S0140-6736(14)60042-8

Stok, C. J. (1987). The influence of model parameters on EEG/MEG single dipole source estimation. *IEEE Transactions on Biomedical Engineering*, *BME-34*(4), 289–296. https://doi.org/10.1109/TBME.1987.326090

Sussman, E., Winkler, I., & Wang, W. (2003). MMN and attention: Competition for deviance detection. *Psychophysiology*, *40*(3), 430–435. https://doi.org/10.1111/1469-8986.00045

Tallon-Baudry, C., & Bertrand, O. (1999). Oscillatory gamma activity in humans and its role in object representation. *Trends in Cognitive Sciences*, *3*(4), 151–162. https://doi.org/10.1016/S1364-6613(99)01299-1

Tapson, K., Sierotowicz, W., Marks-Maran, D., & Thompson, T. M. (2015). 'It's the hearing that is last to go': A case of traumatic head injury. *British Journal of Nursing*, *24*(5), 277–281. https://doi.org/10.12968/bjon.2015.24.5.277

Thomas Yeo, B. T., Krienen, F. M., Sepulcre, J., Sabuncu, M. R., Lashkari, D., Hollinshead, M., Roffman, J. L., Smoller, J. W., Zöllei, L., Polimeni, J. R., Fischl, B., Liu, H., & Buckner, R. L. (2011). The organization of the human cerebral cortex estimated by intrinsic functional connectivity. *Journal of Neurophysiology*, *106*(3), 1125–1165. https://doi.org/10.1152/jn.00338.2011

Thonnard, M., Charland-Verville, V., Brédart, S., Dehon, H., Ledoux, D., Laureys, S., & Vanhaudenhuyse, A. (2013). Characteristics of Near-Death Experiences Memories as Compared to Real and Imagined Events Memories. *PLOS ONE*, *8*(3), e57620. https://doi.org/10.1371/journal.pone.0057620

Tomasi, D., & Volkow, N. D. (2012). Aging and functional brain networks. *Molecular Psychiatry*, *17*(5), 549–558. https://doi.org/10.1038/mp.2011.81

Tomasi, Dardo, & Volkow, N. D. (2011). Functional connectivity hubs in the human brain. *NeuroImage*, *57*(3), 908–917. https://doi.org/10.1016/j.neuroimage.2011.05.024

Treisman, A. M., & Souther, J. (1985). Search asymmetry: A diagnostic for preattentive processing of separable features. *Journal of Experimental Psychology: General*, *114*(3), 285–310. https://doi.org/10.1037/0096-3445.114.3.285

Tresch, D. D., Sims, F. H., Duthie, E. H., Goldstein, M. D., & Lane, P. S. (1991). Clinical Characteristics of Patients in the Persistent Vegetative State. *Archives of Internal Medicine*, *151*(5), 930–932. https://doi.org/10.1001/archinte.1991.00400050078015

Tsolaki, A., Kosmidou, V., Hadjileontiadis, L., Kompatsiaris, I. (Yiannis), & Tsolaki, M. (2015). Brain source localization of MMN, P300 and N400: Aging and gender differences. *Brain Research*, *1603*, 32–49. https://doi.org/10.1016/j.brainres.2014.10.004

van den Heuvel, M. P., & Hulshoff Pol, H. E. (2010). Exploring the brain network: A review on resting-state fMRI functional connectivity. *European Neuropsychopharmacology*, *20*(8), 519–534. https://doi.org/10.1016/j.euroneuro.2010.03.008

van Hooff, J. C., de Beer, N. A. M., Brunia, C. H. M., Cluitmans, P. J. M., & Korsten, H. H. M. (1997). Event-related potential measures of information processing during general anesthesia. *Electroencephalography and Clinical Neurophysiology*, *103*(2), 268–281. https://doi.org/10.1016/S0013-4694(97)00012-6

van Lommel, P., van Wees, R., Meyers, V., & Elfferich, I. (2001). Near-death experience in survivors of cardiac arrest: A prospective study in the Netherlands. *The Lancet*, *358*(9298), 2039–2045. https://doi.org/10.1016/S0140-6736(01)07100-8

Vanhaudenhuyse, A., Laureys, S., & Perrin, F. (2008). Cognitive Event-Related Potentials in Comatose and Post-Comatose States. *Neurocritical Care*, *8*(2), 262–270. https://doi.org/10.1007/s12028-007-9016-0

Vanhaudenhuyse, A., Noirhomme, Q., Tshibanda, L. J.-F., Bruno, M.-A., Boveroux, P., Schnakers, C., Soddu, A., Perlbarg, V., Ledoux, D., Brichant, J.-F., Moonen, G., Maquet, P., Greicius, M. D., Laureys, S., & Boly, M. (2010). Default network connectivity reflects the level of consciousness in non-communicative brain-damaged patients. *Brain*, *133*(1), 161–171. https://doi.org/10.1093/brain/awp313

Varela, F., Lachaux, J.-P., Rodriguez, E., & Martinerie, J. (2001). The brainweb: Phase synchronization and large-scale integration. *Nature Reviews Neuroscience*, *2*(4), 229–239. https://doi.org/10.1038/35067550

Varotto, G., Fazio, P., Rossi Sebastiano, D., Avanzini, G., Franceschetti, S., & Panzica, F. (2012). Music and emotion: An EEG connectivity study in patients with disorders of consciousness. *2012 Annual International Conference of the IEEE Engineering in Medicine and Biology Society*, 5206–5209. https://doi.org/10.1109/EMBC.2012.6347167

Verger, J., Ruiz, S., Tillmann, B., Ben, M. R., De, M. Q., Castro, M., Tell, L., Luauté, J., & Perrin, F. (2014). Beneficial effect of preferred music on cognitive functions in minimally conscious state patients. *Revue neurologique*, *170*(11), 693–699. https://doi.org/10.1016/j.neurol.2014.06.005

Vesco, K. K., Bone, R. C., Ryan, J. C., & Polich, J. (1993). P300 in young and elderly subjects: Auditory frequency and intensity effects. *Electroencephalography and Clinical Neurophysiology/Evoked Potentials Section*, *88*(4), 302–308. https://doi.org/10.1016/0168-5597(93)90054-S

Villanueva, N., E. (1999). Experiences of critical care nurses caring for unresponsive patients. *Journal of Neuroscience Nursing*, *31*(4), 216–223.

Viola, F. C., Thorne, J., Edmonds, B., Schneider, T., Eichele, T., & Debener, S. (2009). Semi-automatic identification of independent components representing EEG artifact. *Clinical Neurophysiology*, *120*(5), 868–877. https://doi.org/10.1016/j.clinph.2009.01.015

Vogel, E. K., Luck, S. J., & Shapiro, K. L. (1998). Electrophysiological evidence for a postperceptual locus of suppression during the attentional blink. *Journal of Experimental*

Psychology: Human Perception and Performance, *24*(6), 1656–1674. https://doi.org/10.1037/0096-1523.24.6.1656

Wannez, S., Heine, L., Thonnard, M., Gosseries, O., & Laureys, S. (2017). The repetition of behavioral assessments in diagnosis of disorders of consciousness. *Annals of Neurology*, *81*(6), 883–889. https://doi.org/10.1002/ana.24962

Wijdicks, E. F., & Pfeifer, E. A. (2008). Neuropathology of brain death in the modern transplant era. *Neurology*, *70*(15), 1234–1237.

Wijnen, V. J. M., van Boxtel, G. J. M., Eilander, H. J., & de Gelder, B. (2007). Mismatch negativity predicts recovery from the vegetative state. *Clinical Neurophysiology*, *118*(3), 597–605. https://doi.org/10.1016/j.clinph.2006.11.020

Worden, M. S., Foxe, J. J., Wang, N., & Simpson, G. V. (2000). Anticipatory biasing of visuospatial attention indexed by retinotopically specific-band electroencephalography increases over occipital cortex. *Journal of Neuroscience*, *20*(6), 1–6.

Wróbel, A. (2000). Beta activity: A carrier for visual attention. *Acta Neurobiologiae Experimentalis*, *60*(2), 247–260.

Wronka, E. A., Kaiser, J., & Coenen, A. M. L. (2008). The auditory P3 from passive and active three-stimulus oddball paradigm. *Acta Neurobiologiae Experimentalis*, *68*, 362–372.

Wronka, E. A., Kaiser, J., & Coenen, A. M. L. (2012). Neural generators of the auditory evoked potential components P3a and P3b. *Acta Neurobiologiae Experimentalis*, *72*(1), 51–64.

Wu, J.-T., Wu, H.-Z., Yan, C.-G., Chen, W.-X., Zhang, H.-Y., He, Y., & Yang, H.-S. (2011). Aging-related changes in the default mode network and its anti-correlated networks: A resting-state fMRI study. *Neuroscience Letters*, *504*(1), 62–67. https://doi.org/10.1016/j.neulet.2011.08.059

Yordanova, J., & Kolev, V. (1998a). Single-sweep analysis of the theta frequency band during an auditory oddball task. *Psychophysiology*, *35*(1), 116–126. https://doi.org/10.1111/1469-8986.3510116

Yordanova, J., & Kolev, V. (1998b). Event-related alpha oscillations are functionally associated with P300 during information processing. *NeuroReport*, *9*(14), 3159.

Yordanova, J., Kolev, V., & Polich, J. (2001). P300 and alpha event-related desynchronization (ERD). *Psychophysiology*, *38*(1), 143–152. https://doi.org/10.1111/1469-8986.3810143

Appendix A

Supplementary ERSP figures (Chapter 2)

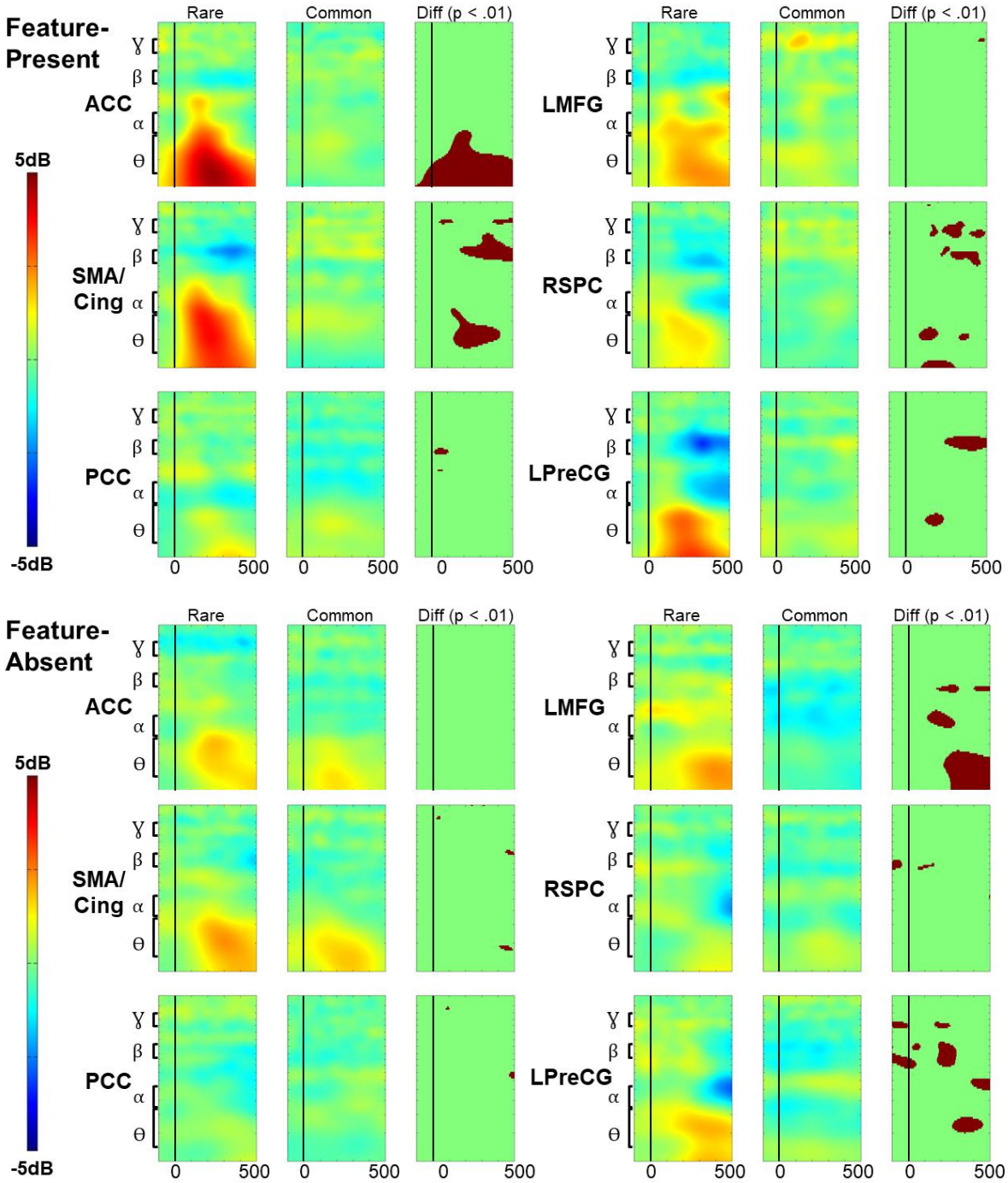

Appendix A: ERSPs in response to Feature-Present (top) and Feature-Absent (bottom) rare and common runs. For each panel the x axis is time, the y axis is frequency. Warmer colours represent spectral power increases relative to baseline, cooler colours represent spectral power

decreases relative to baseline, green represents no difference relative to baseline. ERSPs are baseline corrected to a common baseline across all trials within a condition. Significant differences (burgundy) represent local power differences (both increases and decreases) in rare runs relative to common runs (rare – common). Only the 6 ROIs that were found to have contributed to detection of the oddball targets are shown.

Appendix B

Supplementary PLV figures (Chapter 2)

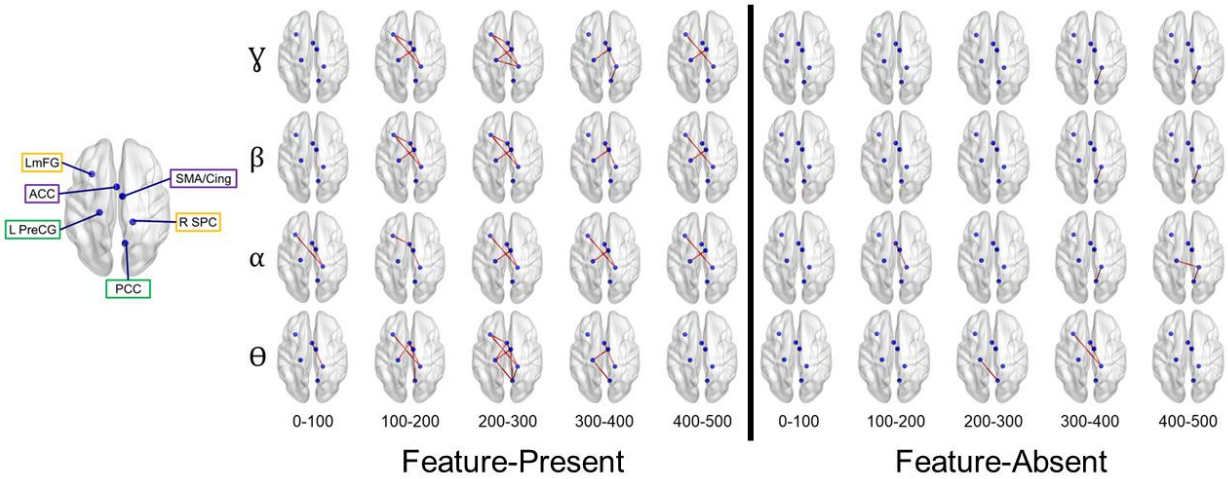

Appendix B: PLVs by frequency and time bin. Red lines represent significant connectivity between ROIs (p <0 .05). Only significantly larger connectivity to rare vs common runs are shown. Legend (left) indicates which network each node corresponds to. ROIs in purple are associated with the VAN, ROIs in gold are associated with the DAN, ROIs in green are associated with detecting auditory oddball targets.

Appendix C

Supplementary medication information (Chapter 3)

Medication Name	**Description and Usage in a Hospice Context**
clonazepam	A tranquilizer of the benzodiazepine class usually used for treating persistent anxiety.
dexamethasone	Corticosteroid used in in controlling pain, nausea, raised intracranial pressure and lymphedema.
escitalopram	Antidepressant of the selective serotonin reuptake inhibitor class used to treat major depressive disorder or generalized anxiety disorder.
fentanyl	Opioid used to treat pain or shortness of breath due to advanced disease.
gabapentin	Anticonvulsant medication used to treat neuropathic pain.
glycopyrrolate	Anticholinergic used to reduce salivary production in deeply unconscious patients in order to avoid noisy respiration.
hydromorphone	Opioid used to treat pain or shortness of breath due to advanced disease
levetiracetam	Anticonvulsant medication used to treat seizures secondary to primary tumors of the brain and/or brain metastases.
levothyroxine sodium	Manufactured form of the thyroid hormone thyroxine used to treat thyroid hormone deficiency.
lorazepam	Benzodiazepine medication used to treat anxiety, insomnia, active seizures including status epilepticus,
methadone	Opioid used for pain management, usually when other opioids not tolerated or not effective.
methylphenidate	Stimulant medication used to counter sedation secondary to the use of opioids for pain management or shortness of breath.
oxycodone	Opioid used to treat pain or shortness of breath due to advanced disease.
trazodone	Antidepressant medication used in smaller doses for sleep and anxiety.
zopiclone	Hypnotic agent used in the treatment of insomnia with a similar side effect profile to benzodiazepines.

Appendix C: List of medications administered to hospice patients summarized in Tables 1a & 1b. List includes a description of each medication and its use in a hospice context

Appendix D

Supplementary Patient Resting State Dipole Info (Chapter 5)

Participant ID	Network	ROI	Brodmann Area	Number of ICs	Mean Talairach Coords (x,y,z)	Mean Dipole fit (% scalp variance accounted for)
Responsive						
P002*		N/A				
P003	DMN	vMPFC	11	1	9, 53, -26	0.94
		PCC	31	3	-8, -41, 35	0.91
	Other	CC	24	2	7, 3, 41	0.84
		R PC	5	1	30, -37, 72	0.84
		L VC	19	1	-39, -75, 19	0.91
P004*	DMN	vMPFC	32	6	-5, 36, -5	0.93
		PCC	5	2	4, -34, 54	0.91
	Other	CC	24	1	1, -8, 25	0.91
		L pMC	6	1	-36, -3, 38	0.94
		R FG	37	1	32, -50, -12	0.96
		R VC	19	1	24, -44, -3	0.91
P005	DMN	vMPFC	11	6	-8, 47, -21	0.90
		R dMPFC	8	1	28, 46, 38	0.86
	Other	R FC	N/A	1	33, 16, 23	0.93
		L Ins	13	1	-46, 13, 1	0.98
		SMA	6	1	18, 8, 50	0.85
		R AC	21	1	47, -29, -7	0.94
P006	DMN	PCC	31	1	14, -41, 33	0.86
		L IPL	40	1	-64, -31, 43	0.94
	Other	SMA	6	1	15, 7, 62	0.94
		R VC	19	1	24, -94, 30	0.87
		L VC	18	1	-38, -91, -4	0.87
P007*	DMN	vMPFC	11	2	17, 41, -22	0.86
		L dMPFC	9	2	-29, 48, 35	0.85
		PCC	31	2	-3, -59, 25	0.95
		R IPL	39	1	47, -50, 10	0.94
		L IPL	40	2	-57, -37, 35	0.90
	Other	SMA	6	2	-24, 4, 69	0.83
		R pMC	6	1	47, 16, 51	0.83
		R PSC	3	1	47, -20, 61	0.94
		R AC	21	1	71, -29, 0	0.92
		L AC	22	2	-68, -32, 7	0.91
		L VC	19	1	-43, -82, 22	0.91
P008*	DMN	vMPFC	11	1	-3, 48, -31	0.95
		R dMPFC	10	1	37, 43, 9	0.93
		PCC	31	3	-8, -45, 33	0.89
		L IPL	N/A	1	-29, -20, 32	0.80

		R FC	10	1	30, 66, -8	0.80
		L Ins	N/A	1	-26, -18, 26	0.81
		CC	24	1	7, -6, 26	0.84
		R ITC	38	1	23, 15, -43	0.95
P009	DMN	vMPFC	11	3	-8, 47, -15	0.95
		PCC	7	1	-8, -49, 46	0.95
		R IPL	41	1	39, -33, 13	0.94
	Other	R FC	38	1	49, 9, -13	0.81
		SMA	6	1	1, 14, 68	0.93
Unresponsive						
P001	DMN	vMPFC	32	1	4, 42, 6	0.98
		PCC	5	3	12, -32, 51	0.90
		R IPL	40	3	45, -50, 36	0.92
		L IPL	22	1	-67, -50, 20	0.81
	Other	R FC	9	1	46, 33, 40	0.87
		CC	N/A	1	-21, 9, 23	0.90
		SMA	6	4	8, 0, 67	0.89
		L pMC	6	1	-39, -8, 28	0.90
		PCU	31	1	-25, -74, 18	0.91
		R ITC	37	1	61, -76, 1	0.94
P002*	Other	L FC	38	1	-47, 24, -35	0.95
P004*	DMN	vMPFC	11	1	-7, 61, -22	0.92
		R dMPFC	9	2	4, 39, 28	0.94
		PCC	N/A	1	20, -27, 30	0.91
	Other	R Ins	13	1	37, -23, 16	0.91
		CC	24	1	8, 5, 33	0.83
		L pMC	6	1	-37, -4, 31	0.93
		MTL	28	1	-19, -1, -22	0.84
P007*	DMN	vMPFC	47	1	14, 27, -28	0.85
		R dMPFC	10	1	11, 55, 15	0.94
		PCC	23	2	6, -33, 24	0.89
		R IPL	40	1	68, -38, 27	0.81
	Other	R Ins	13	1	26, 15, 10	0.87
		L Ins	13	1	-38, -11, -2	0.94
		SMA	6	1	29, 8, 55	0.90
		R VC	17	1	5, -82, 11	0.87
P008*	DMN	PCC	31	1	-19, -25, 33	0.87
	FPN	L pMC	6	1	-35, -7, 52	0.84

Appendix D: Complete list of valid ICs for all responsive and unresponsive patients. ICs are grouped by network (column 2) and region (column 3). If multiple ICs were localized to the same region, then only the mean Talairach coordinates and PVAF values of all ICs within that region are reported. Recall that ICs were localized to regions within DMN using a seeding algorithm (see methods). All other ICs were grouped based on their nearest neural region and Brodmann area. Starred patients contributed data both when they were responsive and again when they became unresponsive.